COORDINATED NEUROMORPHOLOGY IN THE DEVELOPMENT OF SOCIAL INFORMATION PROCESSING

A Dissertation
Submitted to
the Temple University Graduate Board

In Partial Fulfillment
of the Requirements for the Degree
DOCTOR OF PHILOSOPHY

---

by
Karla C. Fettich
July 2016

Examining Committee Members:

Jason M. Chein, Advisory Chair, Department of Psychology
Laurence Steinberg, Department of Psychology
Michael S. McCloskey, Examining Chair, Department of Psychology
Thomas Olino, Department of Psychology
Tania Giovannetti, Department of Psychology
Hongling Xie, Department of Psychology

ABSTRACT

Changes in social information processing that occur during adolescence are thought to rely on the functional and structural maturation of a network of interconnected brain regions referred to as "the social brain." The morphology of these brain regions, individually, is thought to be associated with functional specialization and/or ability, but little is known about the relationship between the morphology of the network and its functional specialization. Studies suggest that repeatedly executed psychological processes are not only reflected in functional networks, but may also be related to coordinated morphological changes in the brain across multiple regions that are functionally and structurally connected. The present study sought to explore changes in neuromorphological covariation that occur in the social brain network between adolescence and adulthood (Aim 1), using magnetic resonance imaging and graph theory, and link the properties of this covariance to self-reported and behavioral aspects of social information processing, specifically resistance to peer influence (Aim 2.1), rejection sensitivity (Aim 2.2), and the control of automatic reactions to socially relevant stimuli (Aim 2.3). The specificity of these results to social stimuli was assessed by also analyzing covariance properties in relation to a non-social measure of cognitive functioning (Aim 2.4). Subjects were 217 healthy right-handed individuals between the ages of 13 and 25 – 77 adolescents (ages 13-17), 73 young adults (ages 18-21), and 67 adults (ages 22-25). Analyses involved extracting cortical thickness values for the social brain network for each subject, and conducting group-level graph theoretic analyses. Results suggest that older subjects, subjects who are less sensitive to social stimuli and those who perform better on a behavioral inhibition task, all share one characteristic: the density of covariance in the structural social brain network is low compared to individuals who are younger, more sensitive to social stimuli, and who perform worse on a behavioral inhibition task.

Furthermore, this pattern was not observed in a non-social measure of cognitive functioning, suggesting a level of specificity to social information processing in the reported findings. By suggesting that selective structural covariance in the social brain may be characteristic of maturity but also more adaptive in social contexts, the findings from the present study contribute to the idea that adolescence is a time of great opportunity for shaping the brain's structural architecture.

ACKNOWLEDGMENTS

This dissertation would not have been possible without the help and guidance of my advisors, Jason Chein, Mike McCloskey, and Larry Steinberg, who have encouraged and supported me in exploring new scientific ideas and methodologies. I am especially grateful to Jason Chein for welcoming me into his lab, allowing me to pursue novel research approaches, spending countless hours with me brainstorming and troubleshooting, and providing me with the guidance I needed to stay on track. I am thankful to Mike McCloskey for always giving honest feedback and for supporting my interest in new statistical methods; and to Larry Steinberg I am grateful for challenging my thinking through dynamic, creative, and ethical scientific discussions in the lab, and for making it possible for me to work with the MacArthur Foundation Research Network on Law and Neuroscience.

I consider myself very fortunate to have had access to the resources that made this research possible. Specifically, I would like to thank the MacArthur Foundation Research Network on Law and Neuroscience, in particular BJ Casey and Larry Steinberg for making the present dataset available to me, Kaitlyn Breiner, Alexandra Cohen and Danielle Dellarco, for transferring the data and answering all my questions almost immediately, and Damien Fair for sharing his insights on graph theory methods. Furthermore, I would like to acknowledge that the speedy processing of the dataset was greatly facilitated by the Temple University High Performance Computing resource.

I have found that the phrase “it takes a village” also applies to writing a dissertation. I would like to extend my deep appreciation to Gail Rosenbaum, Harry Wilmer, Karol Silva, Grace Icenogle, Natasha Duell, Morgan Botdorf, Jamie Patrianakos,

Jamielyn Samper, Dan Kulper, and Brooke Ammerman for their friendship and for repeatedly reminding me of the importance of having a work-life balance. I am particularly grateful to Ashley Smith and Amy Look, who have been incredibly supportive and helpful, and have never asked me to stop sending them screenshots of graphs.

Finally, I would like to thank my parents. They have been there for me through all the ups and downs of grad school and have always believed in me. My skills and knowledge today are built on a foundation that I owe to them: my father always emphasized that math is beautiful and that coding is invaluable for efficient problem-solving. Unintentionally, those beliefs are deeply embedded in my work.

I am sincerely grateful to everyone who, directly or indirectly, helped me see this research to completion. I hope that I will have the opportunity to repay and share with others the kindness that was shown to me.

TABLE OF CONTENTS

LIST OF TABLES

TABLE Page

LIST OF FIGURES

FIGURE Page

CHAPTER 1

INTRODUCTION

Adolescence is a sensitive period for social information processing: compared to other age groups, adolescents spend more time with their peers, place greater emphasis on the expectations and opinions of their peers, experience new types of interpersonal relationships, develop their social skills and learn to negotiate their role within their social contexts (Brown & Larson, 2009; Steinberg & Morris, 2001).

These changes are thought to rely on the functional and structural maturation of a network of interconnected brain regions referred to as "the social brain" (Blakemore, 2008). The "social brain" is a term coined by Brothers in 1990, and was used to describe a set of brain regions that were involved in social cognition, with the amygdala, orbital frontal cortex and temporal cortex as major components (see a discussion in Frith, 2007). Recent research has expanded Brothers' original set of regions to a broader and more complex network (Blakemore, 2008; Frith, 2007; Skuse & Gallagher, 2009). Primarily, the social brain is considered to support processes related to mentalizing, i.e., the ability to infer the intentions, beliefs and desires of others (Mills, Lalonde, Clasen, Giedd, & Blakemore, 2014), but aspects such as face processing, peer influence, and social evaluation have also been subsumed under the social brain network's functionality (Burnett, Sebastian, Cohen Kadosh, & Blakemore, 2011).

While the functional involvement of regions and sub-networks of the social brain in social information processing has received increasing scientific attention, the importance of its structural properties in the context of social behavior remains to be clarified. The present study will seek to address this gap in the literature, building on the understanding that brain structure and function are intertwined, and that differences in brain morphology are related to observable

differences in psychological processes and their associated behavior.

The notion of a relationship between structure and function in the brain is not new. Research in healthy adults has shown differences in gray matter volume and/or cortical thickness between experts and controls in a range of functional domains, including spatial knowledge in cab drivers (Maguire et al., 2000, 2003; Maguire, Woollett, & Spiers, 2006), attention and self-perception in meditators (Kang et al., 2013), and musical tasks in musicians (Bermudez, Lerch, Evans, & Zatorre, 2009). Not only are gray matter volume and cortical thickness related to expertise, but they are also related to functional impairments in clinical populations, including mild cognitive impairment (Karas et al., 2004), Alzheimer's disease (Thompson et al., 2003), and schizophrenia (Sui et al., 2015). An extensive body of literature has also documented structural changes in the brain during development (e.g., Giedd et al., 1999; Giedd & Rapoport, 2010; P. Shaw et al., 2008) and discussed the potential implications of these changes for cognitive development (e.g., Casey, Giedd, & Thomas, 2000).

If brain morphology in specific areas can be indicative of functional specialization and/or ability, then a better understanding of morphological changes and their relationship to behavior is warranted. In this context, adolescence is of particular interest, as it is a period of extensive structural and functional reorganization across the entire brain. Studies show an accelerated cortical thinning process across the entire brain in adolescence, compared to childhood and young adulthood (Zhou, Lebel, Treit, Evans, & Beaulieu, 2015). In brain areas relevant for socio-affective processing, heterogeneous functional and structural changes have also been documented (Gogtay et al., 2004; Ostby et al., 2009). Given these widespread structural changes during a critical time for social development, an obvious question arises: how might the development of brain morphology be related to the increased sensitivity to social stimuli that has

been found during this period?

Emergence of a structural covariance network approach

Studies investigating the brain-behavior relationship have been moving away from focusing on single brain regions, and have moved towards a more network-oriented framework. Within that conceptualization, psychological phenomena are thought to emerge from patterns of inter-regional functional co-activation, rather than from activation in one key area of the brain. This functional co-activation in the brain may be facilitated by direct inter-regional white matter tracts, although this is not a necessary condition for co-activation (Johnson, Grossmann, & Kadosh, 2009). Thus, inter-regional co-activation is thought to provide the functional basis for behavior. In light of the research summarized above, it is also likely that this co-activation either relies on, or results in, coordinated anatomical changes in frequently co-activating brain regions (Alexander-Bloch, Giedd, & Bullmore, 2013).

Given the notion that networks, rather than individual regions, form the neuroanatomical basis for psychological processes, research has sought to focus on analyses that include data from multiple regions. One approach to studying gray matter morphology at the network level is through analysis of the pairwise correlations observed across a broad range of brain regions, an approach referred to as structural covariance. Developmental studies of inter-regional morphological correlations in gray matter structures have provided initial support for this approach. For example, female adolescents who scored high (vs. low) on a resistance to peer influence (RPI) measure also showed greater morphological similarity in cortical thickness between brain regions in premotor and prefrontal networks (Paus et al., 2008). These same networks were found in a previous study to have stronger functional connectivity in high-RPI

children when they viewed salient social stimuli (Grosbras et al., 2007).

These findings suggest that psychological processes can be directly related to interregional correlations in gray matter, and, it has been speculated that this link between function and structure is a result of repeated and concurrent engagement of specific groupings of brain regions (e.g., Bermudez et al., 2009; Munte, Altenmuller, & Jancke, 2002). Thus, increased functional connectivity may be reflected in an increased covariance in gray matter morphology. Indeed, resting-state functional networks have a high degree of overlap with structural covariance networks, as high as 60% for positive relationships (Hosseini & Kesler, 2013). In addition, up to 40% overlap has been found between structural covariance networks and white-matter tract networks (Gong, He, Chen, & Evans, 2012). A more detailed discussion of the relationship between gray matter structural covariance and other connectivity methods will be presented in the following sections. However, here it is important to note that gray matter covariance reflects an underlying connectivity between brain regions that is also found with other connectivity methods, but that the information obtained with this approach is not equivalent to that provided by other connectivity methods.

The research presented thus far suggests that repeatedly executed psychological processes are not only reflected in functional networks, but may also be related to coordinated morphological changes in the brain across multiple regions that are functionally and structurally connected. Because adolescence is a time of both extensive neuroanatomical remodeling and increased salience of social stimuli, the present study seeks to clarify: 1) how this remodeling impacts anatomical network topology, and 2) how behavioral phenotypes may differ according to anatomical network topology. To focus on these aims, the study restricts the breadth of its scope to the social brain and sub-networks described in the literature, rather than the whole brain.

After a discussion of gray matter changes in adolescence and their relationship to social information processing, the present study will introduce the structural covariance analysis approach and how it compares to other brain connectivity methods, specifically resting-state functional magnetic resonance imaging (resting-state fMRI) and diffusion tensor imaging (DTI). In Chapter 2, the specific methodology used in this study will be discussed in further detail, including the extraction of morphology metrics and the application of graph theoretic concepts. Findings are then presented for two separate network properties (cost and efficiency, discussed in the next chapters), for 1) maturation, 2) resistance to peer influence, 3) rejection sensitivity, 4) behavioral inhibition of automatic reactions to social stimuli, and 5) a non-social cognitive functioning measure. Chapter 4 discusses these results in context, and provides avenues for further research.

Gray matter changes in adolescence

Quantifying gray matter (GM) morphology in the living human brain continues to pose a challenge (Alexander-Bloch et al., 2016), but three MRI-derived metrics have been used more widely – GM density, cortical thickness, and GM volume. GM density refers to the probability that a voxel classifies as gray matter (Chung, 2013; Thompson et al., 2001). Cortical thickness refers to the distance between the outer (pial/cortical) surface of the cortex and its inner (gray/white matter) surface (Fischl & Dale, 2000; MacDonald, Kabani, Avis, & Evans, 2000). Finally, GM volume estimates the amount of GM that lies between these two cortical surfaces, and is a product of cortical area and thickness (Winkler et al., 2010). Among these metrics, cortical thickness and GM volume are among the most well-replicated MRI markers of macroscopic development (Giedd & Rapoport, 2010) and have been successfully used in

previous research to map covariance in brain networks (Vértes & Bullmore, 2015). Since gray matter volume is a function of surface area and cortical thickness in cortical areas, and these two metrics are believed to be driven by different underlying mechanisms (Vijayakumar et al., 2016) and have been shown to be genetically and phenotypically independent (Winkler et al., 2010), it is important that gray matter volume and cortical thickness metrics are not viewed as interchangeable descriptors of brain morphology. The present study focused primarily on cortical thickness; however, gray matter volume analyses were also conducted and results are shown in the Appendix.

The large-scale and regional neuroplasticity that is observed in adolescence appears to be coordinated in some regions, but uncoordinated in others. For instance, a longitudinal study of individuals between 4 and 22 years of age found similar change trajectories in GM volume in frontal and parietal regions, peaking around 10-12 years of age, but different trajectories in the temporal lobes, where GM volume peaked in late adolescence, and in the occipital lobe, where volume increased linearly over the studied age range (Giedd et al., 1999). Furthermore, across the cortex, GM thickness is higher during childhood and lower in early adulthood, with regional differences in change trajectories over the course of adolescence (Zhou et al., 2015). Developmental trajectories across the lateral frontal, lateral temporal, parietal and occipital cortices follow a cubic trend, with an increase in cortical thickness during childhood followed by a decrease during adolescence and stabilization during adulthood (P. Shaw et al., 2008). These patterns of change across brain regions have been theorized to relate to social cognitive processes that depend on these regions (Choudhury, Blakemore, & Charman, 2006). The present study will extend this line of research through a network-based approach that takes into account morphological properties across a range of regions.

A recent comprehensive review of tract-tracing, functional connectivity, electrophysiology and lesion neuropsychology literature related to social cognition and the social brain suggests the existence of several large-scale brain networks that subserve specific processes (Bickart, Dickerson, & Feldman Barrett, 2014), including a *social perception* network, an *affiliation* network, an *aversion* network, a *mentalizing* network and a *mirror* network.

Gray matter development has been documented in some of the regions considered to belong to the social brain. For instance, in the amygdala, which is identified as a social brain hub region that participates in social perception, affiliation and aversion processes (Bickart et al., 2014), volume was found to increase linearly with age between 5 and 18 years (Giedd et al., 1996). In the insula, which is viewed as a component in the aversion network in (Bickart et al., 2014) but whose role may be more nuanced (Brooks & Tracey, 2007; Craig, 2009; Smith, Steinberg, & Chein, 2014), cortical thickness decreases linearly with age in anterior portions, but follows a quadratic and cubic fit in the body and posterior portions, respectively (P. Shaw et al., 2008). The anterior cingulate cortex, whose sub-structures participate in affiliation (rostral) and aversion (caudal) based on the Bickart et al.(2014) review, follows a quadratic trajectory in its cortical thickness development (P. Shaw et al., 2008), while the lateral orbitofrontal cortex (perception network; Bickart et al., 2014) follows a cubic trajectory. These findings are an important step towards understanding the anatomy that underlies social cognition, and highlight the complexity that needs to be considered in the study of brain networks whose patterns of coordinated activity or anatomical covariance may not be immediately apparent from a region-centric approach.

Neural connectivity approaches

Researchers have increasingly recognized the importance of studying the brain at a network level, and the three most widely used approaches for doing so are resting-state functional magnetic resonance imaging (resting-state fMRI), diffusion tensor imaging (DTI) and more recently, the novel approach of studying structural covariance. Below is a brief overview of research to date related to the neural development of brain networks as measured through these different modalities and a consideration of the convergent evidence they provide.

DTI. Ongoing maturation of inter-regional white matter connectivity during adolescence was noted in a large study of 114 healthy participants between ages 8 and 28 years, particularly in fibers connecting prefrontal regions with subcortical areas (Asato, Terwilliger, Woo, & Luna, 2010). This finding may potentially provide an anatomical substrate for the ability to apply top-down cognitive control over affective- and reward-related processing (Asato et al., 2010). In the social brain, particularly with regard to affiliative behavior, white matter structural connectivity between the amygdala, the orbitofrontal cortex and the anterior temporal lobe was strongly related to the number of friends in female adolescents' and adults' social support networks, while amygdala – temporo-parietal junction connectivity did not explain a significant portion of this variance (Hampton, Unger, Von Der Heide, & Olson, 2016). Studies such as these suggest that white matter tracts that are important for cognitive control of emotion continue to mature over adolescence, and play a role in social behavior. However, establishing such direct connections, while increasing the speed of signal transmission, may also raise wiring and/or metabolic costs. In a recent review of research on the economy of brain network organization, Bullmore and Sporns (2012) suggest that the cost of developing and maintaining white matter connections, and the speed with which signals travel across those tracts, increase with wiring volume, which is

proportional to the distance of inter-neuronal connections (Chklovskii, 2004) and axon diameter (Niven & Laughlin, 2008). Thus, with the increased development of long-range connections, more distant or widely distributed brain regions can more easily participate in information processing. Based on these findings, it would be expected that functional networks would also show stronger connectivity between more distant regions with maturation.

Resting-state fMRI. Over the course of development from childhood to adulthood, functional connections among cortical regions become more prominent (for a review, see Uddin, 2010). Despite DTI findings showing strengthening anatomical connections between prefrontal and subcortical areas with maturation (Asato et al., 2010), functional connections between cortical and subcortical regions become weaker and less abundant (Uddin, 2010). In addition, maturation also involves a shift towards more hierarchically organized networks, with more regions involved in larger and longer-distance clusters of activity, as well as weaker short-range connections and stronger long-range connections (Fair et al., 2009). The comparison between DTI and resting-state fMRI findings is interesting, as it suggests that there may not be a direct correspondence between anatomical and functional connectivity.

Structural covariance. Structural covariance is a relatively new approach that seeks to leverage the structural images that are typically collected from all participants in neuroimaging studies, but that are oftentimes used only for registering functional data. The benefit of this approach is that it reduces the time burden on the participant, as it does not require additional scans, as well as the cost burden on the researcher, and ample datasets are already freely available through various open-access databases (e.g., http://www.oasis-brains.org/). In this approach, networks are

typically studied through either seed analysis, principal component analysis or graph analysis. Unlike fMRI and DTI networks, inter-regional connectivity in structural covariance networks cannot be easily estimated within the individual subject, although some studies have begun exploring such approaches (e.g., Saggar et al., 2015). Accordingly, structural covariance networks are typically based on inter-regional correlations derived from groups of subjects (Alexander-Bloch, Giedd, et al., 2013).

It is believed that anatomical features that covary are also functionally connected with each other (Worsley, Chen, Lerch, & Evans, 2005), either through direct anatomical projections or through more indirect and functionally-dependent routes. Several studies have shown such a structure-function relationship. For instance, in a large cross-sectional sample of 292 children and adolescents, areas whose cortical thickness had the highest number of associations with other cortical areas tended to be regions known for their integrative functions (i.e., the association cortices; Lerch et al., 2006). In addition, cortical thickness covariance among language-processing regions revealed a relationship pattern similar to the fiber pathway that connects these areas (Lerch et al., 2006). Another study examined the relationship between cross-sectional cortical thickness covariance and covariance of longitudinal rate of change in regional cortical thickness per year during adolescence (Alexander-Bloch, Raznahan, Bullmore, & Giedd, 2013). Here, the brain was divided into 360 regions, and for each region in each subject, the rate of change (thickness/year) was estimated based on within-subject longitudinal scans. Maturational covariance was calculated using these rate of change values. Results showed that cross-sectional structural covariance networks had a very similar topology with maturational networks, supporting the notion that regions that have similar morphologies also grow and shrink at a coordinated rate.

A recent study of structural covariance using voxel-based morphometry further suggests that structural covariance may also be informative for understanding social information processes. Shaw et al (2016) explored the maturation of face processing from a neuromorphological covariance perspective in a longitudinal study of adolescents between 10 and 15 years of age. The authors found that trajectories of structural covariance paralleled the developmental increases in functional covariance among extrastriate (V2/V3, LOC, FFA and posterior STS) and frontal cortical regions (mid-dorsolateral frontal cortex and mid-ventrolateral frontal cortex, and PMC). Furthermore, their findings suggest that greater functional and structural integration of extra-striate and frontal cortices over time could be related to improved discrimination between emotional facial expressions (D. J. Shaw et al., 2016).

Thus, statistical correlations between morphological measurements across brain regions are likely to reflect synchronized changes between these regions as a result of anatomical and functional connections (Vértes & Bullmore, 2015). Although the exact mechanisms that drive these correlations are not fully understood, covariance studies have not only advanced our understanding of the morphological organization and development of brain structures, but they have also demonstrated initial clinical utility. For instance, one study found that not only did early-blind and sighted individuals differ with regard to structural covariance between areas involved in visual processing, but structural covariance metrics also strongly predicted behavioral performance in the early-blind group (Voss & Zatorre, 2015). Another recent study used the features of individual subjects' cortical thickness-derived networks (e.g., nodal degree, clustering coefficient) and found that, when entered into a classification algorithm, these network features discriminated between cognitively impaired individuals and healthy controls with a 70% sensitivity and 69% specificity, respectively (Raamana, Weiner, Wang, & Beg, 2015).

Together, the recent findings using the gray matter structural covariance approach demonstrate that this technique offers an additional avenue for understanding brain structure, function, and maturation, and offers an approach with unique benefits that can be used in parallel with white matter tract analyses and functional MRI.

Structural covariance graphs

The social brain has not been studied at a complex network level using a structural covariance approach. The few studies that have examined structural covariance within the social brain have only assessed a small number of brain regions. However, because this network is believed to be rather complex, encompassing multiple sub-networks, it may benefit from an analytic approach that can shed light on characteristics of complex networks (enacting such an analysis is the central goal of the present study).

One such approach is graph theory. Graph theory defines networks as sets of nodes and the edges between them (Bullmore & Sporns, 2009). In structural covariance networks, the nodes represent brain regions, and the edges between them represent the group-level statistical correlation between the regions' GM morphology (e.g., volume or thickness). Information from nodes and edges can then be computed to form indices characterizing the entire network, or sub-parts of the network. While many metrics are available, node degree, path length, and clustering coefficient are among the more widely used (Bullmore & Sporns, 2009) and are the building blocks for more complex network metrics. Node degree – the most fundamental network measure – refers to the number of correlations that link a node to the rest of the network. Path length is a measure of efficiency within the network, and is defined as the minimum number of

edges that must be traversed to go from one node to another. Short path length is indicative of greater efficiency, and in the context of covariance networks, shorter path lengths are indicative of more direct interregional correlations, while longer path lengths may suggest mediated relationships between regions. While path length is a measure of network integration, the clustering coefficient is a measure of segregation (i.e., the extent to which nodes in a network cluster together, or the probability that the adjacent vertices of a vertex are connected) and serves as the basis for higher-level metrics that identify and characterize 'communities' of nodes.

It is important to stress here that structural covariance networks derived using graph theoretical approaches are statistically based, and thus edges between nodes may or may not reflect direct anatomical links (e.g., white matter tracts) between brain regions. Because graph theory is useful in assessing the relationships between a large number of elements and has often been used to characterize different types of connections within a given network (e.g., relationships between people in social networks, white matter fibers between regions in diffusion tensor MRI), its terminology often implies connectivity. While “graph” and “network” are terms used interchangeably in this dissertation, the relationships mapped using graph theory should be understood as statistical covariance, and an interpretation of these graphs as biological networks should therefore be done within this context.

Aims

Aim 1: Structural covariance changes in the social brain across development

Aim 1 used MRI to explore the neuromorphological covariation changes that occur in the social brain network between adolescence and adulthood. To assess structural covariation at the network level, the social brain network was conceptualized as a mathematical graph in which

morphological correlations in cortical thickness represent links between individual regions. This graph theoretical approach allowed a large-scale assessment of the morphological similarity between all pairs of regions at different stages in development. Specifically, properties of structural covariance graphs in the social brain and its sub-networks were assessed at different stages of maturation – adolescence (ages 13-17 years), young adulthood (18-21 years) and adulthood (22-25 years) – specifically with regard to network cost and efficiency (these concepts are discussed in more detail in Chapter 2). It was hypothesized that increased functional specialization within the social brain as a result of maturation (Bickart et al., Dickerson, & Feldman Barrett, 2014; Johnson et al., 2009) would also be reflected by increased segregation in the network.

Aim 2: Aim 2 was to link the properties of these structural covariance graphs (graph cost and efficiency, discussed in more detail in Chapter 2) to self-reported and behavioral aspects of social information processing, specifically resistance to peer influence (Aim 2.1), rejection sensitivity (Aim 2.2), and the control of automatic reactions to socially relevant stimuli (Aim 2.3). Furthermore, in order to assess the specificity of these results to social stimuli, network cost and efficiency were also assessed in relation to a non-social measure of cognitive functioning (Aim 2.4).

Aim 2.1: Resistance to Peer Influence

Functional connectivity studies have shown that a number of cortical regions involved in decision making and social information processing are more tightly interconnected in adolescents who are more effective at resisting peer influence (Grosbras et al., 2007).

Furthermore, female adolescents who are high in resistance to peer influence also show greater morphological similarity between areas in premotor and prefrontal networks than female adolescents who score low in their ability to resist the influence of their peers (Paus et al., 2008). Therefore, Aim 2.1 hypothesized that, independently of age, structural covariance in the social brain network would also increase as a function of the ability to resist peer influence.

Aim 2.2: Rejection Sensitivity

With the exception of one study reporting regional differences in cortical morphology between adults high and low in rejection sensitivity (Sun et al., 2014), research studies have not examined how structural covariance between the regions of the social brain relates to rejection sensitivity.

Findings from functional MRI studies have identified a number of regions of the social brain that are involved in processing social rejection stimuli, including the posterior cingulate cortex, dorsal anterior cingulate cortex, medial frontal gyri, middle frontal gyri, right inferior frontal gyrus, precentral gyrus and parahippocampal gyrus, with increased activation in lateral prefrontal cortex and dorsal superior frontal gyrus in low rejection-sensitive adults compared to their high-rejection sensitive counterparts (Kross, Egner, Ochsner, Hirsch, & Downey, 2007). In addition, the experience of social exclusion is associated with activity in a network of regions that include the dorsal anterior cingulate cortex, the insula, and the right ventral and ventrolateral prefrontal cortices in adults (Eisenberger, 2003; Eisenberger, Way, Taylor, Welch, & Lieberman, 2007), and the insula, right ventral prefrontal cortex, subgenual anterior cingulate cortex, ventral striatum and amygdala in adolescents (Masten et al., 2009). However, negative relationships were found during social exclusion between prefrontal regions and the ventral striatum on the

one hand, and insula, anterior cingulate cortex and amygdala on the other (Masten et al., 2009). Since structural covariance has been discussed predominantly in the context of positive functional co-activation patterns, the effect of inhibitory patterns of activity on structural covariance is unclear and may weaken the covariance between structures. In Aim 2.2, it was therefore hypothesized that higher rejection sensitivity would be associated with greater structural covariance in the social brain.

Aim 2.3: Behavioral inhibition in response to socially relevant stimuli

In Aim 2.3, the goal was to test whether network properties of the structural social brain network were associated not only with relatively stable trait-level characteristics, but also with behavioral effects. To this end, data from an "emotional Go-NoGo" task were used. This task is an experimental paradigm that tests behavioral inhibition in response to socially relevant stimuli, and has been validated (Schulz et al., 2007) and used in previous studies (e.g., Hare et al., 2008; Tottenham, Hare, & Casey, 2011). Because this aim was exploratory in nature, no predictions were made regarding the direction of the effect.

Aim 2.4: Cognitive functioning

Finally, to assess the specificity of findings to social information processing, a non-social measure was also examined. Specifically, participants completed the Wechsler Abbreviated Scale of Intelligence (WASI) Matrix Reasoning sub-test (Wechsler, 2011). It was hypothesized that if structural network characteristics in the social brain were primarily associated with social information processing, effects on this non-social measure would be weaker compared to social measures.

CHAPTER 2

METHOD

Subjects

Subjects were 217 healthy right-handed individuals between the ages of 13 and 25 years – 77 adolescents (ages 13-17 years), 73 young adults (ages 18-21 years), and 67 adults (ages 22-25 years) – recruited at two sites, Cornell University and UCLA, as part of a larger neuroimaging study run by the MacArthur Foundation Research Network on Law and Neuroscience. Subjects were recruited from the local communities and had no history of mental illness, neurologic disorders, or use of psychotropic medications. Protocols were approved by each site's Institutional Review Board. Prior to participation, all adult subjects were consented, and adolescent subjects provided assent and parental consent. All subjects were evaluated for MRI contraindications by the research staff, and underwent MRI scans at either Cornell's (New York, NY) or UCLA's (Los Angeles, CA) neuroimaging facilities. All subjects received monetary compensation for their participation.

Table 1 Demographics

	Adolescents (13-17 years; N=77)	**Young Adults (18-21 years; N=73)**	**Adults (22-25 years; N=67)**
Age: M (SD)	15.14 (1.44)	19.45 (1.12)	23.4 (1.09)
Gender	40 F / 37 M	35 F / 38 M	36 F / 31 M
Race / Ethnicity			
African-American	14	11	15

Asian	3	10	16
White	25	30	16
Hispanic/Latino	23	9	8
Other	7	8	4
NA	5	5	8

In Aim 2, the sample size was reduced as a result of measure-specific missing data. Thus, of the full sample of 217 subjects, RPI analyses (Aim 2.1) included 198 subjects, RSQ analyses (Aim 2.2) included 153 subjects, emotional Go-NoGo analyses (Aim 2.3) included 171 subjects, and WASI analyses (Aim 2.4) included 195 subjects.

Self-Report Measures

In addition to the MRI protocol, subjects were asked to complete a battery of self-report questionnaires that included the Resistance to Peer Influence questionnaire (RPI; Steinberg & Monahan, 2007) and the Rejection Sensitivity Questionnaire (RSQ; Downey & Feldman, 1996).

The *Resistance to Peer Influence* questionnaire consists of 10 pairs of statements from which participants are asked to select the statement that best describes them (e.g. “Some people go along with their friends just to keep their friends happy” BUT “Other people refuse to go along with what their friends want to do, even though they know it will make their friends unhappy”). Participants then rate whether the description is “Really True” or “Sort of True” and responses are coded on a 4-point scale, ranging from “really true” for one descriptor to “really true” for the

other descriptor, and averaged. Higher scores indicate greater resistance to peer influence (Steinberg & Monahan, 2007).

The *Rejection Sensitivity Questionnaire* (Downey & Feldman, 1996) is an 18-item self-report measure that assesses the degree of concern or anxiety about a range of interpersonal situations and the individual's expectations about the likelihood that the other person(s) would respond in an accepting fashion. Ratings are made on a 6-point scale ranging from very unconcerned (1) to very concerned (6), and from very unlikely (1) to very likely (6) respectively. The RSQ has high internal reliability ($\alpha = .83$) and high test–retest reliability after 2-3 weeks (r=.83) and after 4 months (r=.78) (Downey & Feldman, 1996). Higher scores on the RSQ indicate greater rejection sensitivity.

Experimental Measure

"Emotional" Go-NoGo. In addition to the trait-focused measures described above, an experimental task was used to assess subjects' ability to inhibit automatic responses to socio-affective stimuli. The Go-NoGo task is a reliable and robust behavioral measure of cognitive control across multiple age groups (Casey et al., 1997; Durston et al., 2006), with findings suggesting that children make more false alarm errors (i.e., demonstrate weaker cognitive control) relative to adults. In the present study the task was modified to examine cognitive control in the presence of emotional information. Thus, participants were asked to control their impulses to transient social cues (calm, fearful and happy emotional expressions) under three anticipatory emotional contexts: threat (aversive noise), excitement (reward) and neutral (no anticipation).

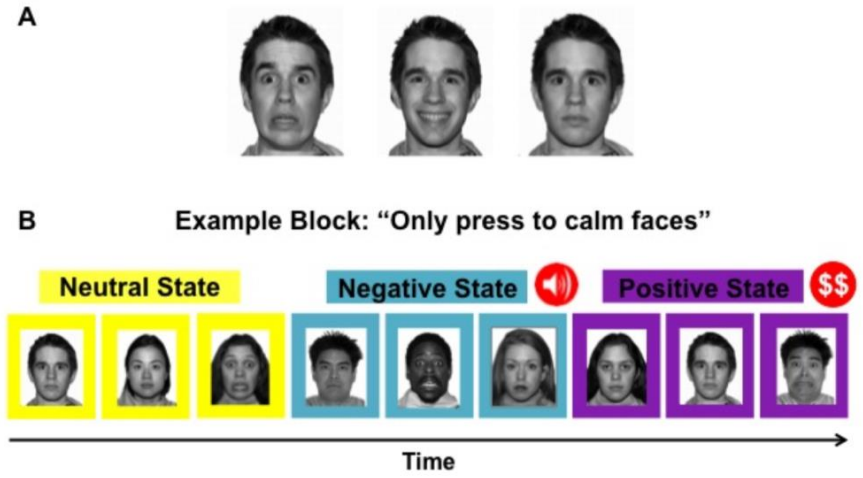

Figure 1: Emotional Go-NoGo task design and presentation.

Impulse control task to transient social cues under sustained neutral, negative (threat: noise) and positive (excitement: reward) emotional contexts. Emotional contexts and six primary social cue trial types of fear/calm, calm/fear, fear/happy, happy/fear, calm/happy, and happy/calm were presented in a pseudo-randomized order. Image reproduced from Rudolph, et al. (unpublished manuscript).

A more detailed description of this task can be found in previous reports (Rudolph et al., unpublished manuscript, Cohen et al., 2016). Stimuli were presented in a pseudorandomized order, with a total of 60 no-go and 168 go trials presented across all three cue types for each emotional state. Because this task was part of a larger study, a portion of the participants underwent a peer condition where a theoretical peer was present; for the purposes of the present study, peer condition was controlled statistically. As in previous research (Tottenham et al., 2011), the D-prime measure was operationally defined as a primary index of behavioral inhibition. D-prime is an index of performance accuracy on this task, accounting for response

bias, and was computed by subtracting the z-transformed false alarm rate from the z-transformed hit rate (Tottenham et al., 2011). False alarm rate and hit rates were calculated as the proportion of total possible events for each type.

Cognitive Functioning Measure

The *Wechsler Abbreviated Scale of Intelligence* (WASI; Wechsler, 2011) Matrix Reasoning subtest was administered as part of a bigger test battery, and was used in this study as a non-social comparison measure and an index of cognitive functioning. This subtest measures nonverbal abstract problem-solving, inductive reasoning and spatial reasoning. The WASI is a widely used measure of cognitive functioning. Here, T-scores were used as an index of cognitive ability.

MRI Data Acquisition

Imaging data were collected on 3T Siemens Magnetom Trio Tim scanners at both UCLA and Cornell. Although both sites used the same hardware, analyses controlled for site to account for any potential site differences in scanning parameters or image processing. Phased-array head coils were used for all scans. A T-1 weighted magnetization-prepared-rapid-acquisition gradient echo (MPRAGE) scan was collected in the sagittal plane at the beginning of each scanning session.

Measurement of Gray Matter Volume and Thickness

All cortical thickness and volume analyses were performed using the FreeSurfer cortical parcellation pipeline (http://surfer.nmr.mgh.harvard.edu/fswiki/recon-all; Massachusetts General

Hospital, Boston, MA). This software and procedure have been validated in the literature (Dale, Fischl, & Sereno, 1999; Fischl, Salat, et al., 2004; Fischl & Dale, 2000). Processing is completed in the following sequence (Dale et al., 1999; Fischl & Dale, 2000; Fischl, Sereno, & Dale, 1999; Fischl, Sereno, Tootell, & Dale, 1999): motion correction, intensity normalization, standardization into Talairach space, skull stripping, volume registration, white/gray matter segmentation and boundary determination, surface reconstruction, spherical mapping, inflation, and registration, and cortical parcellation and subcortical segmentation. This automated process generates thickness and volume measurements across the cortex, as well as an estimate of total intracranial volume. To increase processing speed, the parcellation pipeline was processed on Temple University's Linux-based 64-processor High Performance Computing platform using GNU parallel (Tange, 2011) for parallelization across processors.

Quality assurance was conducted via visual inspection of the FreeSurfer pipeline output using the tools provided for editing in FreeSurfer (http://freesurfer.net/fswiki/FreeviewGuide/FreeviewWorkingWithData/FreeviewEditingaRecon). Of the 263 subjects whose data were processed, 5 were excluded from analysis due to poor image quality and 40 (15%) were corrected and reprocessed. Of the 40 subjects whose data required corrections, 3 had holes in the white matter surface, 36 had incorrectly classified white matter, and 2 subjects needed corrections to the pial surface. Data were corrected manually following the guidelines provided by FreeSurfer, and reprocessed through the pipeline. Of the 40 subjects, reprocessing with corrections was unsuccessful for 3 subjects, who were excluded from subsequent analyses. Additionally, 1 subject reported a diagnosis of clinical depression symptoms and was therefore not included in analyses. The sample after quality assurance consisted of 255 individuals. Further, while the full dataset included four age groups (children,

adolescents, young adults and adults) the current analyses focused only on adolescents, young adults and adults, and therefore children under the age of 12 (N=38) were excluded from analysis. The final sample, after quality assurance and exclusions, was 217 individuals.

Parcellation of the cortical regions was done using the Desikan-Killiany Atlas (Desikan et al., 2006; Fischl, van der Kouwe, et al., 2004), and segmentation of subcortical structures was done using a previously described atlas (Fischl et al., 2002), both of which are part of the FreeSurfer standard package. For a more nuanced analysis of the social brain, the labels for the posterior superior temporal sulcus, the temporo-parietal junction and the anterior temporal pole were obtained from a study of developmental changes in the structure of the social brain in adolescence (Mills et al., 2014). These labels were drawn based on the same surface template as the Desikan-Killiany atlas ("fsaverage"). Furthermore, because sub-sections of the insula (dorsal anterior, ventral anterior, posterior) were not part of the Desikan-Killiany atlas, but have been found to be important during development and in social information processing, thickness and volume measurements for these regions were extracted using pre-existing custom masks created from the Desikan-Killiany Atlas in FreeSurfer (Smith, 2015), where anterior and posterior regions of the insula were defined along the anterior commissure, and ventral and dorsal areas of the anterior insula were defined based on recent meta-analyses (Chang, Yarkoni, Khaw, & Sanfey, 2013; Deen, Pitskel, & Pelphrey, 2011).

Based on research by Bickart and colleagues (2014) and Blakemore and colleagues (2008), the following sub-networks of the social brain were also analyzed individually in the present study (Figures 2 and 3): 1) a social *perception* network, consisting of the lateral orbitofrontal cortex (lOFC), the anterior temporal pole (ATP), the fusiform gyrus (FFG), the posterior superior temporal sulcus (pSTS), and the amygdala (AMY); 2) an *affiliation* network,

consisting of the medial oribitofrontal cortex (mOFC), the anterior temporal pole (ATP), the entorhinal cortex (ERC), the parahippocampal cortex (PHC), the rostral anterior cingulate cortex (rACC), the nucleus accumbens (nACC), and the amygdala (AMY); an *aversion* network, consisting of the caudal anterior cingulate cortex (cACC), the dorsal anterior insula (dAI), ventral anterior insula (vAI), posterior insula (PI), the putamen (PUT) and the amygdala (AMY); and a *mentalizing/mirror* network, consisting of the dorsolateral prefrontal cortex (dlPFC), the posterior cingulate cortex (PCC), the temporoparietal junction (TPJ), the posterior superior temporal sulcus (pSTS). A number of brain regions are represented in more than one sub-network, to reflect their activation across different functional domains. While these sub-networks include both cortical and subcortical structures, the main analyses presented in this dissertation include only cortical thickness values, and therefore only cortical structures. Findings from volume-based networks are shown in the Appendix.

Finally, all individual subjects' thickness and volume measurements were compiled and exported from FreeSurfer for further analyses in the R statistical package (R Core Team, 2014).

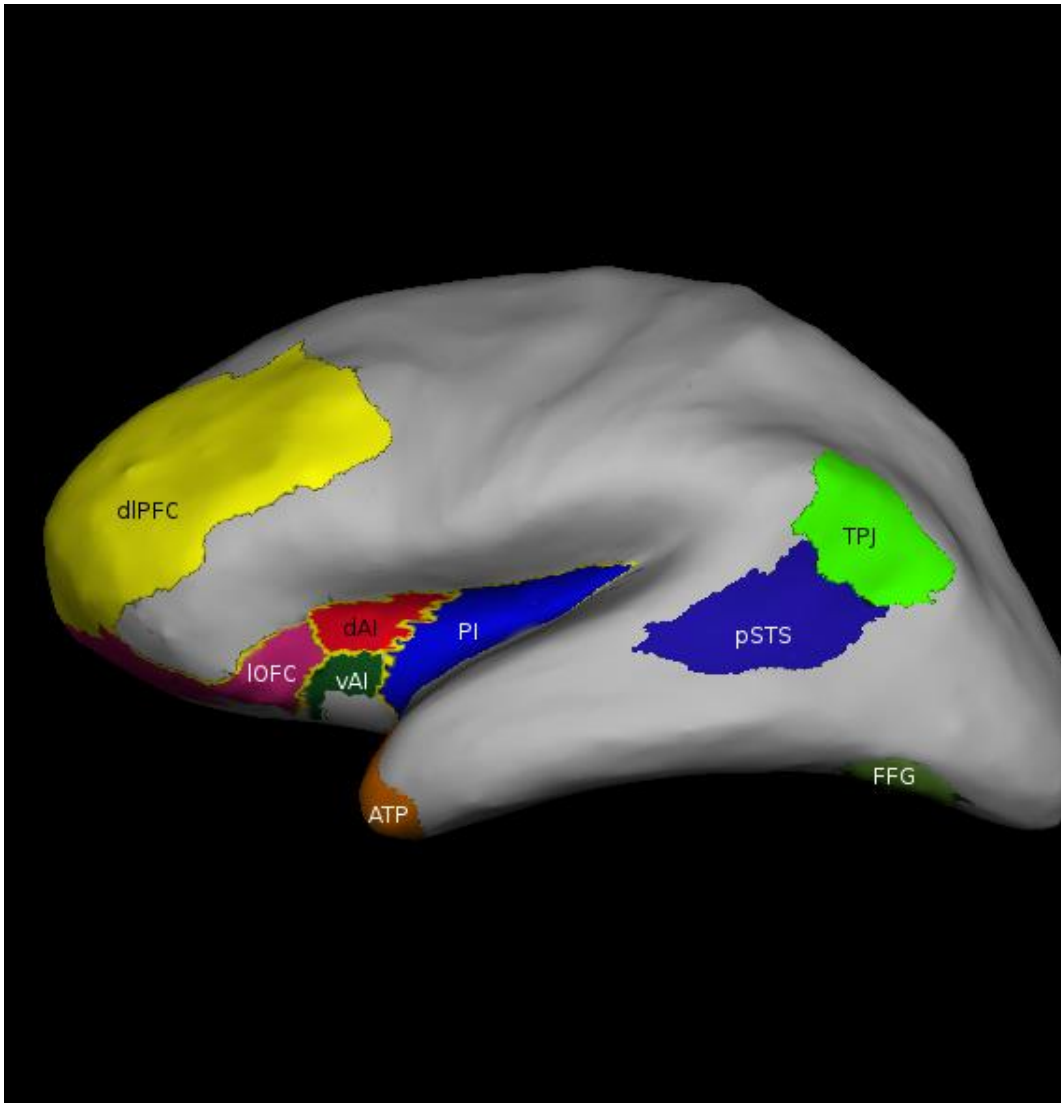

Figure 2: The Social Brain (lateral view)

dlPFC = dorsolateral prefrontal cortex; lOFC = lateral orbitofrontal cortex; dAI = dorsal anterior insula; vAI = ventral anterior insula; PI = posterior insula; ATP = anterior temporal pole; pSTS = posterior superior temporal sulcus; TPJ = temporo-parietal junction; FFG = fusiform gyrus.

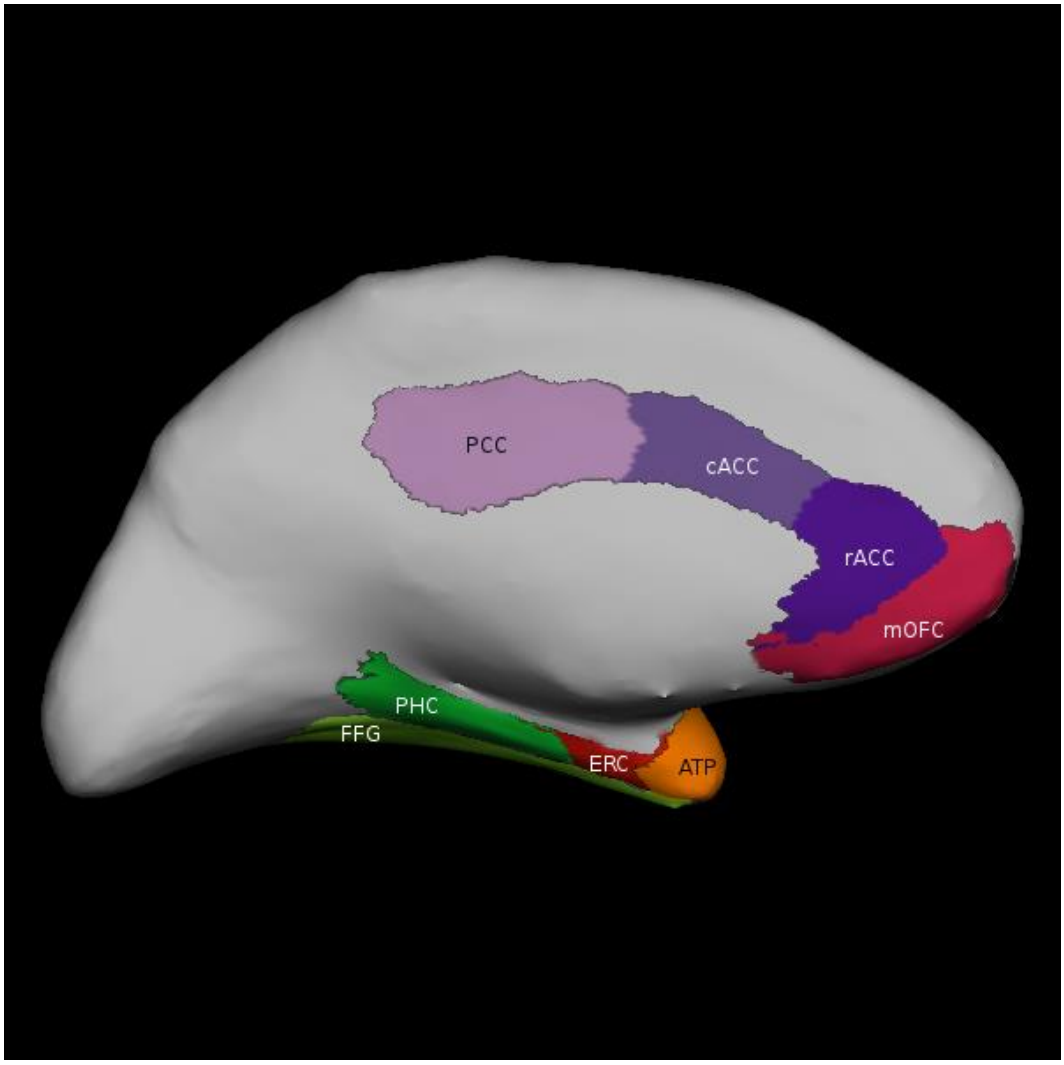

Figure 3: The Social Brain (medial view)

mOFC = medial orbitofrontal cortex; rACC = rostral anterior cingulate cortex; cACC = caudal anterior cingulate cortex; PCC = posterior cingulate cortex; ATP = anterior temporal pole; ERC = entorhinal cortex; PHC = parahippocampal cortex; FFG = fusiform gyrus.

Graph Theoretical Analysis

Construction of Structural Covariance Matrix

All data processing and statistical analyses were completed using R (R Core Team, 2014). To examine the social brain network specifically, morphological values were extracted

bilaterally in the following brain regions: lateral OFC, fusiform gyrus, rostral ACC, medial OFC, entorhinal cortex, parahippocampal gyrus, caudal ACC, posterior cingulate cortex, PFC, putamen, nucleus accumbens, amygdala, anterior temporal cortex, posterior superior temporal sulcus, temporo-parietal junction, posterior insula, dorsal anterior insula, and ventral anterior insula. For cortical thickness measurements, residualized values were obtained for each brain region of interest after controlling for site and gender. Separate structural covariance matrices were constructed for each age group (adolescent, young adult, adult) and for each type of correlation (positive, negative, combined).

In each matrix, correlation coefficients and p-values for multiple biweight midcorrelations were computed based on residualized values ("bicorAndPvalue" function, 'WGCNA' package for R; Langfelder & Horvath, 2008). The present study used biweight midcorrelation as a robust alternative to the Pearson correlation coefficient used in prior studies (He, Chen, & Evans, 2007a; Peng et al., 2014) because it is less sensitive to outliers. An FDR threshold of q=0.01 was then applied for thickness measurements.

Negative correlations did not survive the FDR threshold and resulted in graphs with no edges. As noted earlier, the biological significance of negative correlations in gray matter morphology is not yet fully understood. For these reasons, analyses reported here focused exclusively on graphs derived from positive correlations.

To perform a graph theoretical analysis, the R-based "igraph" software package was used (Csardi & Nepusz, 2006). The FDR-corrected structural covariance matrices obtained above were considered as undirected graphs G with N nodes and K edges, where nodes represent brain regions and edges represent undirected correlations between regions. The graph metrics reported in this study are based on previously reported graph theoretic analyses in the neuroimaging

literature, and include *small-world properties* and *network cost (density)*.

Table 2: Definitions of Network Properties

Characterstic Path Length (L_p)	The smallest number of connections required to connect one node to another, averaged over all pairs of nodes; an index of network efficiency
Node Clustering Coefficient (C_i)	The number of existing connections between a node's neighbors divided by all their possible connections
Network Clustering Coefficient (C_p)	The average clustering coefficient over all nodes
Small-worldness	A network with high C_p and small L_p
Network density	The number of edges present in the graph as a proportion of the total number of possible edges; an index of network cost

Small-world properties

Small-world properties in complex dynamic systems tend to indicate increased signal propagation speed, computational power and synchronizability (Watts & Strogatz, 1998). The brain's structural and functional systems share such small-world characteristics with other complex networks, regardless of system granularity (for a review, see Bullmore & Sporns, 2009).

A graph is considered to have small-world properties if it is highly clustered but has small characteristic path lengths (Watts & Strogatz, 1998). The clustering coefficient C_i of a node *i* reflects the number of existing connections between the node's neighbors divided by all their possible connections (Watts and Strogatz 1998). The network's clustering coefficient C_p is calculated from the average clustering coefficient over all nodes. The characteristic path length L_p is the smallest number of connections required to connect one node to another, averaged over all pairs of nodes. L_p is a measure of the extent of average connectivity or overall routing efficiency of the network.

In a small-world graph, the clustering coefficient C_p is greater than the clustering coefficient that would be observed in a random network, while the characteristic path length L_p should be comparable to the characteristic path length of a random graph. Thus, in small-world graphs, the ratio *r* between C_p / C_{random} and L_p / L_{random} is expected to be greater than 1 (Achard, 2006; He et al., 2007a; Humphries, Gurney, & Prescott, 2006).

In the present study, comparisons with values from random networks were obtained through simulation, by creating 1000 random graphs each with the same number of vertices and edges as the real graph. The clustering coefficient and characteristic path length were obtained for each of the 1000 random graphs, and an average was computed that was then used to calculate small-world properties. Furthermore, the 1000 random graphs were used in one-sample t-tests to assess whether the values obtained from each real graph produced by the data differed significantly from the range of values that would be obtained by chance, given equivalent structural constraints. Small-world properties were assessed in this study primarily to validate the obtained networks against robust findings from the literature. The two primary graph measures of interest, network cost and efficiency, are described below.

Network cost and efficiency

The simplest estimator of the physical cost (i.e., resource requirements) of a network is the graph's density, which refers to the number of edges present in the graph as a proportion of the total number of possible edges (Bullmore & Sporns, 2009). In structural networks, the density of a graph reflects the degree of covariance among the nodes within the graph, with greater density suggesting more covariance among the nodes. Given that the social brain network includes regions that are not always in close spatial proximity to one another, a high density covariance matrix suggests that even regions that are not adjacent to each other are likely to be correlated in morphology, potentially suggesting a more spatially distributed, and inclusive covariance pattern. In contrast, a low covariance density suggests a more segregated pattern of covariance within the graph, which may be more spatially localized.

As mentioned above, the characteristic path length is a measure of the extent of average connectivity or overall routing efficiency of the network.

Since structural covariance analyses are inherently group-based approaches, with a sample of individuals contributing to one overall value for each graph metric, a random sub-sampling approach was employed to support statistical comparisons across graphs. Thus, random subsamples consisting of two thirds of the original sample in each age group were drawn, their data used to inform a graph, and the resulting graph metrics were stored (including graph density). This approach was repeated 100 times, resulting in 100 sub-graphs reflecting graph properties of subsamples of subjects within each age group. These 100 sub-graphs in each age group were then used to estimate differences in graph metrics (characteristic path length, graph density) using analyses of variance (ANOVAs) and pairwise t-tests.

Cost-Efficiency Trade-Offs

Studies have shown that robust patterns of functional connectivity are induced by a combination of direct and indirect anatomical links (Adachi et al., 2012; Honey et al., 2009), and it has been suggested that wiring costs tend to increase with connection density and distance (Bullmore & Sporns, 2012). From a functional point of view, direct connections between nodes at the neural level carry the benefit of faster signal transfer, even if this comes at higher processing costs (Bullmore & Sporns, 2012). Based on the assumption that structural covariance is related to functional connectivity, it may be speculated that increased density in a structural covariance graph would correspond to a significant extent to increased density in functional connections, and thus suggest greater wiring and metabolic costs.

CHAPTER 3

RESULTS

The present study used between-group comparisons to examine changes in the social brain's structural network density and characteristic path length as a function of age (Aim 1) and as a function of social-cognitive processes (Aim 2). For the purpose of clarity, the results will be presented not by specific aims, but by graph feature (density and path length), and will be discussed in relation to each aim in the discussion section.

Data Validation

Prior to conducting graph theoretical analyses, self-report measures and whole-brain and social-brain graphs were analyzed and examined in comparison to existing findings from the literature.

Developmental Trajectories of Behavioral and Self-Report Measures

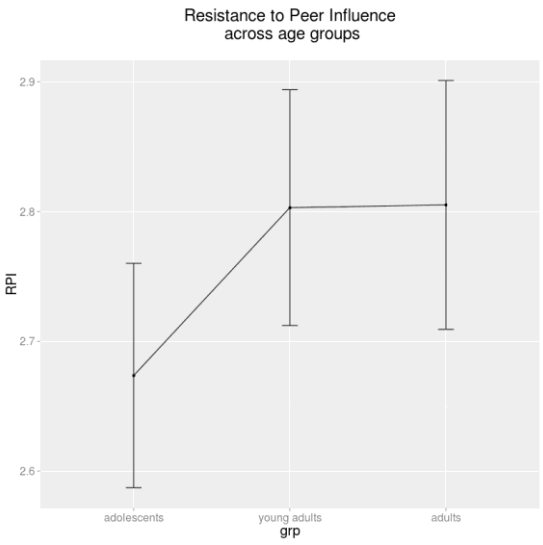

Resistance to Peer Influence.

After eliminating subjects with missing values on the RPI questionnaire, a sample of N=198 individuals was obtained. Across the three age groups studied, chi-square tests showed no significant differences on participant gender and data collection site. Therefore, data were not controlled statistically with regard to

these variables. Findings show that RPI followed a developmental trajectory that increased with age, which corresponds to findings from previous studies (Steinberg & Monahan, 2007). A between-groups analysis of variance (ANOVA) found that groups differed marginally, $F(2,195)=2.85$, $p=0.06$, with adolescents having significantly lower RPI scores ($M=2.67$, $SD=0.37$) than young adults ($M= 2.80$, $SD= 0.37$) and adults ($M=2.81$, $SD=0.37$), p's=0.04. The young adult and adult groups did not differ significantly from each other.

Rejection Sensitivity. After excluding missing cases, the sample for RSQ analyses was smaller than the sample for RPI analyses (N=153). No significant between-group differences were found, $F(2, 150)=0.13$, $p=0.88$. Group-wise comparisons showed no significant differences between adolescents ($M= 8.73$, $SD=3.05$), young adults ($M=8.46$, $SD= 2.86$) and adults ($M=8.71$, $SD=2.89$). While greater rejection sensitivity might be expected in younger age groups given the increased importance of social relationships during this time, the maturational trajectory of rejection sensitivity using the RSQ between adolescence and adulthood has not yet been documented in the literature.

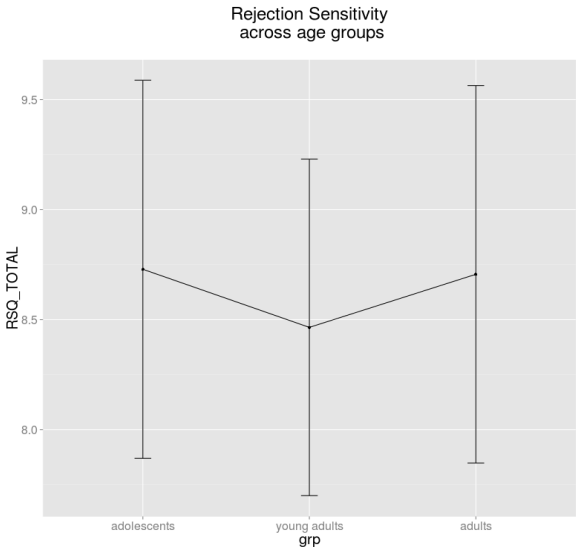

Emotional Go-NoGo. After excluding missing cases and cases affected by a programming error, data from 171 subjects were available for this behavioral task. D-prime values were averaged across arousal conditions (positive, negative and neutral) and then residualized controlling for site, because significant differences were found between sites X^2 (2, N = 171) = 6.48, p < .04.

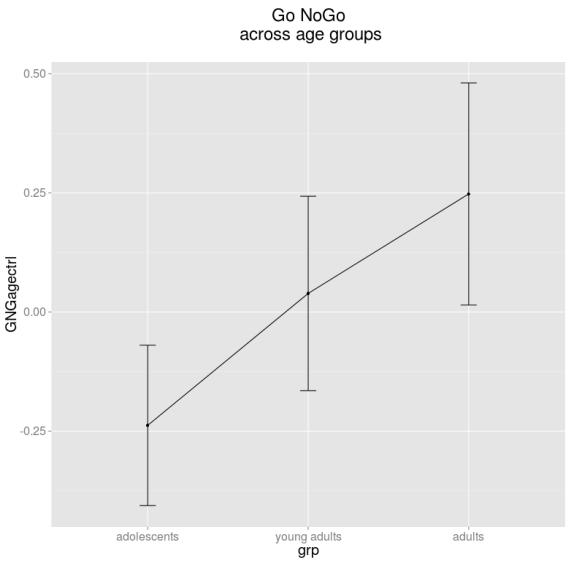

Age groups were significantly different from each other, F(2,168)=6.12, p=0.003. Pair-wise t-tests showed that the performance of adolescents on this task (M=-0.24, SD=0.67) was significantly poorer than the performance of young adults (M=0.04, SD=0.85, p=0.048) and adults (M=0.25, SD=0.85, p<.001).

WASI Matrix Reasoning. After removing missing data, 195 cases were available for analysis. The three age groups had significantly different WASI Matrix Reasoning T-scores, F(2,192)=7.05, p=0.001. Pair-wise t-tests showed that adolescents (M=51.93, SD=7.79) scored marginally lower compared to young adults (M=54.86, SD=7.56, p=0.06), who in turn did not score significantly lower than adults (M=56.73, SD=6.52, p=0.47). However, adolescents had significantly lower WASI Matrix Reasoning T-scores compared to adults (p<.001). Although similar relationships were found between

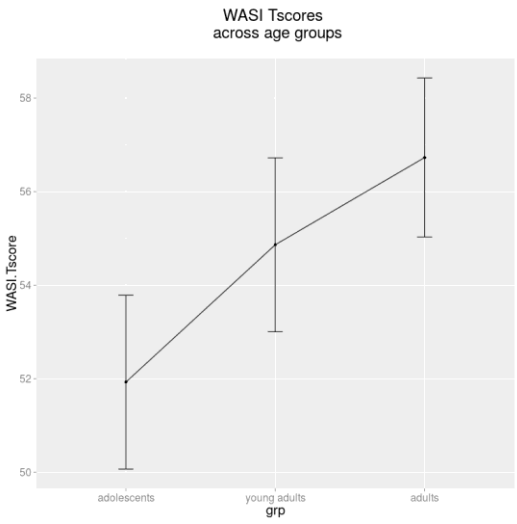

adolescents and adults in previous research using WASI raw scores (e.g., Waber et al., 2007), age and gender normed T-scores would not be expected to show developmental differences. Despite being statistically significant, the differences found in WASI T-scores in this study had a small effect size ($\eta^2 = .07$). Subsequent analyses dividing the sample into low, medium and high WASI scores took these age effects into account.

Self-report and behavioral measures used in this study were found to follow the expected maturational trajectory based on the existing literature, where available, with the exception of WASI T-scores. Additionally, the maturational trajectory of the RSQ remains to be clarified in the developmental literature. Given that the RSQ is designed to measure an individual's disposition to defensively expect, readily perceive, and intensely react to rejection, and is thought to develop from rejection experiences (Purdie & Downey, 2000), these initial findings suggest that this disposition is not a direct function of an individual's maturity, but that other factors may contribute to high or low rejection sensitivity. The present study will explore this possibility with regard to structural covariance.

Graph metrics (Small-world properties)

Before analyzing network topologies in relation to the measures of interest, the present study tested whether structural covariance networks obtained in this study display the same structural features as networks derived from other modalities. Specifically, “small-world” properties were selected for this assessment because these have been identified as a robust characteristic of complex networks, including biological networks. In addition, whole-brain and

social brain networks obtained from the data used in the present study were compared to random networks with similar properties.

Across the three age groups, whole-brain and social brain graphs differed significantly from random graphs on both clustering coefficient and average path length (all *p*'s <.001), and exhibited small-world properties (Table 3).

Table 3: Small-world properties of brain graphs derived from cortical thickness

	Brain Networks **Cortical Thickness (FDR=0.01)**	**N**	**C_p**	**L_p**	**C_p / C_{random}**	**L_p / L_{random}**	**r**
Whole Brain	Adolescents	68	0.77	1.59	1.59	1.05	1.51
	Young Adults	68	0.73	1.55	1.57	1.01	1.56
	Adults	68	0.70	1.65	1.66	1.04	1.59
Social Brain	Adolescents	30	0.66	1.91	2.14	1.11	1.93
	Young Adults	30	0.56	2.02	2.31	1.08	2.14
	Adults	30	0.48	1.89	1.70	1.07	1.59

C = clustering coefficient; L = characteristic path length; r = (Cp / Crandom) / (Lp / Lrandom).

At the whole-brain level, an ANOVA showed that small-worldness differed significantly across groups, F(2, 297) = 16.46, *p*<.001. Post-hoc Bonferroni-adjusted pairwise comparisons revealed that small-worldness was lowest among adolescent graphs (M= 1.97, SD= 0.25) and young adult graphs (M= 2.03, SD= 0.27), which did not differ between each other (p=.50), but

both were significantly lower than adult graphs (M= 2.19, SD=0.34), both p's <.001. Within regions of the social brain, an ANOVA showed that small-worldness values did not differ significantly across groups, $F(2, 297) = 1.11$, $p=.33$.

Small-world properties in the networks obtained in the present study replicate results from prior studies. In the seminal paper on small world network architecture, the graph theoretical representation of the neurons and synaptic connections of the *C. elegans* nervous system had a high clustering coefficient and a short path-length (Watts & Strogatz, 1998). In humans, a study of 124 individuals 18 - 39 years old found that the clustering coefficient of the brain's structural covariance network was approximately twice that of the clustering coefficient from similar random networks (He, Chen, & Evans, 2007). Although this ratio was smaller in the present study (ranging between 1.57 and 2.14 across developmental groups in cortical thickness graphs), the findings suggest a non-random, small world architecture of the human brain over the course of development. Previously, Sporns and Zwi (2004) had also shown small-world properties in cortical connection matrices at both the macro neuroanatomical level, as well as at the level of small cortical neuronal populations. The finding that covariance matrices across stages of development display small-world features suggests that graphs created from macro-anatomical data in the human brain adhere to established organizational principles of brain network topology.

Having established that the measures used in this study generally align with the existing literature, the following sections will focus more specifically on two main characteristics of complex networks – network cost (measured through graph density) and efficiency (measured with characteristic path length).

Graph Density (Network Cost)

1. Maturational Trajectories

It was hypothesized that in more mature groups, there would be increased segregation observed in the social brain network, i.e., decreased covariance density, potentially as a result of increased regional and network specialization. Although the specific focus of the present study was the social brain network, maturational trajectories were also obtained for the whole brain in order to contextualize findings.

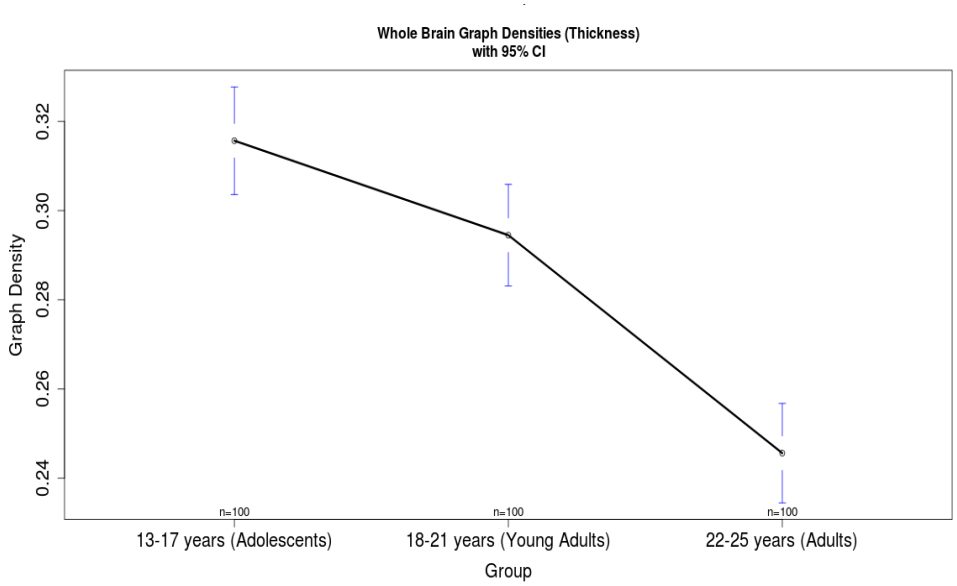

Figure 4: Graph densities across age groups (whole-brain)

Results confirmed the hypothesis, showing decreased density at both the whole-brain level, as well as at the social brain level. At the whole-brain level, an ANOVA showed that density values differed significantly across groups, $F(2, 297) = 38.23$, $p<.001$. Post-hoc Bonferroni-adjusted pairwise comparisons revealed that covariance density was highest in adolescents (M= 0.32, SD= 0.06), lower in young adults (M= 0.29, SD= 0.06, p=.03) and even lower in the adult sample (M= 0.25, SD= 0.06, p<.001).

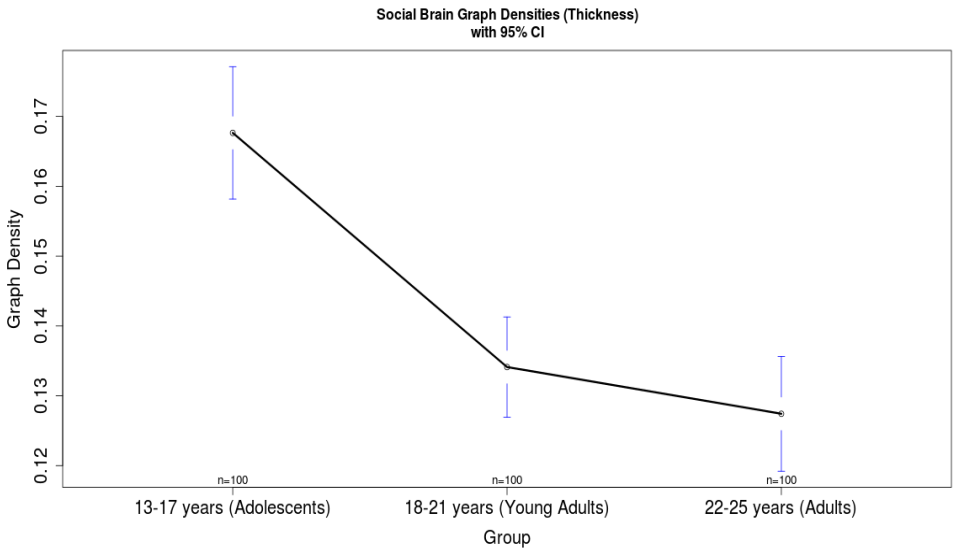

Figure 5: Graph densities across age groups (social brain)

In the social brain network, covariance densities also differed between groups, $F(2,297) = 26.26$, $p<.001$. Post-hoc tests showed that adolescents had the highest densities ($M= 0.17$, $SD= 0.05$), and differed significantly ($p<.001$) from both young adults ($M= 0.13$, $SD= 0.04$) and adults ($M= 0.13$, $SD= 0.04$), which did not differ significantly from one another.

A sub-network analysis further revealed that between adolescence and adulthood, decreases in covariance density occur in the *affiliation, mentalizing/mirror* and *perception* networks. In contrast, an increase in density was noted in the aversion network between adolescence and adulthood (see Table 4 for means and p-values). These findings suggest that across maturation, regions in the perception, affiliation and mentalizing/mirror networks become less similar to other regions within these sub-networks, while regions in the aversion network become more similar in thickness to one another.

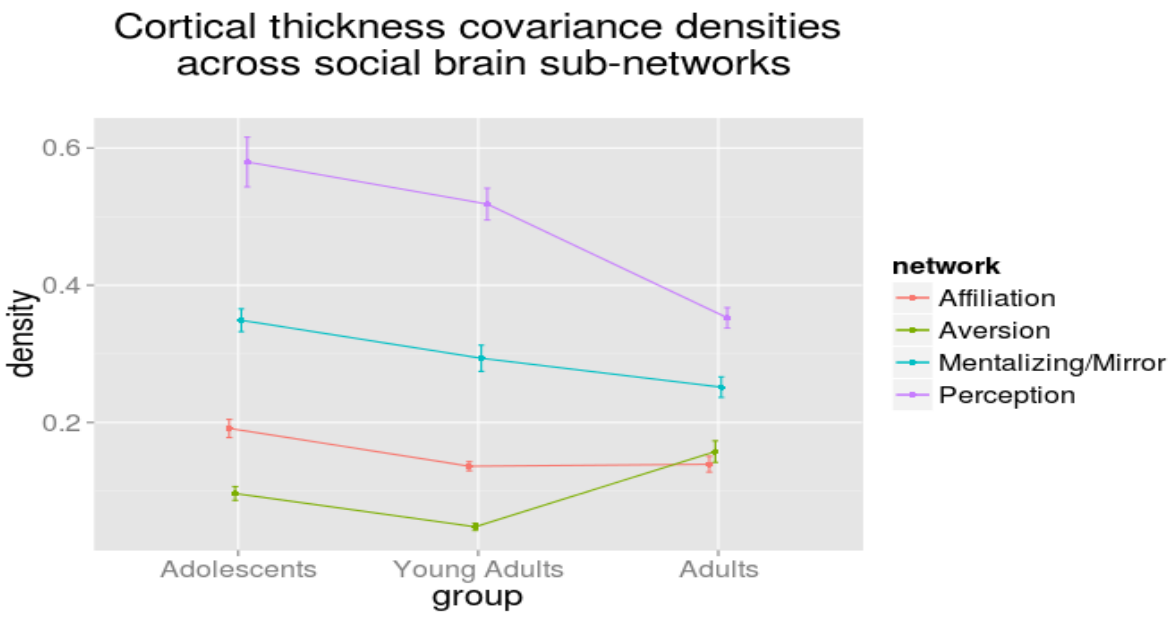

Figure 6: Social brain sub-networks – covariance densities across age groups

Table 4: Social brain sub-networks – covariance densities across age groups

	Covariance Density		
	Adolescents **M (SD)**	**Young Adults** **M (SD)**	**Adults** **M (SD)**
Perception	0.80 (0.16)[2,3]	0.75 (0.11)[1,3]	0.58 (0.12)[1,2]
Affiliation	0.36 (0.10)[2,3]	0.24 (0.06)[1,3]	0.31 (0.10)[1,2]
Aversion	0.20 (0.08)[2,3]	0.16 (0.07)[1,3]	0.37 (0.11)[1,2]
Mentalizing/Mirror	0.51 (0.09)[3]	0.53 (0.11)[3]	0.46 (0.08)[1,2]
	1 = significantly different from adolescents; 2 = significantly different from young adults; 3 = significantly different from adults; $p<.05$		

2. Resistance to Peer Influence (RPI)

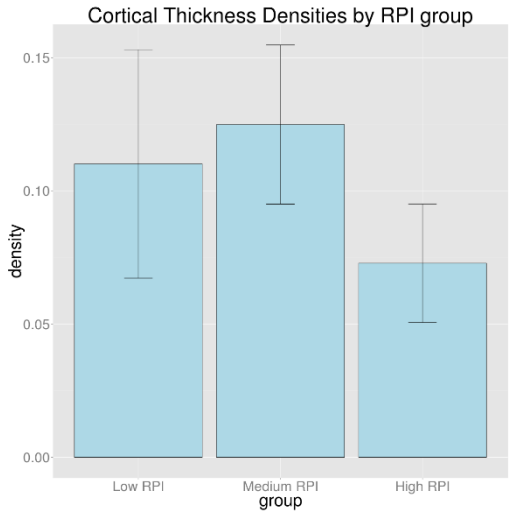

Figure 7: Social brain densities by RPI group

After eliminating cases with missing RPI data, the remaining RPI values were adjusted for site, gender and age using linear regression, and three groups were created based on the adjusted scores: low RPI (bottom third of the group), medium RPI (middle third), and high RPI (top third of the group). Sample sizes were 60 subjects for the high and medium RPI groups, and 61 subjects for the low RPI group. Grouping subjects based on age- and gender-adjusted RPI scores ensured that the groups did not differ in age or gender (all three groups had relatively equal gender representation for each outcome measure, and were comparable in average age). Cortical thickness measurements were further residualized as described in the methods section in order to control for within-group age differences, gender and site influences.

Cortical thickness covariance densities for RPI-based graphs found significant between-group differences, $F(2,297) = 66.91$, $p<.001$, $\eta^2 = 0.31$. Post-hoc tests showed that high RPI groups had a lower covariance density in the social brain overall (M= .07, SD=0.02) compared to medium RPI (M=0.12, SD=0.03) and low RPI (M=0.11, SD=0.04), all p's <.001.

Furthermore, subnetwork covariance analyses showed that *affiliation* and *aversion* network densities remained relatively unchanged across groups, while decreases were observed between low RPI and high RPI groups in the *mentalizing/mirror* and the *perception* networks. Interestingly, a significant increase in network density was noted in the medium RPI group in the

perception network.

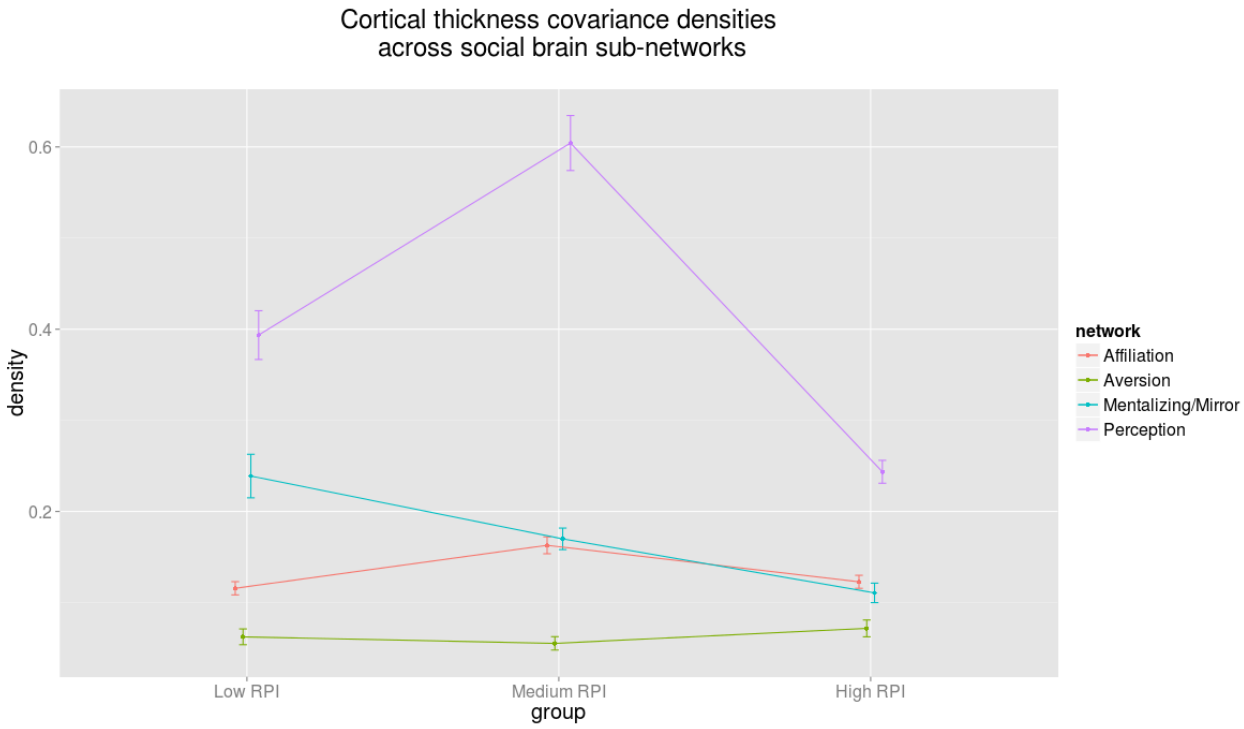

Figure 8: Social brain sub-networks – covariance densities across RPI groups

Together, these findings suggest that differences in covariance density in the social brain between levels of resistance to peer influence are driven primarily by differences in the perception and mentalizing/mirror networks. Furthermore, these findings align with results from maturational trajectories: across maturation, resistance to peer influence decreases, as does structural covariance in the social brain. Beyond the effects of age, greater resistance to peer influence is related to decreased cortical thickness covariance in the social brain.

3. Rejection Sensitivity

For structural covariance analyses, the same procedure as for the RPI analyses was employed, with RSQ values being computed controlling for age, site, and gender. As a result, the groups differed significantly on RSQ total scores (high RSQ M=11.77, SD=1.73; medium RSQ=8.44, SD=0.76; low RSQ=5.63, SD=1.62), but did not differ significantly on age, gender and site. Sample sizes were 52 subjects for the high and low RSQ groups, and 50 for the low RSQ group.

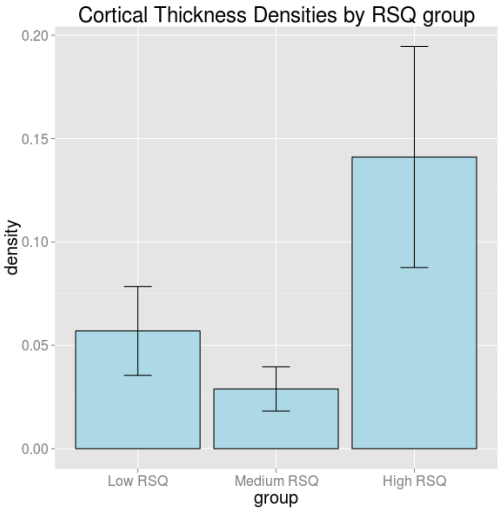

Figure 9: Social brain densities by RSQ group

Cortical thickness covariance densities for graphs of individuals with high RSQ found significant between-group differences, $F(2,297) = 297.6$, $p<.001$, $\eta^2 = 0.67$. Post-hoc tests showed that high RSQ groups had a higher connection density in the social brain overall (M= 0.14, SD=0.05) compared to medium RSQ (M=0.03, SD=0.01) and low RPI (M=0.06, SD=0.02), all p's <.001.

Subnetwork analysis found that between low and high RSQ groups, all sub-networks increased in density.

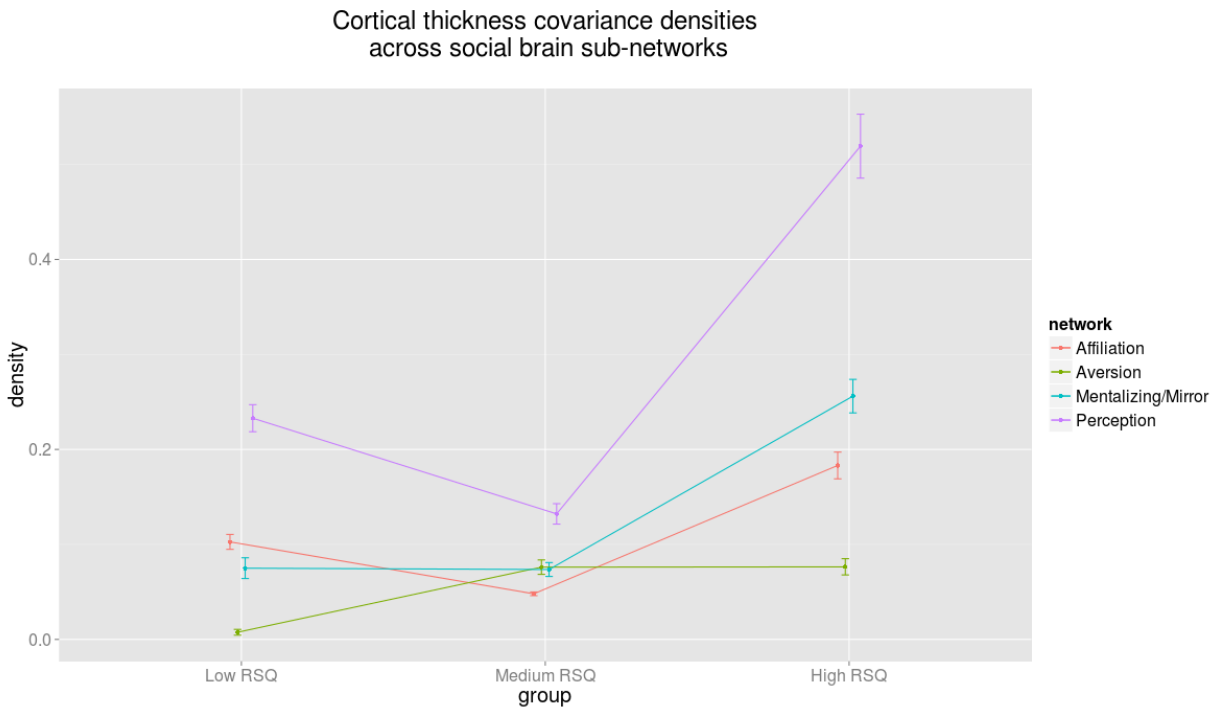

Figure 10: Social brain sub-networks – covariance densities across RSQ groups

Together with findings from RPI analyses, these results suggest that a sensitivity to social stimuli at the trait level, i.e., a decreased ability to resist peer influence and a sensitivity to rejection by others, is related to a more densely covarying social brain network. This increase in density may be indicative of a more costly, but faster (more efficient) signal transmission at a functional level.

4. Behavioral Inhibition

The same procedure as for the previous analyses was employed, with age-adjusted Go-NoGo (GNG) D-prime values being computed, controlling for age, site, gender, and peer condition. As a result, the groups differed significantly on GNG D-prime total scores (high GNG M=2.39, SD=0.54; medium GNG=1.53, SD=0.35; low GNG=0.75, SD=0.44), but did not differ significantly on age, gender and site. Sample sizes were 58 subjects for the high and low GNG groups, and 56 for the medium GNG group.

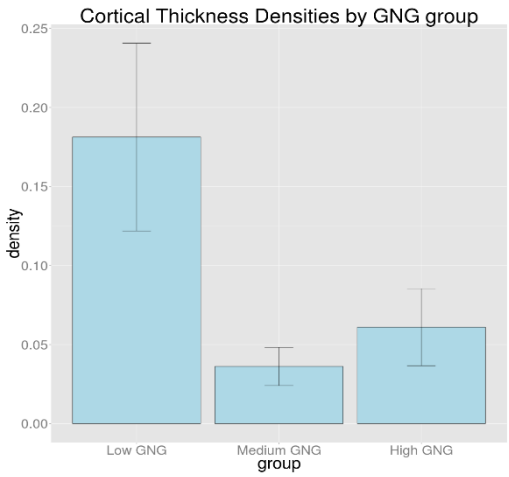

Figure 11: Social brain densities by GNG group

Cortical thickness covariance densities for graphs of individuals with high GNG D-prime found significant between-group differences, $F(2,297) = 423.8$, $p<.001$, $\eta^2 = 0.74$. Post-hoc tests showed that low GNG groups had a higher connection density in the social brain overall (M= 0.18, SD=.06) compared to medium GNG (M=0.04, SD=0.01) and high GNG (M=0.06, SD=0.02), all p's <.001, and that this effect was present across all sub-networks (Figure 12).

Since low GNG D-prime values suggest a decreased ability to control automatic responses to social stimuli, these results align with findings from RPI and RSQ measures. Specifically, individuals in the low GNG D-prime group may experience a more integrated, i.e., a "noisier" response to social stimuli, with simultaneous coactivation across multiple regions, resulting in a diminished ability to quickly identify social cues and control automatic responses to these stimuli.

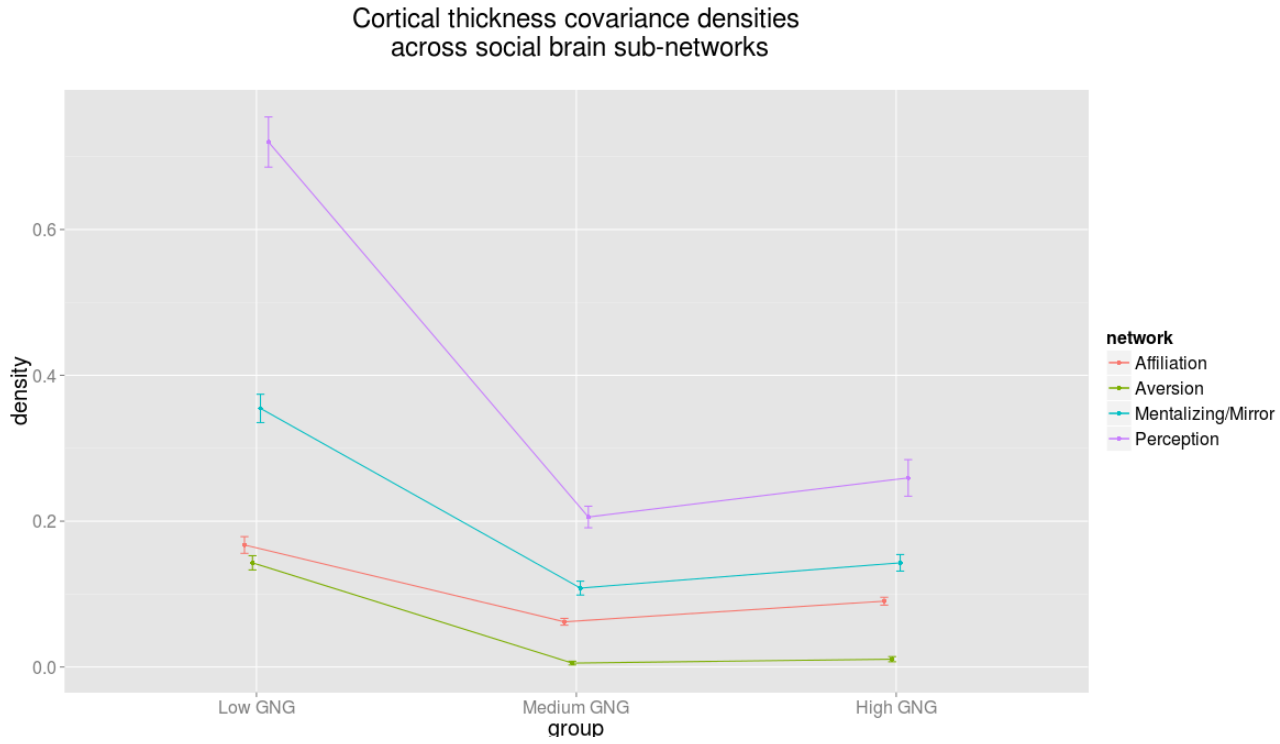

Figure 12: Social brain sub-networks – covariance densities across Go-NoGo groups

5. Non-Social Measure of Cognitive Functioning

The same procedure as for the previous analyses was employed for WASI Matrix Reasoning T scores. After eliminating cases with missing values, a sample of N=195 subjects was obtained. Residuals were computed, controlling for age, site, and gender. As a result, the groups differed significantly on T-scores (high WASI M=61.18, SD=3.26; medium WASI=55.52, SD=3.23; low WASI=46.61, SD=6.31), but did not differ significantly on age, gender and site. Sample sizes were 66 subjects for the high WASI group, 67 for the low WASI

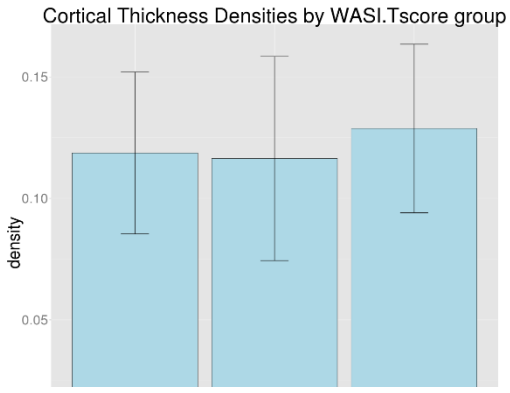

Figure 13: Social brain densities by WASI group

group and 62 for the medium WASI group.

Cortical thickness covariance densities for graphs of individuals with high WASI Matrix Reasoning T-scores found significant between-group differences, $F(2,297) = 3.175$, $p=.04$, but had a small effect size ($\eta^2 = 0.02$). Post-hoc tests showed that low WASI groups ($M= 0.12$, $SD=.03$) did not differ significantly from medium WASI groups ($M= 0.12$, $SD=.04$, $p=1.00$), which did not differ significantly from high WASI groups ($M= 0.13$, $SD=.03$, $p=.07$), and that the difference between medium and high WASI groups was only marginally significant ($p=.056$). At the subnetwork level, an increase in density was noted in the perception and mentalizing/mirror networks.

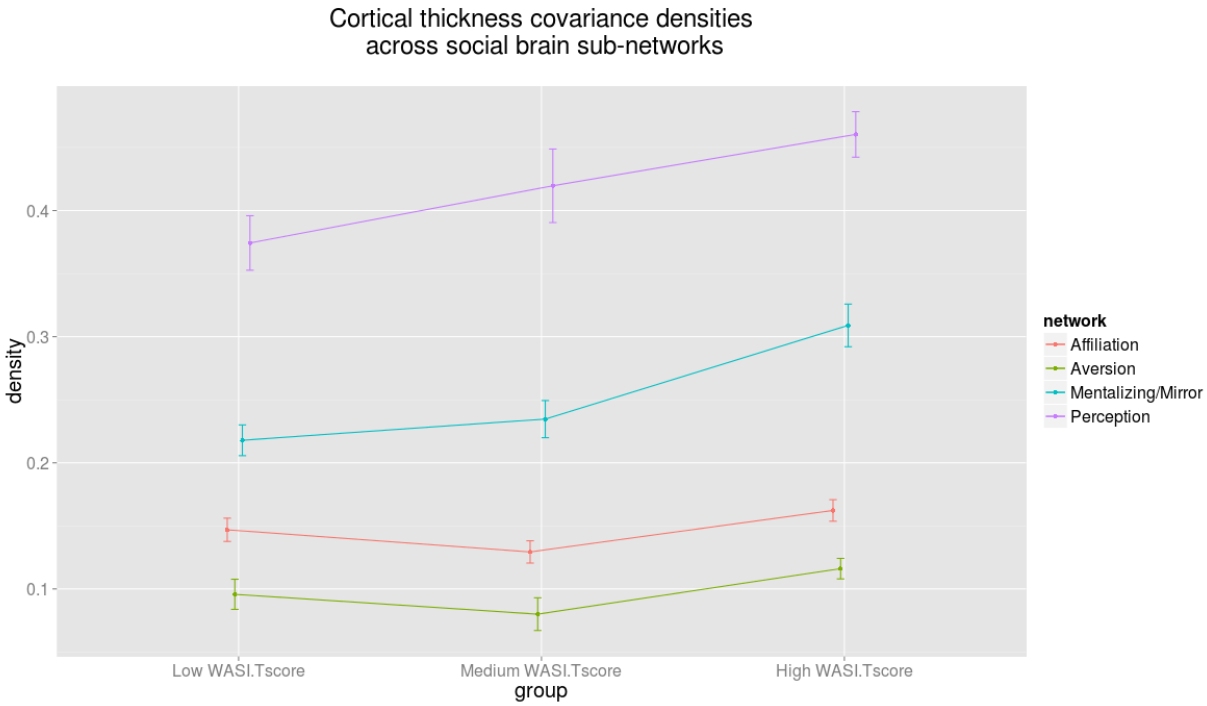

Figure 14: Social brain sub-networks – covariance densities across WASI groups

Characteristic Path Length (Network Efficiency)

1. Maturational Trajectories

An ANOVA showed a significant between-group difference across age groups, F(2,297)= 57.12, p<.001. Post-hoc Bonferroni-adjusted pairwise comparisons revealed that characteristic path length was lowest in adolescents (M= 1.86, SD= 0.13) and young adults (M= 1.87, SD= 0.12; p=1.00), and highest in the adult sample (M= 2.05, SD= 0.17) p's <.001.

Figure 15: Characteristic path length across age groups (whole-brain)

Groups also differed from each other in the social brain, F(2,297) = 37.51, p<.001. Post-hoc tests found that adolescents (M= 2.24, SD= 0.22) and young adults (M= 2.32, SD= 0.29) did not differ significantly from each other (p=.16), while both groups had significantly shorter characteristic path lengths than adults (M= 2.60, SD= 0.39; p's <.001).

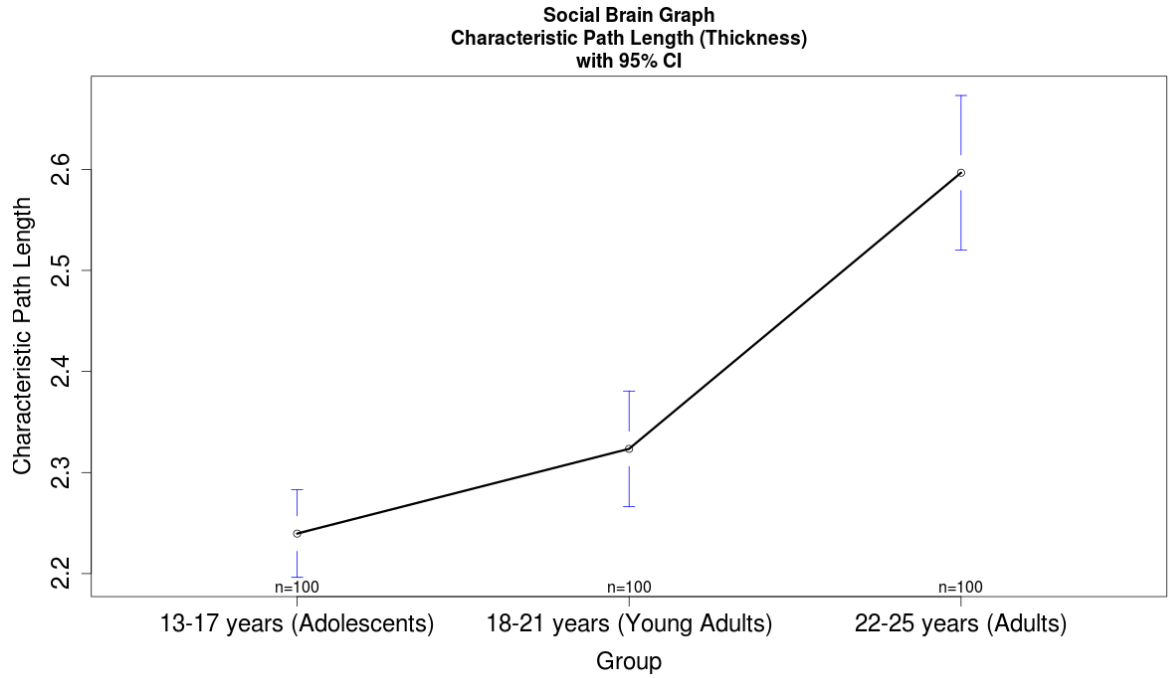

Figure 16: Graph densities across age groups (social brain)

A sub-network analysis was further conducted to examine these findings (see Table 5 for means and p-values). Results suggest that characteristic path lengths increased between adolescence and adulthood in the *perception* and *mentalizing/mirror* networks. Meanwhile, the *aversion* network showed a reorganization during young adulthood, with shorter path lengths compared to both the adolescent and adult networks.

An increase in path length suggests a decrease in communication efficiency in the network. Together with findings from graph density analyses discussed previously, this suggests that during maturation, structural networks become more cost-efficient. In complex networks, increased segregation and longer paths indicate that signals can travel across the network at a lower energy cost.

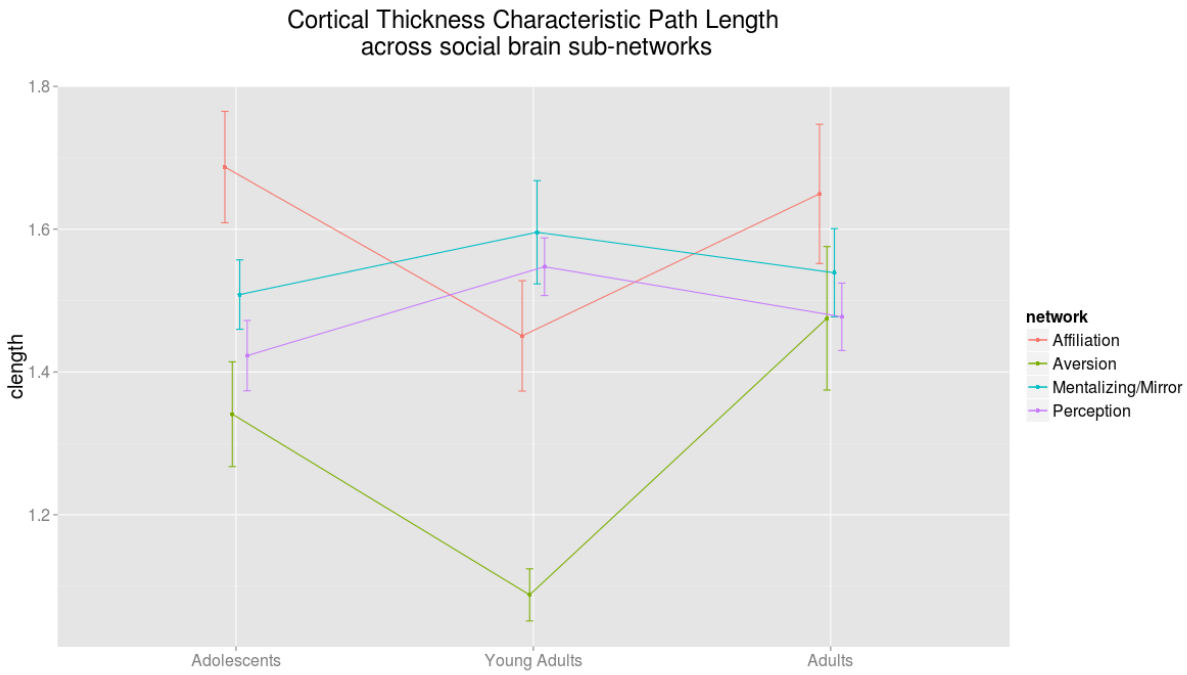

Figure 17: Social brain sub-networks – characteristic path length across age groups

Table 5: Social brain sub-networks – characteristic path length across age groups

	Characteristic Path Length		
	Adolescents **M (SD)**	**Young Adults** **M (SD)**	**Adults** **M (SD)**
Perception	1.21 (0.20)[3]	1.25 (0.11)[3]	1.47 (0.19)[1,2]
Affiliation	1.78 (0.27)	1.84 (0.37)	1.88 (0.33)
Aversion	1.78 (0.38)[2]	1.43 (0.31)[1,3]	1.85 (0.39)[2]
Mentalizing/Mirror	1.47 (0.19)[3]	1.52 (0.22)	1.59 (0.24)[1]
	1 = significantly different from adolescents; 2 = significantly different from young adults; 3 = significantly different from adults; $p<.05$		

2. Resistance to Peer Influence

When grouped by resistance to peer influence, groups were also found to differ, $F(2,297) = 40.12$, $p<.001$, $\eta^2 = 0.21$. Post-hoc tests suggest that high RPI groups (M=2.60, SD=0.42) and low RPI groups (M=2.70, SD= 0.52) have significantly longer path lengths than medium RPI groups (M=2.22, SD=0.23), both p's <.001. This suggests that medium RPI groups are less cost-efficient than the low and high RPI groups. Interestingly, medium RPI groups are also the groups where the social brain network has its highest density, suggesting the possibility that these groups frequently co-activate these regions, more so than low- and high-RPI groups.

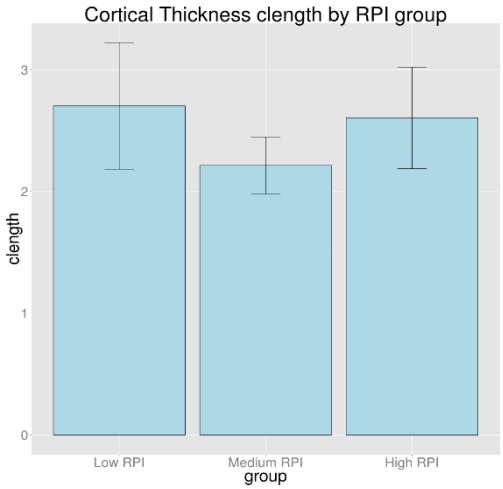

Figure 18: Social brain characteristic path length by RPI group

At the sub-network level, the *affiliation* network appears to be the only network not following this trajectory, showing an increase in path length despite stable covariance density.

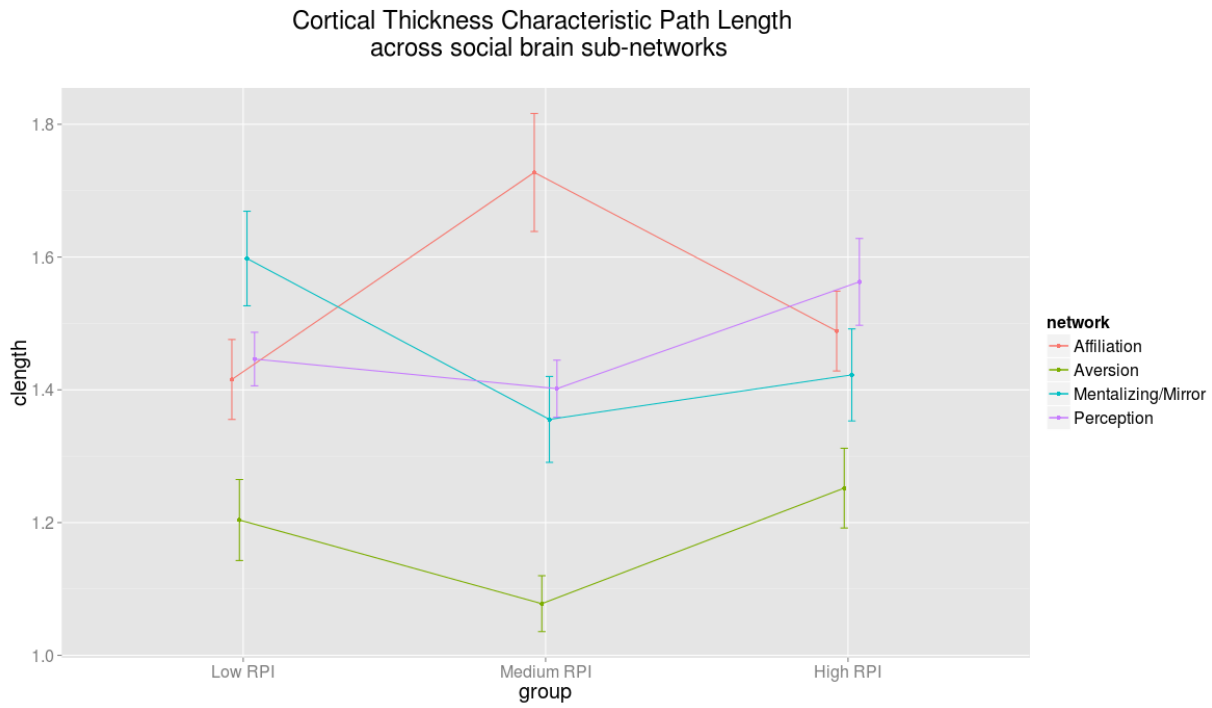

Figure 19: Social brain sub-networks – characteristic path length across RPI groups

3. Rejection Sensitivity

Groups created based on rejection sensitivity scores were also found to differ with regard to their characteristic path length in the social brain network, $F(2,297) = 32.83$, $p<.001$, $\eta^2 = 0.18$. Post-hoc tests suggest that high RSQ groups (M=2.23, SD=0.25) and low RSQ groups (M=2.47, SD= 0.51) have significantly longer path lengths than medium RSQ groups (M=1.92, SD=0.61), all p's <.005.

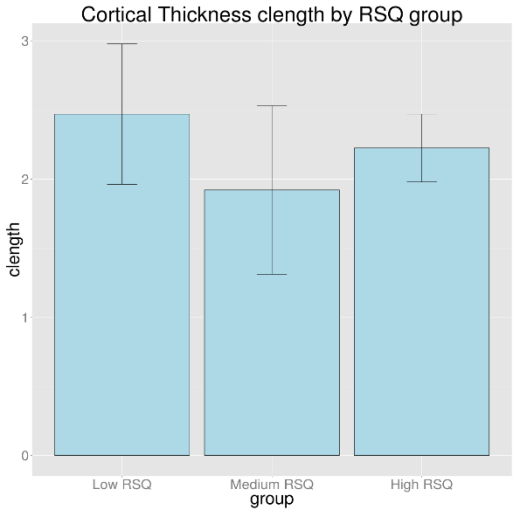

Figure 20: Social brain characteristic path length by RSQ group

At the sub-network level, an increase was

noted between low and high RSQ groups in the *mentalizing/mirror*, *affiliation*, and *aversion* networks.

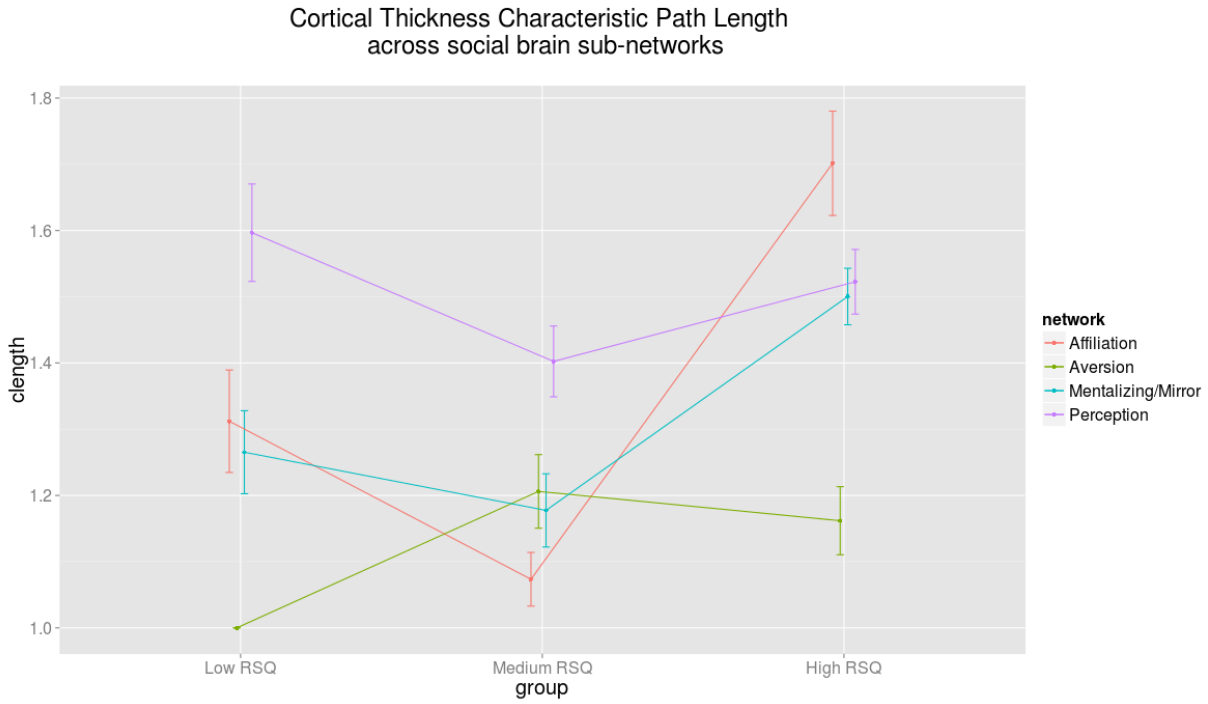

Figure 21: Social brain sub-networks – characteristic path length across RSQ groups

Together with results from density analyses, these results suggest that low-RS individuals' social brain network architecture has decreased efficiency, but also a lower cost, suggesting a cost-efficiency trade-off. Meanwhile, individuals high in RS also have a structural social brain that has decreased efficiency, but is also high in cost.

4. Behavioral Inhibition

Groups based on Go-NoGo D-prime scores also differed in characteristic path lengths in the social brain network, $F(2,297) = 17.74$, $p<.001$, $\eta^2 = 0.11$. Post-hoc tests suggest that groups with low D-prime values on the Go-NoGo task (path length M=2.15, SD=0.27) and groups with medium D-prime values (path length M=2.00, SD= 0.64) do not differ from each other significantly, but that both have significantly shorter path lengths than high GNG groups (M=2.44, SD=0.57), p's <.001.

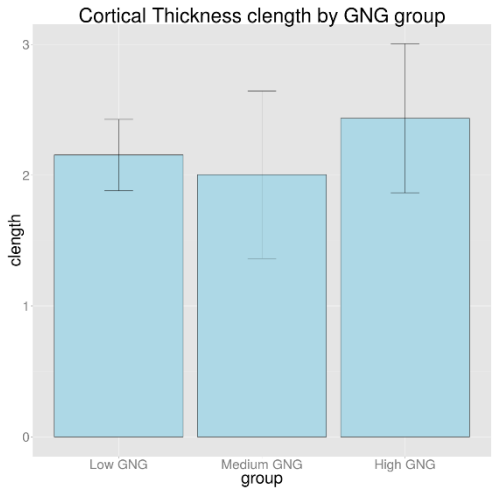

Figure 22: Social brain characteristic path length by Go-NoGo group

Interestingly, at the sub-network level, this pattern was only seen in the perception subnetwork, while the other three subnetworks showed a decrease in path length.

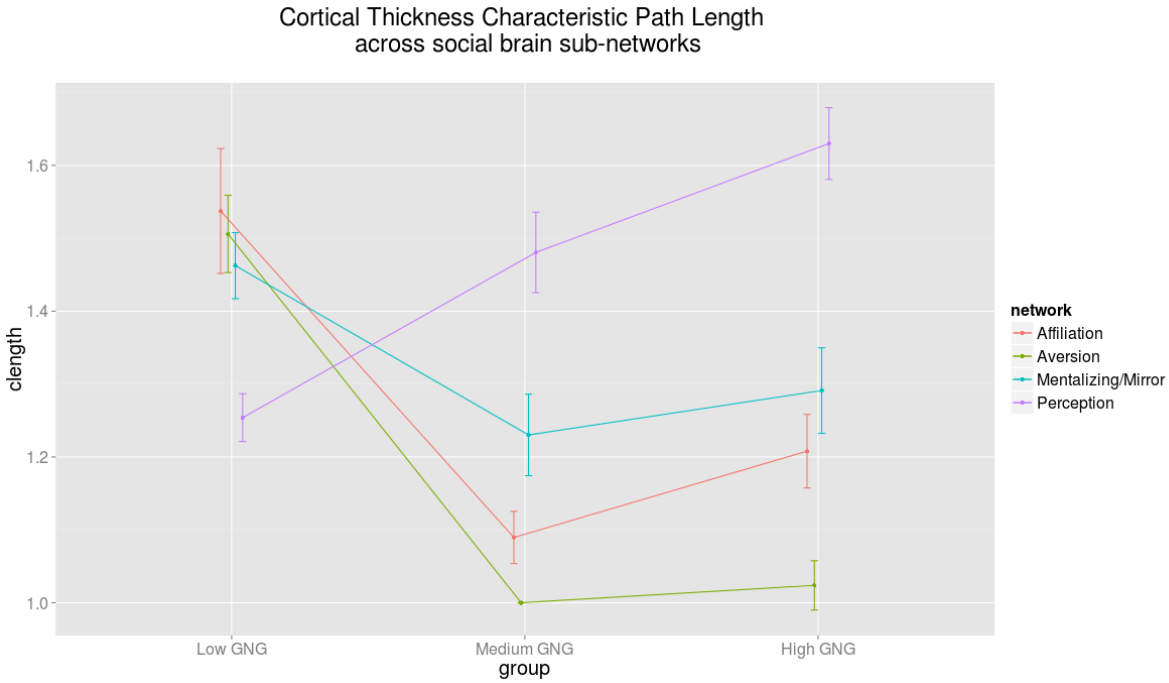

Figure 23: Social brain sub-networks – characteristic path length across Go-NoGo groups

Together with findings from covariance density, these findings suggest that individuals who perform worse on behavioral inhibition in response to socio-emotional stimuli have structural social brain networks that have greater cost and greater efficiency. Meanwhile, these networks in individuals who perform better on this task are lower in cost and comparatively less efficient.

5. Cognitive Functioning

Groups based on WASI Matrix Reasoning T-scores did not differ significantly in characteristic path length, $F(2,297) = 0.47$, $p=.62$, $\eta 2 = 0.003$ (means ranging between 2.52 and 2.57). Post-hoc tests were not computed. These findings suggest that efficiency in the social brain network is not associated with cognitive performance as measured by the WASI. At the sub-network level, an increase was observed in path length in the affiliation sub-network.

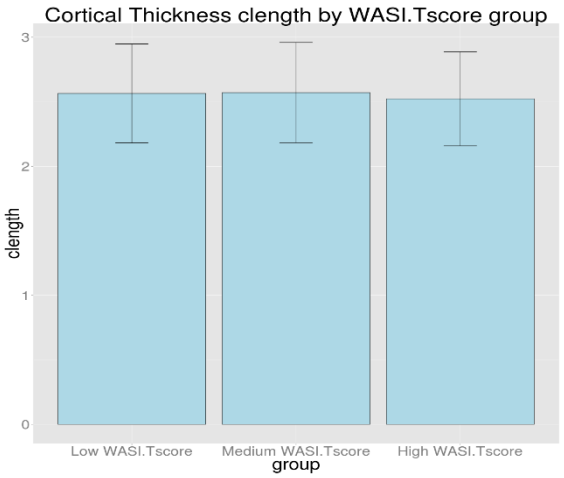

Figure 24: Social brain characteristic path length by WASI group

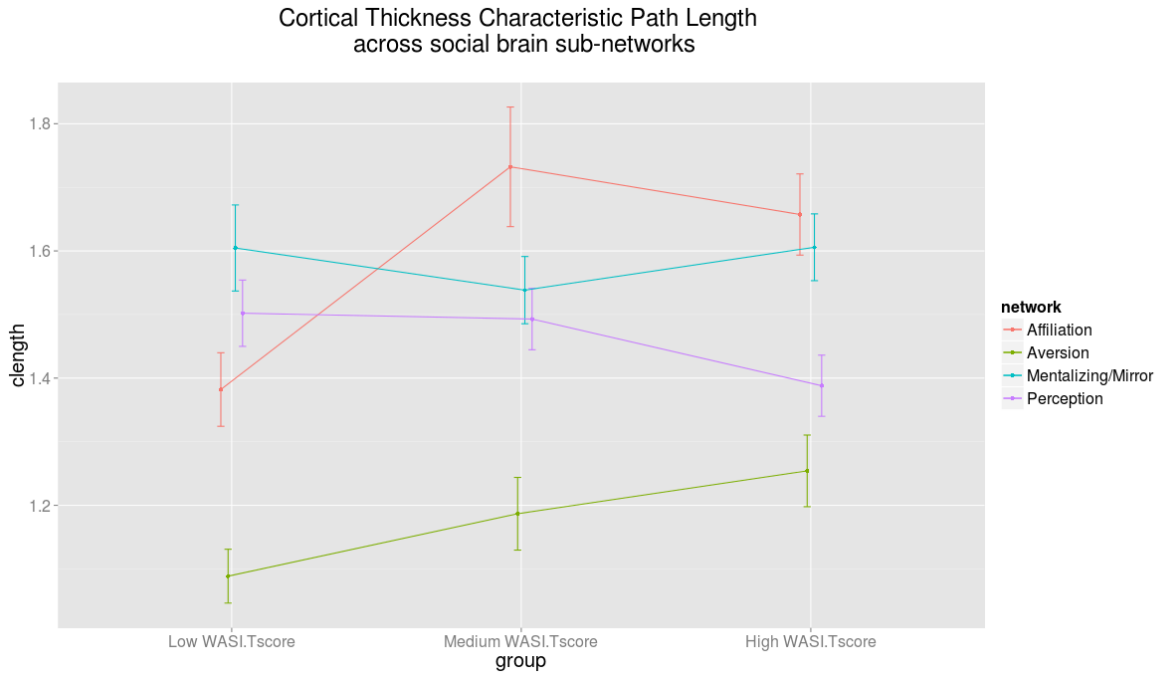

Figure 25: Social brain sub-networks – characteristic path length across WASI groups

CHAPTER 4

DISCUSSION

The present study explored neuromorphological covariation in the social brain network at different stages in the development between adolescence and adulthood. Focusing primarily on cortical thickness, it aimed to clarify how age-dependent anatomical remodeling in the brain impacts the topology of anatomical networks, and whether behavioral phenotypes relevant to social information processing could be differentiated based on the morphological network topology in a brain network known to be involved in processing social information.

Developmental Changes

In Aim 1, the present study focused on the changes that occur within the social brain between adolescence and adulthood, using a cross-sectional approach. Given previous research suggesting increased functional specialization within the social brain as a result of maturation (Bickart et al., 2014; Johnson et al., 2009) it was hypothesized that this specialization would also be reflected at the network level through lower covariance densities. That is, it was expected that in older subjects, the number of inter-regional correlations between regions of the social brain would decrease. Indeed, structural covariance density was found to be higher in networks derived from adolescent groups, and lower in networks derived from adult groups. These patterns were observed not only among regions of the social brain, but also at the whole-brain level. If the cortical thickness in one brain region can influence the cortical thickness of another through functional or synaptic connectivity (Alexander-Bloch, Giedd, et al., 2013), then the significant decrease in cortical thickness covariance between adolescence and adulthood is indicative of structural and/or functional reorganization at the network level.

The interpretation of these findings is challenging, not only because the biological processes driving structural covariance have yet to be fully understood, but also because of the heterogeneous pattern of structural changes that has been documented across brain areas between adolescence and adulthood (e.g., Giedd & Rapoport, 2010; Ostby et al., 2009). However, research has shown that structural covariance using cortical thickness can reflect meaningful white matter connectivity. For instance, cortical thickness covariance was compared with DTI connectivity, and findings showed approximately 35-40% overlap, primarily in positive correlations (Gong, He, Chen, & Evans, 2012). Furthermore, developmental research comparing cortical thickness structural covariance with resting-state fMRI found that in individuals between the ages of 9 and 22 years, there was a systematic association between structural covariance and functional connectivity at the whole-brain level (Alexander-Bloch, Raznahan, et al., 2013). This study also found that regions in the same functional network module showed higher structural covariance than regions in different modules (Alexander-Bloch, Raznahan, et al., 2013). Thus, research suggests that despite the heterogeneity in regional structural development patterns, structural covariance is a meaningful approach to measure connectivity in the brain and overlaps with other connectivity measures.

Therefore, the observed decrease in structural covariance density in the social brain and in the whole brain between adolescence and adulthood might also be found using other modalities. Indeed, developmental resting-state network data show that functional correlations are stronger in anatomically neighboring regions in childhood, but as regions become more functionally specialized as part of functional sub-networks, these local correlations weaken, and the within-network correlations strengthen, resulting in a more segregated overall network (Fair et al., 2009). Since this pattern was observed at both the whole-brain and the social brain

network in the present study, it raises the possibility that the social brain, despite being involved in various aspects of social information processing, is a network whose sub-networks may require closer consideration.

With regard to sub-networks, the present study focused primarily on theory-based sub-networks of the social brain. However, the observed developmentally-decreasing covariance densities in these subnetworks suggests the possibility that this top-down approach to studying sub-networks may be insufficient for identifying covarying structural communities. An exploratory community detection analysis was also conducted within the present study, but a detailed examination of these communities and their components was not the primary focus. Therefore, these results are presented in the Appendix. They suggest that the extent of the overlap between theory-driven sub-networks and data-driven communities is not extensive, but a closer examination of theory vs. data-driven communities and sub-networks should form the focus of future research efforts.

Assuming a relationship between functional co-activation and structural covariance, the finding of increased covariance density in adolescence and decreased covariance density in adulthood suggests that the adolescent social brain is a more metabolically costly network, while the segregation observed in adulthood suggests a more cost-efficient distribution of metabolic needs. This notion is further supported by findings from analyses of characteristic path length. The inverse of the characteristic path length value is considered an index of global network efficiency, with smaller values indicating greater efficiency. While greater efficiency in functional networks facilitate faster signal transfer through direct pathways, high efficiency carries high metabolic costs. The resulting cost-efficiency trade-off creates a small world architecture that has sparse connectivity, local clusters, and a few long-range connections that

bridge short path lengths between pair of regions. In the present study, structural covariance graphs across developmental groups and at both the whole-brain level and in the social brain, exhibited small-world properties. This aligned with previous research on structural covariance matrices (He et al., 2007b) and graph theoretical analyses of cortical connectivity at varying levels of granularity (Sporns & Zwi, 2004), and suggests that the brain's cost-efficiency tradeoffs can be detected even at the macroanatomical level.

It has been suggested that the evolutionary reasons for this small-world architecture in the brain include a pressure to reduce wiring costs, but not to the extent that an overabundance of local connections would result in delayed information transfer and metabolic energy depletion. Therefore, long-range connections are in place to reduce energy costs. In addition, research has shown that the small-world topology facilitates both functional integration and segregation, and thus underlies dynamic complexity in the brain (for a review, see Bassett & Bullmore, 2006).

In conclusion, results from Aim 1 indicate that as the brain matures, structural covariance using cortical thickness results in a network that is less densely connected and has longer path lengths, possibility suggesting increased specialization and selective activation among the different brain regions.

Network properties related to social information processing

In Aim 2, the present study examined the properties of structural covariance graphs, i.e., graph density (an index of cost) and characteristic path length (an index of efficiency), in relation to self-report and behavioral measures of social information processing, specifically resistance to peer influence (Aim 2.1), rejection sensitivity (Aim 2.2), and behavioral inhibition (Aim 2.3). The specificity of these findings with regard to social processes was tested by examining

network properties in relation to non-social cognitive functioning (Aim 2.4).

Resistance to Peer Influence

Results from the present study indicate that graphs obtained from individuals who rated themselves as average on their ability to resist peer influence had a higher covariance density than graphs from both those who rated themselves as low and high on RPI. These results align with previous research on structural covariance in RPI groups in an adolescent sample, where a similar pattern was found (Paus et al., 2008). In that study, 22 regions were used based on prior research using an fMRI paradigm that involved the presentation of angry hand actions. Task-related activity in these regions differed based on the subjects' ability to resist peer influence (Grosbras et al., 2007). Cortical thickness structural covariance density in these regions increased between low and medium RPI individuals, followed by a decrease from medium to high RPI (Paus et al., 2008). However, this finding was only present in males, while a linear increase with greater RPI ability was noted in females (Paus et al., 2008). Since the present study controlled gender statistically, with females as the reference category, the present findings may be more indicative of male effects, thus replicating findings from Paus et al (2008). However, a more targeted sex differences analysis is necessary and should be a focus of investigation in future studies. Furthermore, the present study differs from the study by Paus and colleagues (2008) in that low-RPI individuals also had higher covariance density than high-RPI individuals.

These findings align with the maturational findings discussed above. Given the direct relationship between RPI and age, high-RPI groups would be expected to have similar network properties as older groups, which was indeed found for network density. For path length,

however, a correspondence between maturational trajectories and RPI-based trajectories was not found. Thus, it can be said that the structural covariance network of the social brain has comparable efficiency in low- and high-RPI groups, but is significantly less costly in groups where individuals have an above-average ability to resist the influence of their peers. Thus, findings from the present study indicate that a sensitivity to social context is associated with a higher covariance density in the social brain.

Rejection Sensitivity

The relationship between increased sensitivity to social context and higher covariance density was also found in relation to rejection sensitivity, where high-RS groups had a higher covariance density compared to low-RS groups. Given that this is the first study examining covariance density in structural networks, these results need replication and validation from other modalities before a firm conclusion can be drawn. However, existing findings from resting-state fMRI can be drawn upon to interpret this finding more broadly. In one study, high- and low-rejection sensitive individuals were scanned while viewing rejection vs. acceptance images. Findings from that study suggest that functional activation in regions typically involved in emotional processing and cognitive control (posterior cingulate, insula, dorsal anterior cingulate cortex, and medial frontal cortex) were sensitive to rejection stimuli across groups, but that low-RS individuals had a tendency to activate additional prefrontal structures to regulate distress associated with the stimuli (Kross et al., 2007). Based on this study, it may be inferred that the strength of the co-activation among regions in the social brain decreases in low-RS individuals as a result of inhibitory activity between brain regions.

Furthermore, low-RS individuals are more likely to downplay rejection cues in self-relevant interpersonal situations (Romero-Canyas & Downey, 2013), and may therefore not engage the rejection-processing brain network as frequently as their high-RS counterparts.

With regard to the sub-networks, a pattern emerged in which the high-RS group had sub-networks with greater cost and decreased efficiency (longer path lengths). Further research is needed to examine the functional implications of this structural architecture in the social brain, but it can be speculated that these structural network properties are associated with network specialization and selectivity in patterns of functional activation in response to rejection cues.

Behavioral Inhibition

Findings from Aims 2.1 and 2.2 show that an increased sensitivity to social stimuli at the trait level is associated with an increased covariance density in the structural social brain network. In Aim 2.3, the present study tested whether such an effect would also be observed at the behavioral level in an experimental paradigm. Indeed, groups with poor performance on an emotional Go-NoGo paradigm had higher covariance density in the social brain network compared to groups with average or good performance, and this effect was maintained across all subnetworks studied here.

A possible interpretation for these results is that the high covariance density in regional cortical thickness values facilitates a more diffuse signal in response to social cues, making it more difficult to accurately recognize and/or appropriately respond to socio-affective stimuli.

Conclusions and Future Directions

The present dissertation aimed to characterize structural covariance in the human 'social

brain' network with regard to developmental differences on the one hand, and self-reported and behavioral aspects of social information processing on the other. Results suggest that networks derived from subjects who are older, as well as those from subjects who are less sensitive to social stimuli and from those who perform better on a behavioral inhibition task, all share one characteristic: the density of covariance in the structural social brain network is low compared to individuals who are younger, more sensitive to social stimuli, and who perform worse on a behavioral inhibition task. Furthermore, this increase in covariance density was not observed in a non-social measure of cognitive functioning, suggesting a level of specificity to social information processing in the reported findings.

In addition, the study found that within theory-based sub-networks of the social brain, patterns of density and path length were relatively inconsistent with expectations. That is, if a more segregated social brain network suggests increased specialization, then a higher integration (and greater covariance density) would be expected at the sub-network level. However, the theory-based subnetworks examined in this study were generally found to follow the trajectory of the overall social brain network. It may be that, in this case, a data-driven approach may be more informative. To this end, exploratory analyses employed a data-driven approach to compare groups of regions based on theory and groups of regions emerging from the data. While this was not the main focus of this study, these analyses (see Appendix) do not suggest a strong overlap between the two approaches. Future research is needed to examine these inter-regional communities that emerge from a data-driven approach.

While the findings presented in this dissertation are primarily concerned with cortical thickness, it is important to mention that results using similar methodology with gray matter volume (see Appendix) differed dramatically from the findings obtained from cortical thickness.

This may be due to differences in the number and types of regions examined, the FDR threshold used, or statistical control variables. However, the present study adds to recent advances in understanding the relationships between these metrics (Vijayakumar et al., 2016; Winkler et al., 2010) and suggests that cortical thickness, gray matter volume and gray matter density cannot be used interchangeably as markers of neuroanatomical change, and that a closer examination of each of these measures and their underlying biological processes is needed.

The findings from the present study should be considered given several limitations. In this study, the sample sizes were relatively small (50-60 subjects per group), and therefore the findings need to be replicated with higher sample sizes. In addition, the present study is cross-sectional in nature, and therefore changes in covariance over time need to be examined more directly using longitudinal data, and any developmental changes are only speculative. In a related vein, the present study focused only on a relatively limited age spectrum. Future research should examine a longer developmental trajectory that begins in infancy and traces morphological network topology across the entire lifespan.

Findings presented here may inform future research on neuroplasticity in adolescence, as well as on biomarkers of early socio-affective and socio-cognitive difficulties. Research using graph theoretical approaches with structural covariance of gray matter volume and cortical thickness has already begun to explore the clinical implications of covariance network organization. For instance, studies have found that autism spectrum disorders are accompanied by atypical organization of structural covariance networks, specifically a decreased centrality of regions relevant for social and sensorimotor processing (Balardin et al., 2015). Similarly, schizophrenia is characterized by abnormal network topology in gray matter volume covariance (Bassett et al., 2008). Understanding normative structural topology in the brain using structural

MRI data can help build new avenues for prevention and intervention efforts.

In conclusion, this dissertation adds to our understanding of adolescence as a time of significant structural and functional reorganization in the brain, particularly in relation to social relationships and interpersonal dynamics. Given existing research suggesting that specific behaviors may lead to increases in structural covariance, and results from the present study suggesting that selective covariance in the social brain may be characteristic of maturity but also more adaptive in social contexts, the findings from the present study contribute to the idea that adolescence is a time of great opportunity for shaping the brain's structural architecture.

REFERENCES CITED

Achard, S. (2006). A resilient, low-frequency, small-world human brain functional network with highly connected association cortical hubs. *Journal of Neuroscience*, *26*(1), 63–72. http://doi.org/10.1523/JNEUROSCI.3874-05.2006

Adachi, Y., Osada, T., Sporns, O., Watanabe, T., Matsui, T., Miyamoto, K., & Miyashita, Y. (2012). Functional connectivity between anatomically unconnected areas is shaped by collective network-level effects in the macaque cortex. *Cerebral Cortex*, *22*(7), 1586–1592. http://doi.org/10.1093/cercor/bhr234

Alexander-Bloch, A., Clasen, L., Stockman, M., Ronan, L., Lalonde, F., Giedd, J., & Raznahan, A. (2016). Subtle in-scanner motion biases automated measurement of brain anatomy from in vivo MRI: motion bias in analyses of structural MRI. *Human Brain Mapping*. http://doi.org/10.1002/hbm.23180

Alexander-Bloch, A., Giedd, J. N., & Bullmore, E. (2013). Imaging structural co-variance between human brain regions. *Nature Reviews Neuroscience*, *14*(5), 322–336. http://doi.org/10.1038/nrn3465

Alexander-Bloch, A., Raznahan, A., Bullmore, E., & Giedd, J. (2013). The convergence of maturational change and structural covariance in human cortical networks. *The Journal of Neuroscience: The Official Journal of the Society for Neuroscience*, *33*(7), 2889–2899. http://doi.org/10.1523/JNEUROSCI.3554-12.2013

Asato, M. R., Terwilliger, R., Woo, J., & Luna, B. (2010). White matter development in adolescence: A DTI study. *Cerebral Cortex*, *20*(9), 2122–2131. http://doi.org/10.1093/cercor/bhp282

Balardin, J. B., Comfort, W. E., Daly, E., Murphy, C., Andrews, D., Murphy, D. G. M., … Sato, J. R. (2015). Decreased centrality of cortical volume covariance networks in autism spectrum disorders. *Journal of Psychiatric Research*, *69*, 142–149. http://doi.org/10.1016/j.jpsychires.2015.08.003

Bassett, D. S., & Bullmore, E. (2006). Small-world brain Networks. *The Neuroscientist*, *12*(6), 512–523. http://doi.org/10.1177/1073858406293182

Bassett, D. S., Bullmore, E., Verchinski, B. A., Mattay, V. S., Weinberger, D. R., & Meyer-Lindenberg, A. (2008). Hierarchical organization of human cortical networks in health and schizophrenia. *Journal of Neuroscience*, *28*(37), 9239–9248. http://doi.org/10.1523/JNEUROSCI.1929-08.2008

Bermudez, P., Lerch, J. P., Evans, A. C., & Zatorre, R. J. (2009). Neuroanatomical correlates of musicianship as revealed by cortical thickness and voxel-based morphometry. *Cerebral Cortex (New York, N.Y.: 1991)*, *19*(7), 1583–1596. http://doi.org/10.1093/cercor/bhn196

Bickart, K. C., Dickerson, B. C., & Feldman Barrett, L. (2014). The amygdala as a hub in brain networks that support social life. *Neuropsychologia*, *63*, 235–248. http://doi.org/10.1016/j.neuropsychologia.2014.08.013

Blakemore, S.-J. (2008). The social brain in adolescence. *Nature Reviews Neuroscience*, *9*(4), 267–277. http://doi.org/10.1038/nrn2353

Brooks, J. C. W., & Tracey, I. (2007). The insula: A multidimensional integration site for pain: *Pain*, *128*(1), 1–2. http://doi.org/10.1016/j.pain.2006.12.025

Brothers, L. The social brain: A project for integrating primate behavior and neurophysiology in a new domain. *Concepts in Neuroscience, 1*, 27–51.

Brown, B. B., & Larson, J. (2009). Peer relationships in adolescence. In *Handbook of Adolescent*

Psychology. John Wiley & Sons, Inc. Retrieved from http://dx.doi.org/10.1002/9780470479193.adlpsy002004

Bullmore, E., & Sporns, O. (2009). Complex brain networks: graph theoretical analysis of structural and functional systems. *Nature Reviews Neuroscience*, *10*(3), 186–198. http://doi.org/10.1038/nrn2575

Bullmore, E., & Sporns, O. (2012). The economy of brain network organization. *Nature Reviews Neuroscience*. http://doi.org/10.1038/nrn3214

Burnett, S., Sebastian, C., Cohen Kadosh, K., & Blakemore, S.-J. (2011). The social brain in adolescence: Evidence from functional magnetic resonance imaging and behavioural studies. *Neuroscience & Biobehavioral Reviews*, *35*(8), 1654–1664. http://doi.org/10.1016/j.neubiorev.2010.10.011

Casey, B. J., Giedd, J. N., & Thomas, K. M. (2000). Structural and functional brain development and its relation to cognitive development. *Biological Psychology*, *54*(1-3), 241–257. http://doi.org/10.1016/S0301-0511(00)00058-2

Casey, B. J., Trainor, R. J., Orendi, J. L., Schubert, A. B., Nystrom, L. E., Giedd, J. N., … Rapoport, J. L. (1997). A developmental functional MRI study of prefrontal activation during performance of a Go-No-Go task. *Journal of Cognitive Neuroscience*, *9*(6), 835–847. http://doi.org/10.1162/jocn.1997.9.6.835

Chang, L. J., Yarkoni, T., Khaw, M. W., & Sanfey, A. G. (2013). Decoding the role of the insula in human cognition: Functional parcellation and large-scale reverse inference. *Cerebral Cortex*, *23*(3), 739–749. http://doi.org/10.1093/cercor/bhs065

Chklovskii, D. B. (2004). Exact solution for the optimal neuronal layout problem. *Neural Computation*, *16*(10), 2067–2078. http://doi.org/10.1162/0899766041732422

Choudhury, S., Blakemore, S.-J., & Charman, T. (2006). Social cognitive development during adolescence. *Social Cognitive and Affective Neuroscience*, *1*(3), 165–174. http://doi.org/10.1093/scan/nsl024

Chung, M. K. (2013). *Computational neuroanatomy: the methods*. Singapore ; Hackensack, NJ: World Scientific.

Cohen, A. O., Dellarco, D. V., Breiner, K., Helion, C., Heller, A. S., Rahdar, A., … Casey, B. (2016). The impact of emotional states on cognitive control circuitry and function. *Journal of Cognitive Neuroscience*, *28*(3), 446–459. http://doi.org/10.1162/jocn_a_00906

Craig, A. D. (2009). How do you feel — now? The anterior insula and human awareness. *Nature Reviews Neuroscience*, *10*(1), 59–70.

Csardi, G., & Nepusz, T. (2006). The igraph software package for complex network research. *InterJournal*, *Complex Systems*, 1695.

Dale, A. M., Fischl, B., & Sereno, M. I. (1999). Cortical surface-based analysis. I. Segmentation and surface reconstruction. *NeuroImage*, *9*(2), 179–194. http://doi.org/10.1006/nimg.1998.0395

Deen, B., Pitskel, N. B., & Pelphrey, K. A. (2011). Three systems of insular functional connectivity identified with cluster analysis. *Cerebral Cortex*, *21*(7), 1498–1506. http://doi.org/10.1093/cercor/bhq186

Desikan, R. S., Ségonne, F., Fischl, B., Quinn, B. T., Dickerson, B. C., Blacker, D., … Killiany, R. J. (2006). An automated labeling system for subdividing the human cerebral cortex on MRI scans into gyral based regions of interest. *NeuroImage*, *31*(3), 968–980. http://doi.org/10.1016/j.neuroimage.2006.01.021

Downey, G., & Feldman, S. I. (1996). Implications of rejection sensitivity for intimate

relationships. *Journal of Personality and Social Psychology*, *70*, 1327–1343. http://doi.org/10.1037/0022-3514.70.6.1327

Durston, S., Davidson, M. C., Tottenham, N., Galvan, A., Spicer, J., Fossella, J. A., & Casey, B. J. (2006). A shift from diffuse to focal cortical activity with development. *Developmental Science*, *9*(1), 1–8. http://doi.org/10.1111/j.1467-7687.2005.00454.x

Eisenberger, N. I. (2003). Does rejection hurt? An fMRI Study of social exclusion. *Science*, *302*, 290–292. http://doi.org/10.1126/science.1089134

Eisenberger, N. I., Way, B. M., Taylor, S. E., Welch, W. T., & Lieberman, M. D. (2007). Understanding genetic risk for aggression: Clues from the brain's response to social exclusion. *Biological Psychiatry*, *61*(9), 1100–1108. http://doi.org/10.1016/j.biopsych.2006.08.007

Fair, D. A., Cohen, A. L., Power, J. D., Dosenbach, N. U. F., Church, J. A., Miezin, F. M., … Petersen, S. E. (2009). Functional brain networks develop from a "local to distributed" organization. *PLoS Computational Biology*, *5*(5), e1000381. http://doi.org/10.1371/journal.pcbi.1000381

Fischl, B., & Dale, A. M. (2000). Measuring the thickness of the human cerebral cortex from magnetic resonance images. *Proceedings of the National Academy of Sciences*, *97*(20), 11050–11055. http://doi.org/10.1073/pnas.200033797

Fischl, B., Salat, D. H., Busa, E., Albert, M., Dieterich, M., Haselgrove, C., … Dale, A. M. (2002). Whole brain segmentation. *Neuron*, *33*(3), 341–355. http://doi.org/10.1016/S0896-6273(02)00569-X

Fischl, B., Salat, D. H., van der Kouwe, A. J. W., Makris, N., Ségonne, F., Quinn, B. T., & Dale, A. M. (2004). Sequence-independent segmentation of magnetic resonance images.

NeuroImage, *23 Suppl 1*, S69–84. http://doi.org/10.1016/j.neuroimage.2004.07.016

Fischl, B., Sereno, M. I., & Dale, A. M. (1999). Cortical surface-based analysis. II: Inflation, flattening, and a surface-based coordinate system. *NeuroImage*, *9*(2), 195–207. http://doi.org/10.1006/nimg.1998.0396

Fischl, B., Sereno, M. I., Tootell, R. B., & Dale, A. M. (1999). High-resolution intersubject averaging and a coordinate system for the cortical surface. *Human Brain Mapping*, *8*(4), 272–284.

Fischl, B., van der Kouwe, A., Destrieux, C., Halgren, E., Ségonne, F., Salat, D. H., … Dale, A. M. (2004). Automatically parcellating the human cerebral cortex. *Cerebral Cortex (New York, N.Y.: 1991)*, *14*(1), 11–22.

Frith, C. D. (2007). The social brain? *Philosophical Transactions of the Royal Society B: Biological Sciences*, *362*(1480), 671–678. http://doi.org/10.1098/rstb.2006.2003

Giedd, J. N., Blumenthal, J., Jeffries, N. O., Castellanos, F. X., Liu, H., Zijdenbos, A., … Rapoport, J. L. (1999). Brain development during childhood and adolescence: a longitudinal MRI study. *Nat Neurosci*, *2*(10), 861–863. http://doi.org/10.1038/13158

Giedd, J. N., & Rapoport, J. L. (2010). Structural MRI of pediatric brain development: what have we learned and where are we going? *Neuron*, *67*(5), 728–734. http://doi.org/10.1016/j.neuron.2010.08.040

Giedd, J. N., Vaituzis, A. C., Hamburger, S. D., Lange, N., Rajapakse, J. C., Kaysen, D., … Rapoport, J. L. (1996). Quantitative MRI of the temporal lobe, amygdala, and hippocampus in normal human development: Ages 4-18 years. *The Journal of Comparative Neurology*, *366*(2), 223–230. http://doi.org/10.1002/(SICI)1096-9861(19960304)366:2<223::AID-CNE3>3.0.CO;2-7

Gogtay, N., Giedd, J. N., Lusk, L., Hayashi, K. M., Greenstein, D., Vaituzis, A. C., … Thompson, P. M. (2004). Dynamic mapping of human cortical development during childhood through early adulthood. *Proceedings of the National Academy of Sciences, 101*(21), 8174–8179. http://doi.org/10.1073/pnas.0402680101

Gong, G., He, Y., Chen, Z. J., & Evans, A. C. (2012). Convergence and divergence of thickness correlations with diffusion connections across the human cerebral cortex. *NeuroImage, 59*(2), 1239–1248. http://doi.org/10.1016/j.neuroimage.2011.08.017

Grosbras, M.-H., Jansen, M., Leonard, G., McIntosh, A., Osswald, K., Poulsen, C., … Paus, T. (2007). Neural mechanisms of resistance to peer influence in early adolescence. *Journal of Neuroscience, 27*(30), 8040–8045. http://doi.org/10.1523/JNEUROSCI.1360-07.2007

Hampton, W. H., Unger, A., Von Der Heide, R. J., & Olson, I. R. (2016). Neural connections foster social connections: A diffusion-weighted imaging study of social networks. *Social Cognitive and Affective Neuroscience*, nsv153. http://doi.org/10.1093/scan/nsv153

Hare, T. A., Tottenham, N., Galvan, A., Voss, H. U., Glover, G. H., & Casey, B. J. (2008). Biological substrates of emotional reactivity and regulation in adolescence during an emotional Go-Nogo task. *Biological Psychiatry, 63*(10), 927–934. http://doi.org/10.1016/j.biopsych.2008.03.015

He, Y., Chen, Z. J., & Evans, A. C. (2007a). Small-world anatomical networks in the human brain revealed by cortical thickness from MRI. *Cerebral Cortex, 17*(10), 2407–2419. http://doi.org/10.1093/cercor/bhl149

He, Y., Chen, Z. J., & Evans, A. C. (2007b). Small-world anatomical networks in the human brain revealed by cortical thickness from MRI. *Cerebral Cortex (New York, N.Y.: 1991), 17*(10), 2407–2419. http://doi.org/10.1093/cercor/bhl149

Honey, C. J., Sporns, O., Cammoun, L., Gigandet, X., Thiran, J. P., Meuli, R., & Hagmann, P. (2009). Predicting human resting-state functional connectivity from structural connectivity. *Proceedings of the National Academy of Sciences*, *106*(6), 2035–2040. http://doi.org/10.1073/pnas.0811168106

Hosseini, S. M. H., & Kesler, S. R. (2013). Comparing connectivity pattern and small-world organization between structural correlation and resting-state networks in healthy adults. *NeuroImage*, *78*, 402–414. http://doi.org/10.1016/j.neuroimage.2013.04.032

Humphries, M. ., Gurney, K., & Prescott, T. . (2006). The brainstem reticular formation is a small-world, not scale-free, network. *Proceedings of the Royal Society B: Biological Sciences*, *273*(1585), 503–511. http://doi.org/10.1098/rspb.2005.3354

Johnson, M. H., Grossmann, T., & Kadosh, K. C. (2009). Mapping functional brain development: Building a social brain through interactive specialization. *Developmental Psychology*, *45*(1), 151–159. http://doi.org/10.1037/a0014548

Kang, D.-H., Jo, H. J., Jung, W. H., Kim, S. H., Jung, Y.-H., Choi, C.-H., … Kwon, J. S. (2013). The effect of meditation on brain structure: cortical thickness mapping and diffusion tensor imaging. *Social Cognitive and Affective Neuroscience*, *8*(1), 27–33. http://doi.org/10.1093/scan/nss056

Karas, G. B., Scheltens, P., Rombouts, S. A. R. B., Visser, P. J., van Schijndel, R. A., Fox, N. C., & Barkhof, F. (2004). Global and local gray matter loss in mild cognitive impairment and Alzheimer's disease. *NeuroImage*, *23*(2), 708–716. http://doi.org/10.1016/j.neuroimage.2004.07.006

Kross, E., Egner, T., Ochsner, K., Hirsch, J., & Downey, G. (2007). Neural dynamics of rejection sensitivity. *Journal of Cognitive Neuroscience*, *19*(6), 945–956.

http://doi.org/10.1162/jocn.2007.19.6.945

Langfelder, P., & Horvath, S. (2008). WGCNA: an R package for weighted correlation network analysis. *BMC Bioinformatics*, *9*(1), 559. http://doi.org/10.1186/1471-2105-9-559

Lerch, J. P., Worsley, K., Shaw, W. P., Greenstein, D. K., Lenroot, R. K., Giedd, J., & Evans, A. C. (2006). Mapping anatomical correlations across cerebral cortex (MACACC) using cortical thickness from MRI. *NeuroImage*, *31*(3), 993–1003. http://doi.org/10.1016/j.neuroimage.2006.01.042

MacDonald, D., Kabani, N., Avis, D., & Evans, A. C. (2000). Automated 3-D extraction of inner and outer surfaces of cerebral cortex from MRI. *NeuroImage*, *12*(3), 340–356. http://doi.org/10.1006/nimg.1999.0534

Maguire, E. A., Gadian, D. G., Johnsrude, I. S., Good, C. D., Ashburner, J., Frackowiak, R. S. J., & Frith, C. D. (2000). Navigation-related structural change in the hippocampi of taxi drivers. *Proceedings of the National Academy of Sciences*, *97*(8), 4398–4403. http://doi.org/10.1073/pnas.070039597

Maguire, E. A., Spiers, H. J., Good, C. D., Hartley, T., Frackowiak, R. S. J., & Burgess, N. (2003). Navigation expertise and the human hippocampus: a structural brain imaging analysis. *Hippocampus*, *13*(2), 250–259. http://doi.org/10.1002/hipo.10087

Maguire, E. A., Woollett, K., & Spiers, H. J. (2006). London taxi drivers and bus drivers: A structural MRI and neuropsychological analysis. *Hippocampus*, *16*(12), 1091–1101. http://doi.org/10.1002/hipo.20233

Masten, C. L., Eisenberger, N. I., Borofsky, L. A., Pfeifer, J. H., McNealy, K., Mazziotta, J. C., & Dapretto, M. (2009). Neural correlates of social exclusion during adolescence: understanding the distress of peer rejection. *Social Cognitive and Affective Neuroscience*,

4, 143–157. http://doi.org/10.1093/scan/nsp007

Mills, K. L., Lalonde, F., Clasen, L. S., Giedd, J. N., & Blakemore, S.-J. (2014). Developmental changes in the structure of the social brain in late childhood and adolescence. *Social Cognitive and Affective Neuroscience*, *9*(1), 123–131. http://doi.org/10.1093/scan/nss113

Munte, T. F., Altenmuller, E., & Jancke, L. (2002). The musician's brain as a model of neuroplasticity. *Nat Rev Neurosci*, *3*(6), 473–478. http://doi.org/10.1038/nrn843

Niven, J. E., & Laughlin, S. B. (2008). Energy limitation as a selective pressure on the evolution of sensory systems. *Journal of Experimental Biology*, *211*(11), 1792–1804. http://doi.org/10.1242/jeb.017574

Ostby, Y., Tamnes, C. K., Fjell, A. M., Westlye, L. T., Due-Tonnessen, P., & Walhovd, K. B. (2009). Heterogeneity in subcortical brain development: A structural magnetic resonance imaging study of brain maturation from 8 to 30 years. *Journal of Neuroscience*, *29*(38), 11772–11782. http://doi.org/10.1523/JNEUROSCI.1242-09.2009

Paus, T., Toro, R., Leonard, G., Lerner, J. V., Lerner, R. M., Perron, M., … Steinberg, L. (2008). Morphological properties of the action-observation cortical network in adolescents with low and high resistance to peer influence. *Social Neuroscience*, *3*(3-4), 303–316. http://doi.org/10.1080/17470910701563558

Peng, Z., Shi, F., Shi, C., Yang, Q., Chan, R. C. K., & Shen, D. (2014). Disrupted cortical network as a vulnerability marker for obsessive–compulsive disorder. *Brain Structure and Function*, *219*(5), 1801–1812. http://doi.org/10.1007/s00429-013-0602-y

Pons, P., & Latapy, M. (2005). Computing communities in large networks using random walks (long version). *ArXiv Physics E-Prints*.

Purdie, V., & Downey, G. (2000). Rejection sensitivity and adolescent girls' vulnerability to

relationship-centered difficulties. *Child Maltreatment*, *5*(4), 338–349. http://doi.org/10.1177/1077559500005004005

Raamana, P. R., Weiner, M. W., Wang, L., & Beg, M. F. (2015). Thickness network features for prognostic applications in dementia. *Neurobiology of Aging*, *36*, S91–S102. http://doi.org/10.1016/j.neurobiolaging.2014.05.040

R Core Team. (2014). *R: A Language and Environment for Statistical Computing*. Vienna, Austria: R Foundation for Statistical Computing. Retrieved from http://www.R-project.org/

Romero-Canyas, R., & Downey, G. (2013). What I see when I think it's about me: People low in rejection-sensitivity downplay cues of rejection in self-relevant interpersonal situations. *Emotion*, *13*(1), 104–117. http://doi.org/10.1037/a0029786

Rudolph, M. D., Miranda-Dominguez, O., Cohen, A. O., Breiner, K., Steinberg, L., Bonnie, R. J., … Fair, D. A. (unpublished manuscript). At risk of being risky: the relationship between "brain age" under emotional states and risk preference.

Saggar, M., Hosseini, S. M. H., Bruno, J. L., Quintin, E.-M., Raman, M. M., Kesler, S. R., & Reiss, A. L. (2015). Estimating individual contribution from group-based structural correlation networks. *NeuroImage*, *120*, 274–284. http://doi.org/10.1016/j.neuroimage.2015.07.006

Schulz, K., Fan, J., Magidina, O., Marks, D., Hahn, B., & Halperin, J. (2007). Does the emotional go/no-go task really measure behavioral inhibition? Convergence with measures on a non-emotional analog. *Archives of Clinical Neuropsychology*, *22*(2), 151–160. http://doi.org/10.1016/j.acn.2006.12.001

Shaw, D. J., Mareček, R., Grosbras, M.-H., Leonard, G., Bruce Pike, G., & Paus, T. (2016). Co-

ordinated structural and functional covariance in the adolescent brain underlies face processing performance. *Social Cognitive and Affective Neuroscience*, nsv138. http://doi.org/10.1093/scan/nsv138

Shaw, P., Kabani, N. J., Lerch, J. P., Eckstrand, K., Lenroot, R., Gogtay, N., … Wise, S. P. (2008). Neurodevelopmental trajectories of the human cerebral cortex. *Journal of Neuroscience*, *28*(14), 3586–3594. http://doi.org/10.1523/JNEUROSCI.5309-07.2008

Skuse, D. H., & Gallagher, L. (2009). Dopaminergic-neuropeptide interactions in the social brain. *Trends in Cognitive Sciences*, *13*(1), 27–35. http://doi.org/10.1016/j.tics.2008.09.007

Smith, A. R. (2015). *Development of the Anterior Insula: Implications for Adolescent Risk-Taking*. Unpublished Manuscript (Dissertation), Philadelphia, PA.

Smith, A. R., Steinberg, L., & Chein, J. (2014). The role of the anterior insula in adolescent decision making. *Developmental Neuroscience*. http://doi.org/10.1159/000358918

Sporns, O., & Zwi, J. D. (2004). The small world of the cerebral cortex. *Neuroinformatics*, *2*(2), 145–162. http://doi.org/10.1385/NI:2:2:145

Steinberg, L., & Monahan, K. C. (2007). Age differences in resistance to peer influence. *Developmental Psychology*, *43*(6), 1531–1543. http://doi.org/10.1037/0012-1649.43.6.1531

Steinberg, L., & Morris, A. S. (2001). Adolescent development. *Annual Review of Psychology*, *52*(1), 83–110. http://doi.org/10.1146/annurev.psych.52.1.83

Sui, J., Pearlson, G. D., Du, Y., Yu, Q., Jones, T. R., Chen, J., … Calhoun, V. D. (2015). In search of multimodal neuroimaging biomarkers of cognitive deficits in schizophrenia. *Biological Psychiatry*. http://doi.org/10.1016/j.biopsych.2015.02.017

Sun, J., Li, H., Li, W., Wei, D., Hitchman, G., Zhang, Q., & Qiu, J. (2014). Regional gray matter volume is associated with rejection sensitivity: A voxel-based morphometry study. *Cognitive, Affective, & Behavioral Neuroscience*. http://doi.org/10.3758/s13415-014-0249-z

Tange, O. (2011). GNU Parallel - The command-line power tool. *;login: The USENIX Magazine*, *February*, 42–47.

Thompson, P. M., Cannon, T. D., Narr, K. L., van Erp, T., Poutanen, V.-P., Huttunen, M., … Toga, A. W. (2001). Genetic influences on brain structure. *Nat Neurosci*, *4*(12), 1253–1258. http://doi.org/10.1038/nn758

Thompson, P. M., Hayashi, K. M., de Zubicaray, G., Janke, A. L., Rose, S. E., Semple, J., … Toga, A. W. (2003). Dynamics of gray matter loss in Alzheimer's disease. *The Journal of Neuroscience: The Official Journal of the Society for Neuroscience*, *23*(3), 994–1005.

Tottenham, N., Hare, T. A., & Casey, B. J. (2011). Behavioral assessment of emotion discrimination, emotion regulation, and cognitive control in childhood, adolescence, and adulthood. *Frontiers in Psychology*, *2*. http://doi.org/10.3389/fpsyg.2011.00039

Uddin, L. Q. (2010). Typical and atypical development of functional human brain networks: insights from resting-state fMRI. *Frontiers in Systems Neuroscience*, *4*. http://doi.org/10.3389/fnsys.2010.00021

Vértes, P. E., & Bullmore, E. T. (2015). Annual research review: Growth connectomics - the organization and reorganization of brain networks during normal and abnormal development. *Journal of Child Psychology and Psychiatry*, *56*(3), 299–320. http://doi.org/10.1111/jcpp.12365

Vijayakumar, N., Allen, N. B., Youssef, G., Dennison, M., Yücel, M., Simmons, J. G., &

Whittle, S. (2016). Brain development during adolescence: A mixed-longitudinal investigation of cortical thickness, surface area, and volume. *Human Brain Mapping*, n/a–n/a. http://doi.org/10.1002/hbm.23154

Voss, P., & Zatorre, R. J. (2015). Early visual deprivation changes cortical anatomical covariance in dorsal-stream structures. *NeuroImage*, *108*, 194–202. http://doi.org/10.1016/j.neuroimage.2014.12.063

Waber, D. P., De Moor, C., Forbes, P. W., Almli, C. R., Botteron, K. N., Leonard, G., … THE BRAIN DEVELOPMENT COOPERATIVE GROUP. (2007). The NIH MRI study of normal brain development: Performance of a population based sample of healthy children aged 6 to 18 years on a neuropsychological battery. *Journal of the International Neuropsychological Society*, *13*(05). http://doi.org/10.1017/S1355617707070841

Watts, D. J., & Strogatz, S. H. (1998). Collective dynamics of `small-world' networks. *Nature*, *393*(6684), 440–442. http://doi.org/10.1038/30918

Wechsler, D. (2011). *Wechsler Abbreviated Scale of Intelligence–Second Edition Manual*. Bloomington, MN: Pearson.

Winkler, A. M., Kochunov, P., Blangero, J., Almasy, L., Zilles, K., Fox, P. T., … Glahn, D. C. (2010). Cortical thickness or grey matter volume? The importance of selecting the phenotype for imaging genetics studies. *NeuroImage*, *53*(3), 1135–1146. http://doi.org/10.1016/j.neuroimage.2009.12.028

Worsley, K. J., Chen, J.-I., Lerch, J., & Evans, A. C. (2005). Comparing functional connectivity via thresholding correlations and singular value decomposition. *Philosophical Transactions of the Royal Society B: Biological Sciences*, *360*(1457), 913–920. http://doi.org/10.1098/rstb.2005.1637

Zhou, D., Lebel, C., Treit, S., Evans, A., & Beaulieu, C. (2015). Accelerated longitudinal cortical thinning in adolescence. *NeuroImage, 104,* 138–145. http://doi.org/10.1016/j.neuroimage.2014.10.005

APPENDIX A

GRAY MATTER VOLUME – METHODS AND SMALL-WORLD PROPERTIES

While not the main focus of the present dissertation, a less comprehensive analysis of gray matter volume structural covariance networks was also conducted. The methods were the same as the ones used in cortical thickness analyses, with the following exceptions: all residualized values also controlled for estimated total intracranial volume; the FDR threshold was set at 0.05 as in previous studies (He et al., 2007a); sub-networks included the sub-cortical regions described in the methods section.

Whole brain graphs, as well as graphs restricted to the social brain network, for both gray matter volume and cortical thickness across the three age groups differed significantly from random graphs on both clustering coefficient and average path length (all *p*'s <.001) and exhibited small-world properties.

	Brain Networks GM Volume (FDR=0.05)	**N**	**C_p**	**L_p**	**C_p / C_{random}**	**L_p / L_{random}**	**r**
Whole Brain	Adolescents	82	0.36	2.68	4.05	1.11	3.65
	Young Adults	82	0.49	1.79	1.79	1.04	1.72
	Adults	82	0.50	1.92	2.10	1.09	1.94
Social Brain	Adolescents	36	0.40	2.26	2.30	1.07	2.15
	Young Adults	36	0.55	1.78	1.59	1.08	1.48
	Adults	36	0.52	1.93	1.84	1.10	1.67

At the whole-brain level, an ANOVA showed that small-worldness values differed significantly across groups, $F(2, 297) = 409.1$, $p<.001$. Post-hoc Bonferroni-adjusted pairwise comparisons revealed that small-worldness was highest in adolescents (M= 7.15, SD= 1.81), lowest in young adults (M= 2.72, SD= 0.53) and lower than in adolescents but higher than in young adults in the adult sample (M= 3.37, SD= 0.80), all *p*'s <.001. In the social brain, small-worldness values differed significantly across groups, $F(2, 297) = 49.19$, $p<.001$. Post-hoc Bonferroni-adjusted pairwise comparisons revealed that small-worldness was highest in adolescents (M= 4.03, SD= 1.93), lowest in young adults (M= 2.32, SD= 0.51), and lower than in adolescents but higher than in young adults in the adult sample (M= 2.89, SD= 0.83), all *p*'s <.005.

APPENDIX B

GRAY MATTER VOLUME – COVARIANCE ACROSS DEVELOPMENT

Analyses of variance on graph density values and characteristic path length obtained via sub-sampling suggest that at both the whole-brain level and in the social brain network, graph densities change across development groups.

At the whole-brain level, an ANOVA showed that density values differed significantly across groups, F(2, 297) = 253.2, p<.001. Post-hoc Bonferroni-adjusted pairwise comparisons revealed that small-worldness was lowest in adolescents (M= 0.04, SD= 0.01), highest in young adults (M= 0.14, SD= 0.04) and higher than in adolescents but lower than in young adults in the adult sample (M= 0.11, SD= 0.03), all p's <.001.

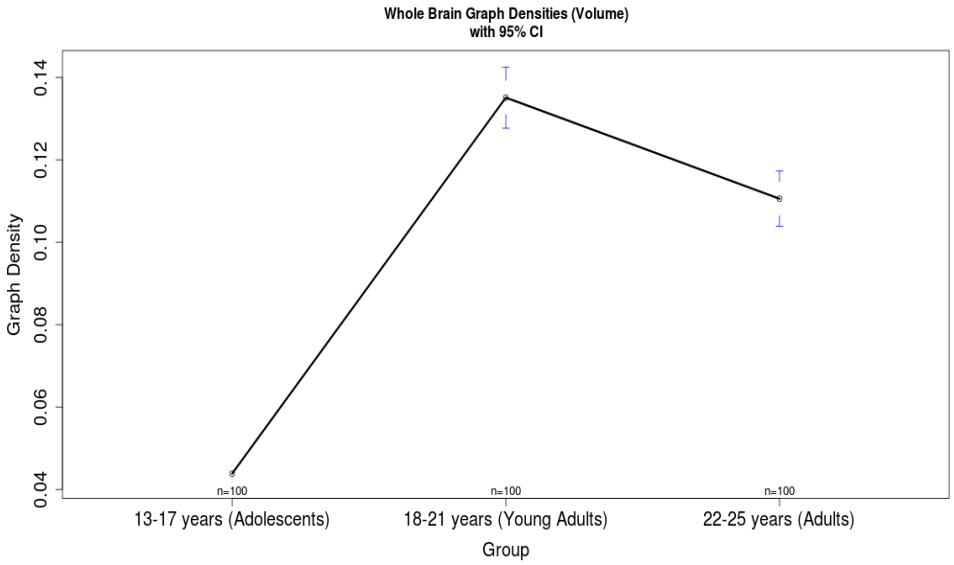

While there was an increase in covariance density between adolescence and adulthood, characteristic path lengths decreased across age groups. The ANOVA showed a significant between-group difference, F(2,297)= 379.5, p<.001. Post-hoc Bonferroni-adjusted pairwise comparisons revealed that characteristic path length was highest in adolescents (M= 3.97, SD= 0.63), lowest in young adults (M= 2.37, SD= 0.31), and lower than in adolescents but higher than in young adults in the adult sample (M= 2.58, SD= 0.32), all p's <.005.

In the social brain network, an ANOVA showed that density values differed significantly across groups, F(2, 297) = 253.2, p<.001. Post-hoc Bonferroni-adjusted pairwise comparisons revealed that small-worldness was lowest in adolescents (M= 0.04, SD= 0.01), highest in young adults (M= 0.14, SD= 0.04) and higher than in adolescents but lower than in young adults in the adult sample (M= 0.11, SD= 0.03), all p's <.001.

While there was an increase in covariance density (network cost) between adolescence and adulthood, characteristic path lengths again decreased during this time. An ANOVA showed a significant between-group difference, F(2,297)= 128.8, p<.001. Post-hoc Bonferroni-adjusted pairwise comparisons revealed that characteristic path length was highest in adolescents (M= 3.11, SD= 0.52), and stabilized by young adulthood, with no significant differences between young adults (M= 2.33, SD= 0.32) and adults (M= 2.39, SD= 0.26); p's between adolescents and

young adults, and adolescents and adults, were <.001.

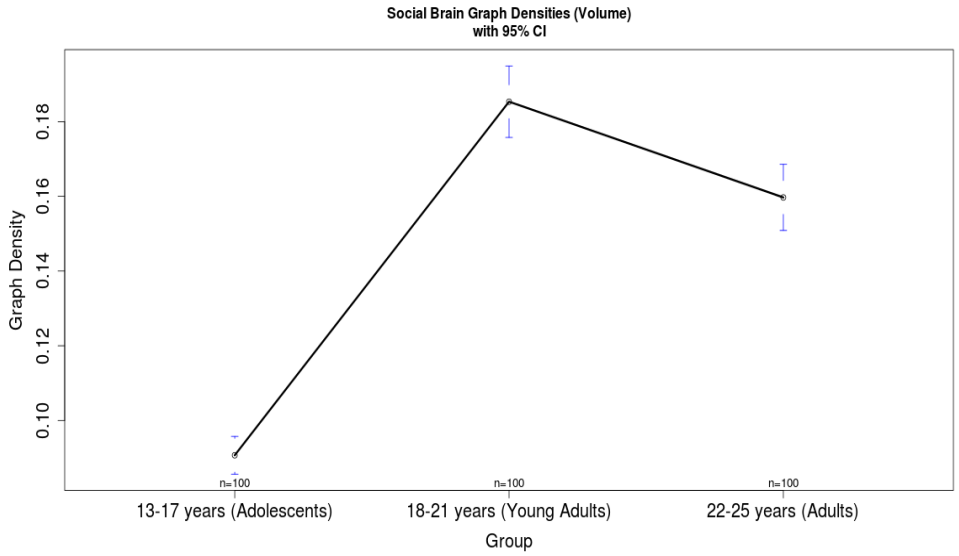

	Social Brain Sub-Networks (Gray Matter Volume)					
	Density			Path Length		
	Adolescents M (SD)	**Y. Adults M (SD)**	**Adults M (SD)**	**Adolescents M (SD)**	**Y. Adults M (SD)**	**Adults M (SD)**
Perception	0.25 (0.07)[2,3]	0.30 (0.09)[1]	0.33 (0.09)[1]	1.97 (0.39)[2,3]	1.89 (0.30)[3]	1.77 (0.30)[1,2]
Affiliation	0.14 (0.04)[2,3]	0.23 (0.07)[1,3]	0.16 (0.05)[1,2]	2.21 (0.50)[2]	2.32 (0.42)[1]	2.11 (0.46)[2]
Aversion	0.15 (0.04)[2,3]	0.36 (0.07)[1,3]	0.26 (0.06)[1,2]	1.86 (0.37)	1.88 (0.31)	1.79 (0.23)
Mentalizing/Mirror	0.12 (0.04)[2]	0.19 (0.07)[1,3]	0.11 (0.05)[2]	1.24 (0.25)[2,3]	1.55 (0.37)[1,3]	1.41 (0.33)[1,2]
	1 = significantly different from adolescents; 2 = significantly different from young adults; 3 = significantly different from adults; p<.05					

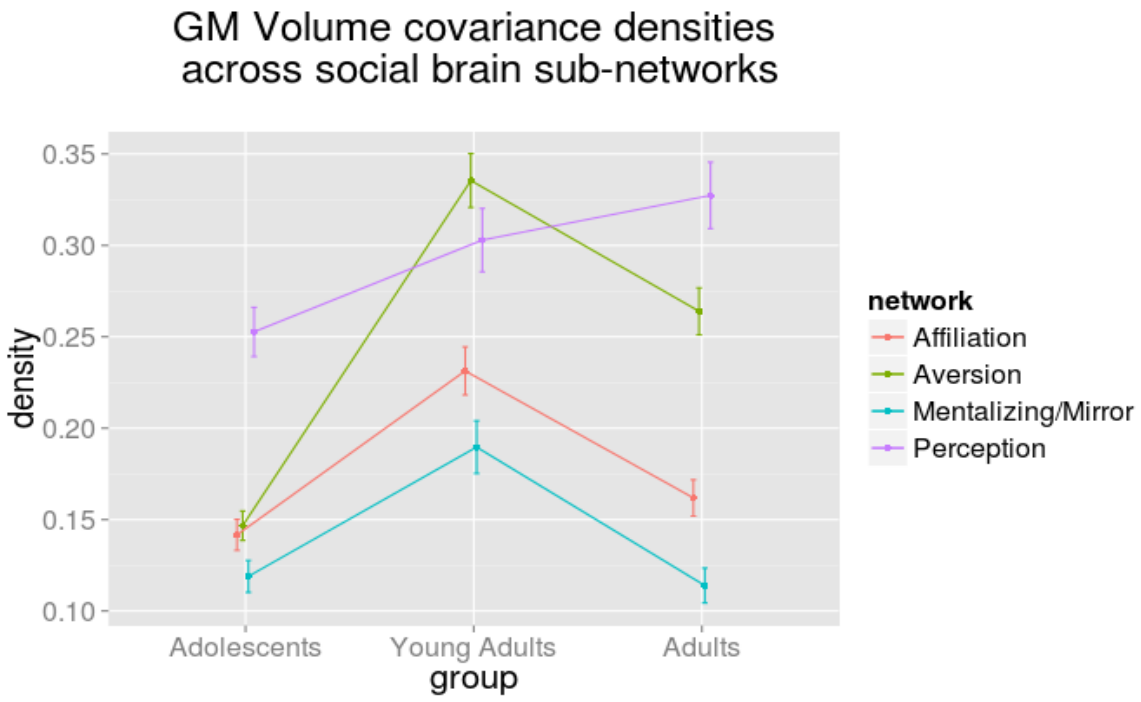
GM Volume covariance densities
across social brain sub-networks
density
0.35
0.30
0.25
0.20
0.15
0.10
Adolescents
Young Adults
Adults
group
network
Affiliation
Aversion
Mentalizing/Mirror
Perception

APPENDIX C

GRAY MATTER VOLUME – RESISTANCE TO PEER INFLUENCE

Gray matter volume covariance densities for graphs of individuals with high RPI found significant between-group differences, $F(3,297) = 155.3$, $p<.001$. Post-hoc tests showed that high RPI groups had a lower covariance density in the social brain overall (M= .08, SD=0.03) compared to medium RPI (M=0.12, SD=0.03) and low RPI (M=0.18, SD=0.06), all p's <.001. Significant between-group differences were also found in characteristic path length, $F(2,297) = 68.64$, $p<.001$. Post-hoc tests suggest that high RPI groups (M=2.80, SD=0.42) and medium RPI groups (M=2.81, SD= 0.35) have significantly longer path lengths than low RPI groups (M=2.29, SD=0.29), both p's <.001.

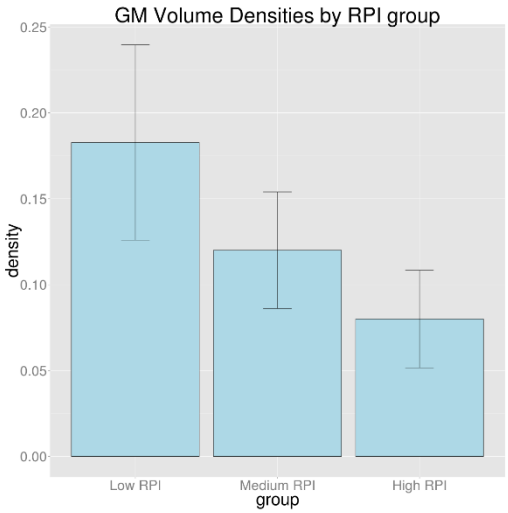

A further investigation of the sub-networks revealed more nuanced findings.

	GM Volume					
	Density			**Path Length**		
	Low RPI M (SD)	**Med. RPI M (SD)**	**High RPI M (SD)**	**Low RPI M (SD)**	**Med. RPI M (SD)**	**High RPI M (SD)**
Perception	0.35 (0.09)[3]	0.36 (0.07)[3]	0.11 (0.04)[1,2]	1.64 (0.26)[2,3]	1.86 (0.24)[1,3]	1.40 (0.42)[1,2]
Affiliation	0.13 (0.05)[2,3]	0.17 (0.05)[1,3]	0.08 (0.03)[1,2]	2.17 (0.57)[3]	2.11 (0.51)[3]	1.52 (0.45)[1,2]
Aversion	0.26 (0.08)[2,3]	0.13 (0.05)[1,3]	0.19 (0.06)[1,2]	1.84 (0.31)[3]	1.86 (0.46)[3]	1.69 (0.36)[1,2]
Mentalizing/Mirror	0.25 (0.09)[3]	0.24 (0.08)[3]	0.07 (0.03)[1,2]	1.78 (0.23)[2,3]	1.68 (0.27)[1,3]	1.25 (0.21)[1,2]
	1 = significantly different from adolescents; 2 = significantly different from young adults; 3 = significantly different from adults; p<.05					

APPENDIX D

GRAY MATTER VOLUME – REJECTION SENSITIVITY

Gray matter volume covariance densities for RSQ graphs found significant between-group differences, F(3,297) = 314.2, p<.001. Post-hoc tests showed that high RSQ groups had a higher connection density in the social brain overall (M= 0.16, SD=0.05) compared to medium RSQ (M=0.04, SD=0.02) and low RSQ (M=0.08, SD=0.03), all p's <.001. Significant between-group differences were also found in characteristic path length, F(2,297) = 14.55, p<.001. Post-hoc tests suggest that high RSQ groups (M=2.48, SD=0.44) and low RSQ groups (M=2.49, SD= 0.78) do not differ from each other significantly, but have significantly shorter path lengths than medium RSQ groups (M=2.87, SD=0.43), both p's <.001.

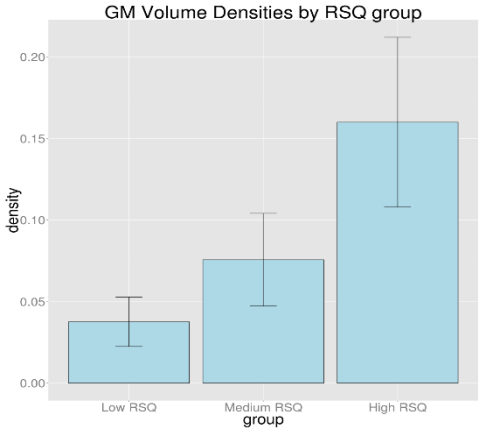

	GM Volume					
	Density			Path Length		
	Low RSQ M (SD)	**Med. RSQ M (SD)**	**High RSQ M (SD)**	**Low RSQ M (SD)**	**Med. RSQ M (SD)**	**High RSQ M (SD)**
Perception	0.09 (0.03)[2,3]	0.13 (0.05)[1]	0.14 (0.05)[1]	1.16 (0.29)[2,3]	1.67 (0.33)[1]	1.72 (0.49)[1]
Affiliation	0.02 (0.01)[3]	0.03 (0.02)[3]	0.07 (0.03)[1,2]	1.03 (0.12)[2,3]	1.18 (0.31)[1,3]	1.60 (0.52)[1,2]
Aversion	0.06 (0.02)[2,3]	0.09 (0.03)[1,3]	0.11 (0.04)[1,2]	1.11 (0.22)[2,3]	1.35 (0.27)[1]	1.44 (0.35)[1]
Mentalizing/Mirror	0.05 (0.03)[2,3]	0.004 (0.01)[1,3]	0.08 (0.04)[1,2]	1.02 (0.08)[3]	1.03 (0.10)[3]	1.19 (0.27)[1,2]
	1 = significantly different from adolescents; 2 = significantly different from young adults; 3 = significantly different from adults; p<.05					

APPENDIX E

GRAY MATTER VOLUME – GO NOGO

Gray matter volume covariance densities for GNG graphs found significant between-group differences, F(3,297) = 38.37, p<.001. Post-hoc tests showed that high GNG groups had a higher connection density in the social brain overall (M= 0.11, SD=0.04) compared to medium GNG (M=0.09, SD=0.03) and low GNG (M=0.07, SD=0.02), all p's <.001. Significant between-group differences were also found in characteristic path length, F(2,297) = 14.01, p<.001. Post-hoc tests suggest that low GNG groups (M=3.06, SD=0.61) and medium GNG groups (M=3.10, SD= 0.63) do not differ from each other significantly, but have significantly longer path lengths than high GNG groups (M=2.71, SD=0.48), both p's <.001.

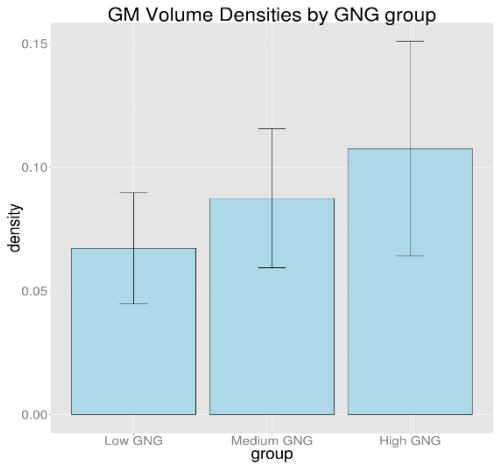

	GM Volume					
	Density			Path Length		
	Low GNG M (SD)	Med. GNG M (SD)	High RSQ M (SD)	Low GNG M (SD)	Med. GNG M (SD)	High GNG M (SD)
Perception	0.08 (0.04)[2,3]	0.11 (0.04)[1]	0.10 (0.04)[1]	1.31 (0.39)	1.25 (0.30)	1.37 (0.41)
Affiliation	0.04 (0.02)[2,3]	0.06 (0.02)[1,3]	0.07 (0.02)[1,2]	1.17 (0.22)[2,3]	1.40 (0.37)[1,3]	1.53 (0.34)[1,2]
Aversion	0.07 (0.02)[3]	0.08 (0.02)[3]	0.12 (0.05)[1,2]	1.20 (0.28)[3]	1.25 (0.29)[3]	1.55 (0.43)[1,2]
Mentalizing/Mirror	0.06 (0.04)[3]	0.05 (0.03)[3]	0.02 (0.02)[1,2]	1.19 (0.27)[2,3]	1.03 (0.09) [1]	1.07 (0.16)[1]
	1 = significantly different from adolescents; 2 = significantly different from young adults; 3 = significantly different from adults; p<.05					

APPENDIX F

COMMUNITY STRUCTURE - METHODS

While graph properties are descriptive of the overall organization of the graph, an interesting avenue of investigation for structural covariance in the brain is the study of how specific groups of brain regions may coordinate their structural development. Using the graphs obtained from the overall sample in each age group, a walktrap algorithm was employed to detect latent subsets of highly-correlated regions within the graphs (Pons & Latapy, 2005). The walktrap algorithm uses the *random walk approach*, which operates under the assumption that from any given vertex, when moving at random from one neighbor to another and recording the visited nodes, the vertices within a community have a higher probability of being visited. The walktrap algorithm runs this process for every vertex, and computes a distance between all vertex pairs. A hierarchical clustering technique is then applied to this distance matrix, and communities are detected by minimizing the sum of squared distances of each node to the other nodes within the community, using modularity optimization as a stopping mechanism. The reliability of community detection algorithms remains an area of fruitful debate and research, but recent work suggests that this community detection algorithm is the most reliable method for community detection in both sparse networks and weighted correlation matrices (Gates, Steinley, & Fair, under review).

Appendices G, I, K, M, O, Q: Graphs show communities identified using the data-driven walktrap algorithm; communities were first identified in the adult group, and then tracked in the two younger groups. Each community is color coded to facilitate structure tracking across groups.

Appendices H, J, L, N, P, R: Graphs show the brain structures belonging to the 4 social brain networks discussed in the present study, as represented in the communities observed in each age group: perception network (turquoise), affiliation network (gray), aversion network (green) and mirror/mentalizing (fuchsia).

APPENDIX G

DATA-DRIVEN COMMUNITIES, ADULTS (GRAY MATTER VOLUME)

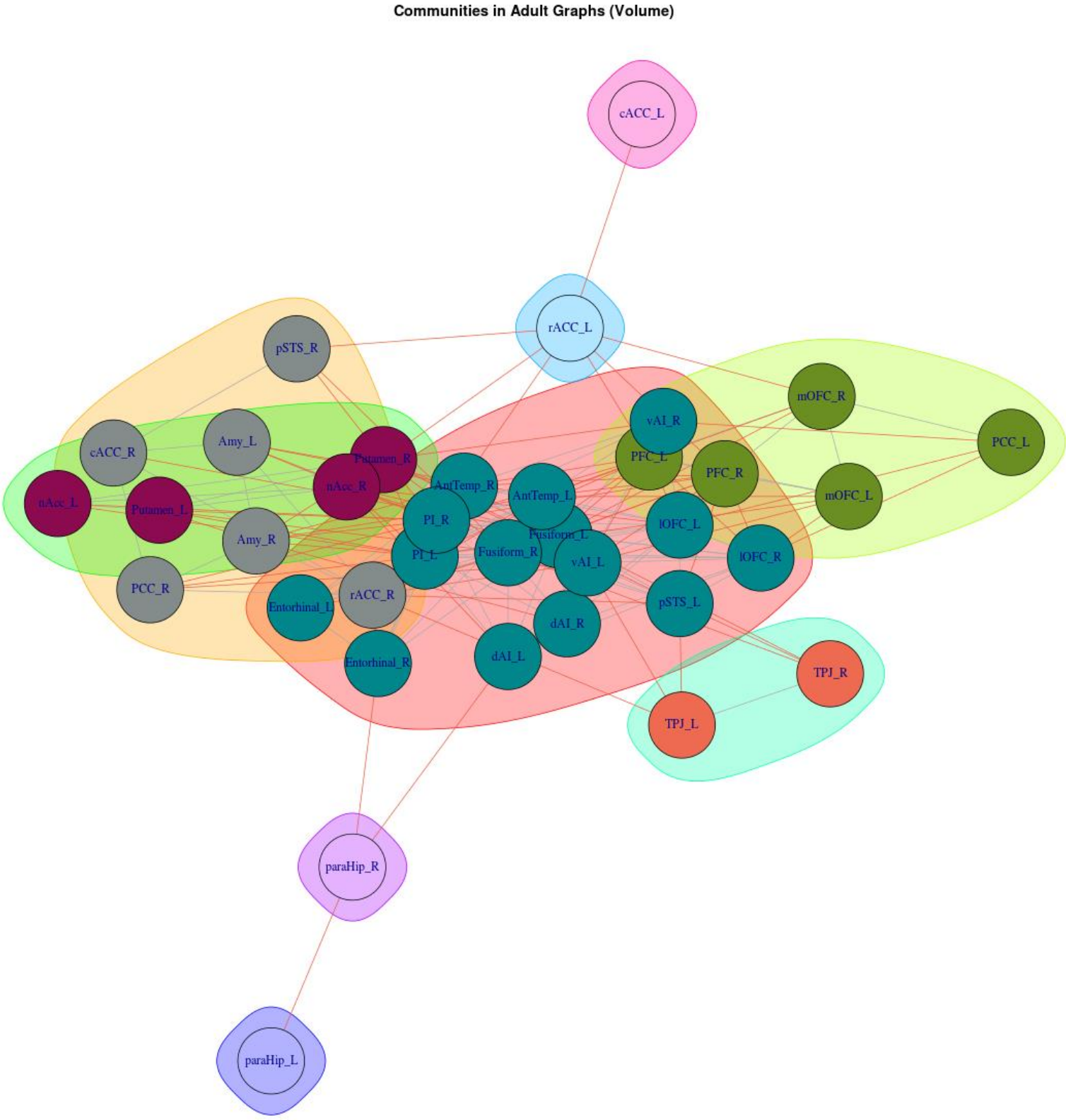

APPENDIX H

THEORY-BASED COMMUNITIES, ADULTS (GRAY MATTER VOLUME)

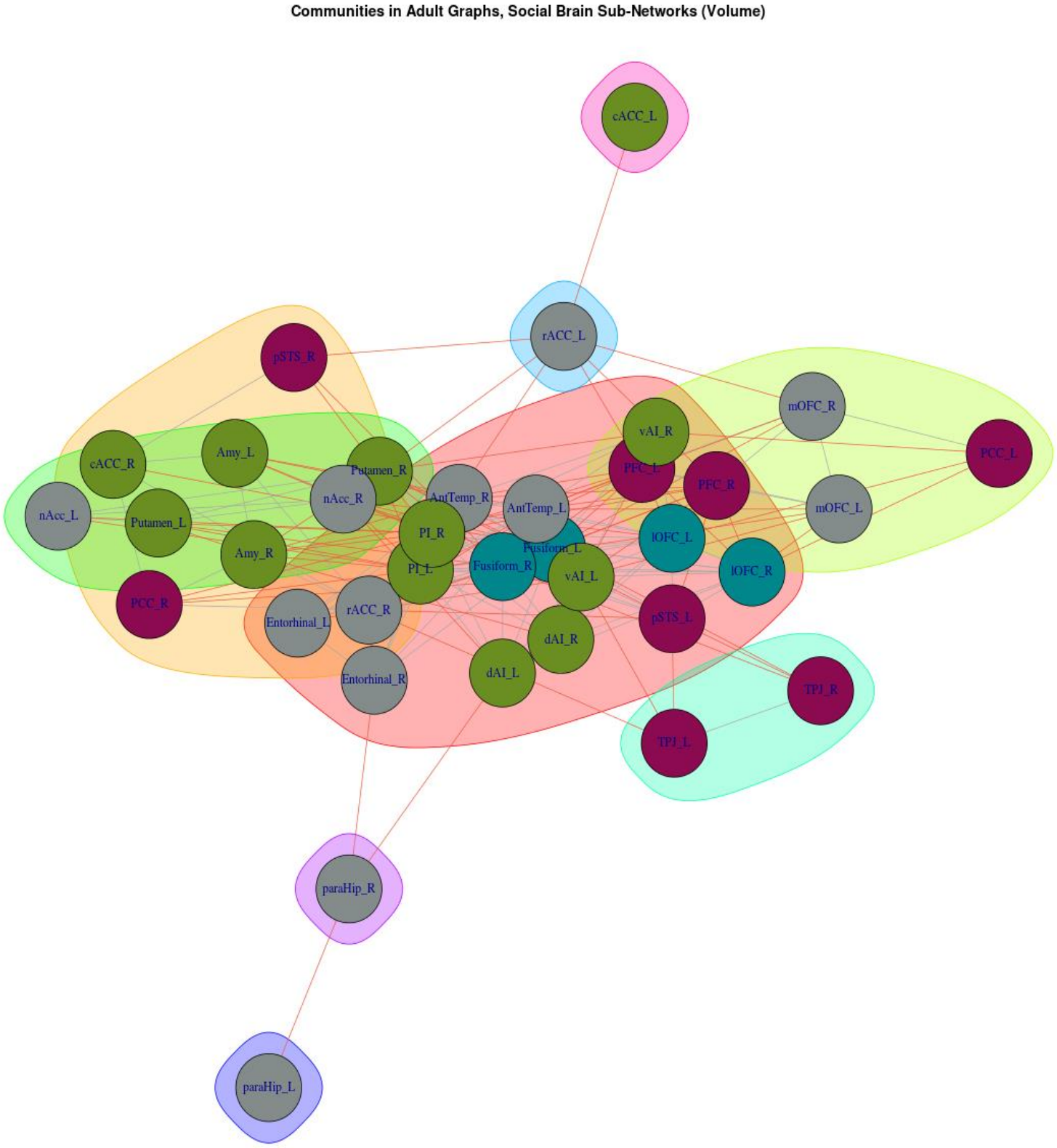

APPENDIX I

DATA-DRIVEN COMMUNITIES, YOUNG ADULTS (GRAY MATTER VOLUME)

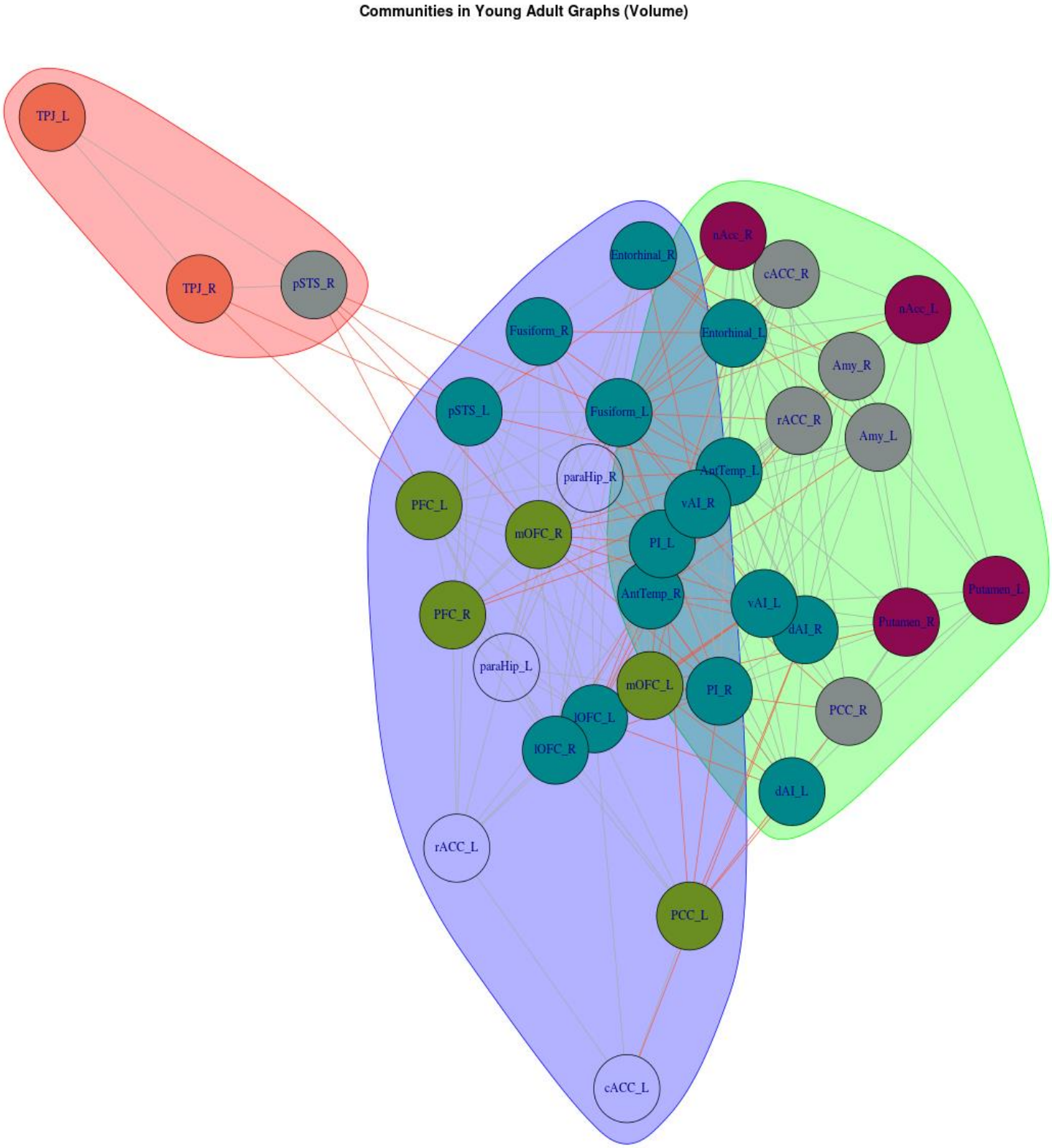

APPENDIX J

THEORY-BASED COMMUNITIES, YOUNG ADULTS (GRAY MATTER VOLUME)

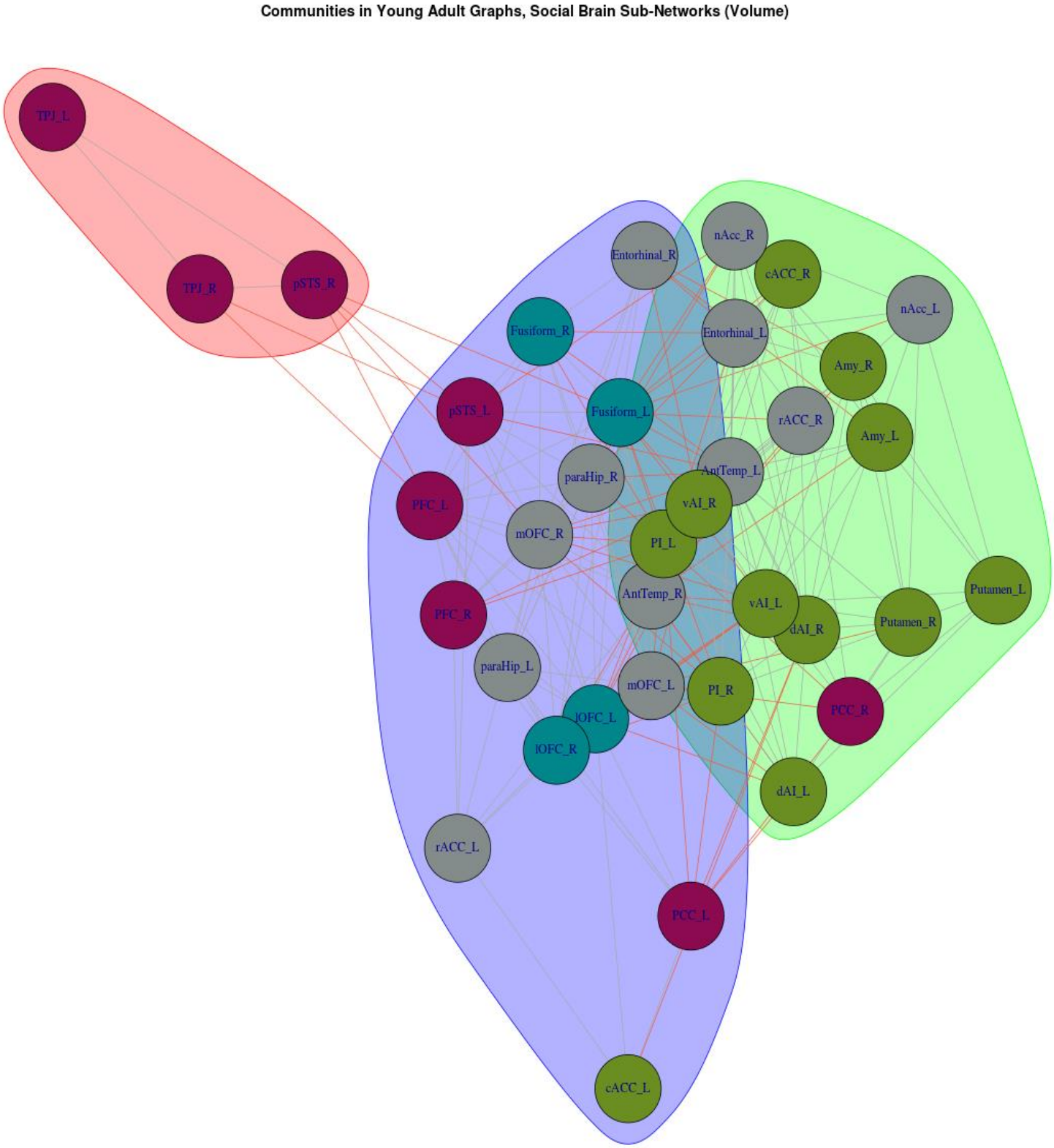

APPENDIX K

DATA-DRIVEN COMMUNITIES, ADOLESCENTS (GRAY MATTER VOLUME)

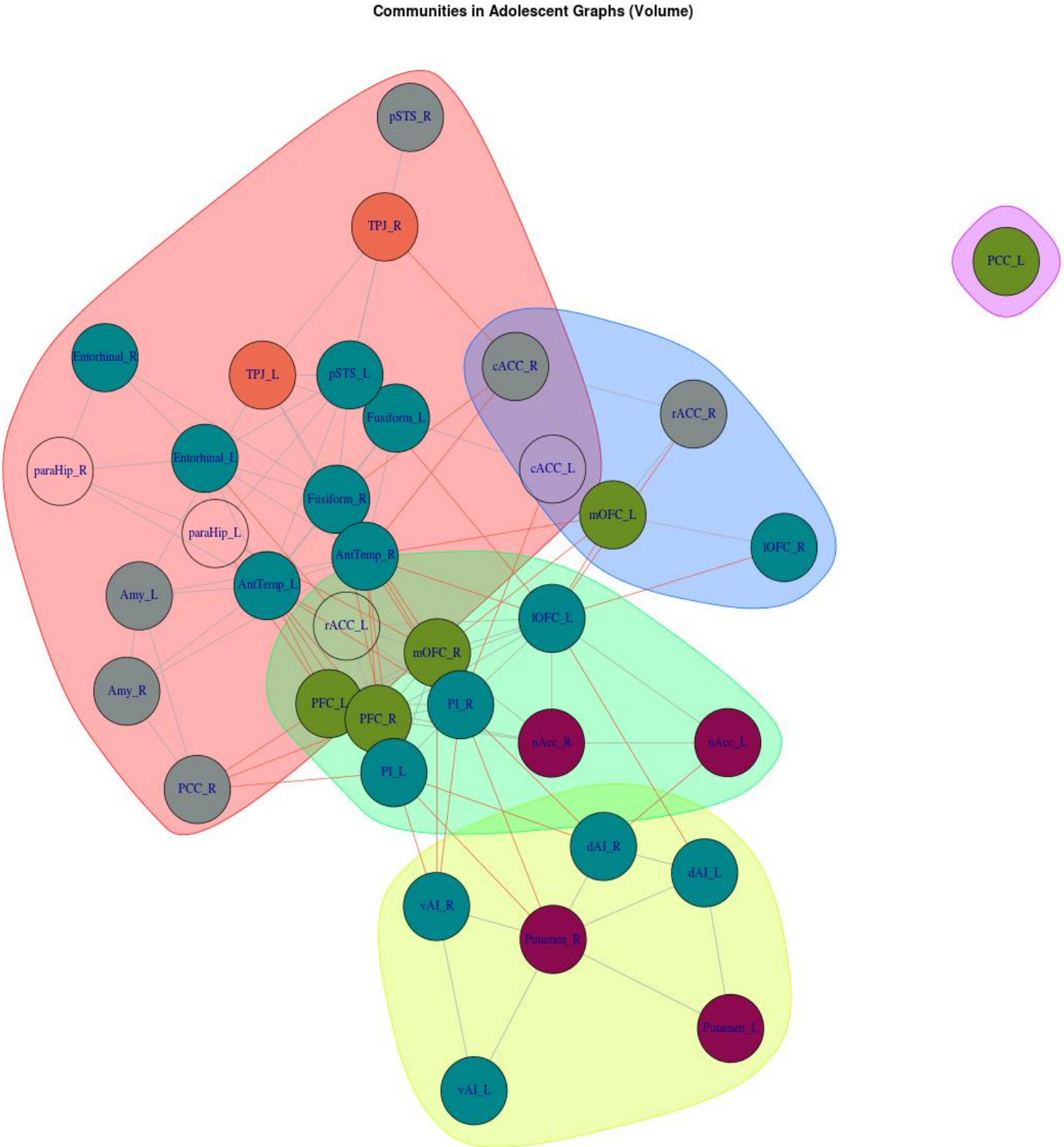

APPENDIX L

THEORY-BASED COMMUNITIES, ADOLESCENTS (GRAY MATTER VOLUME)

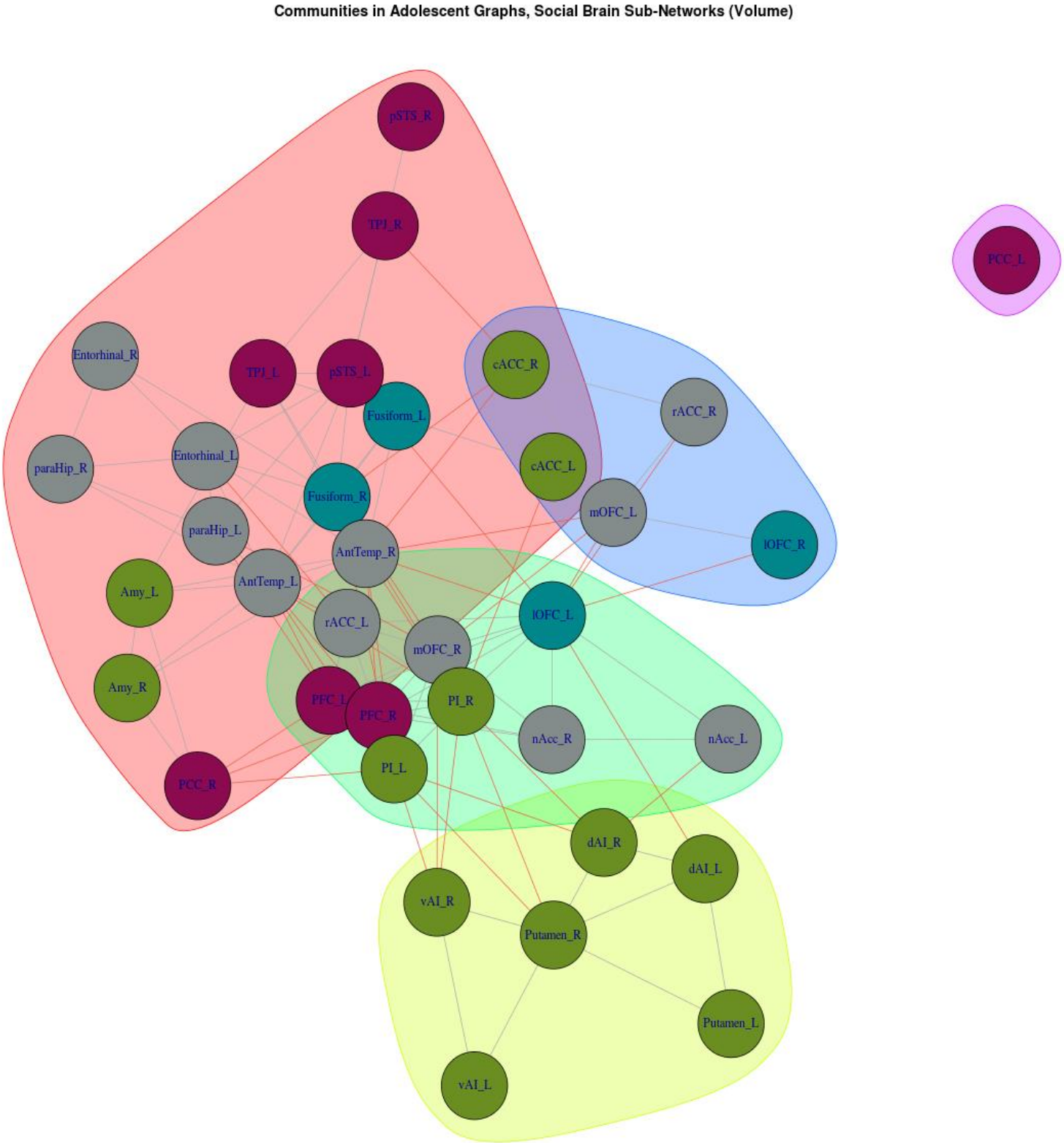

APPENDIX M

DATA-DRIVEN COMMUNITIES, ADULTS (CORTICAL THICKNESS)

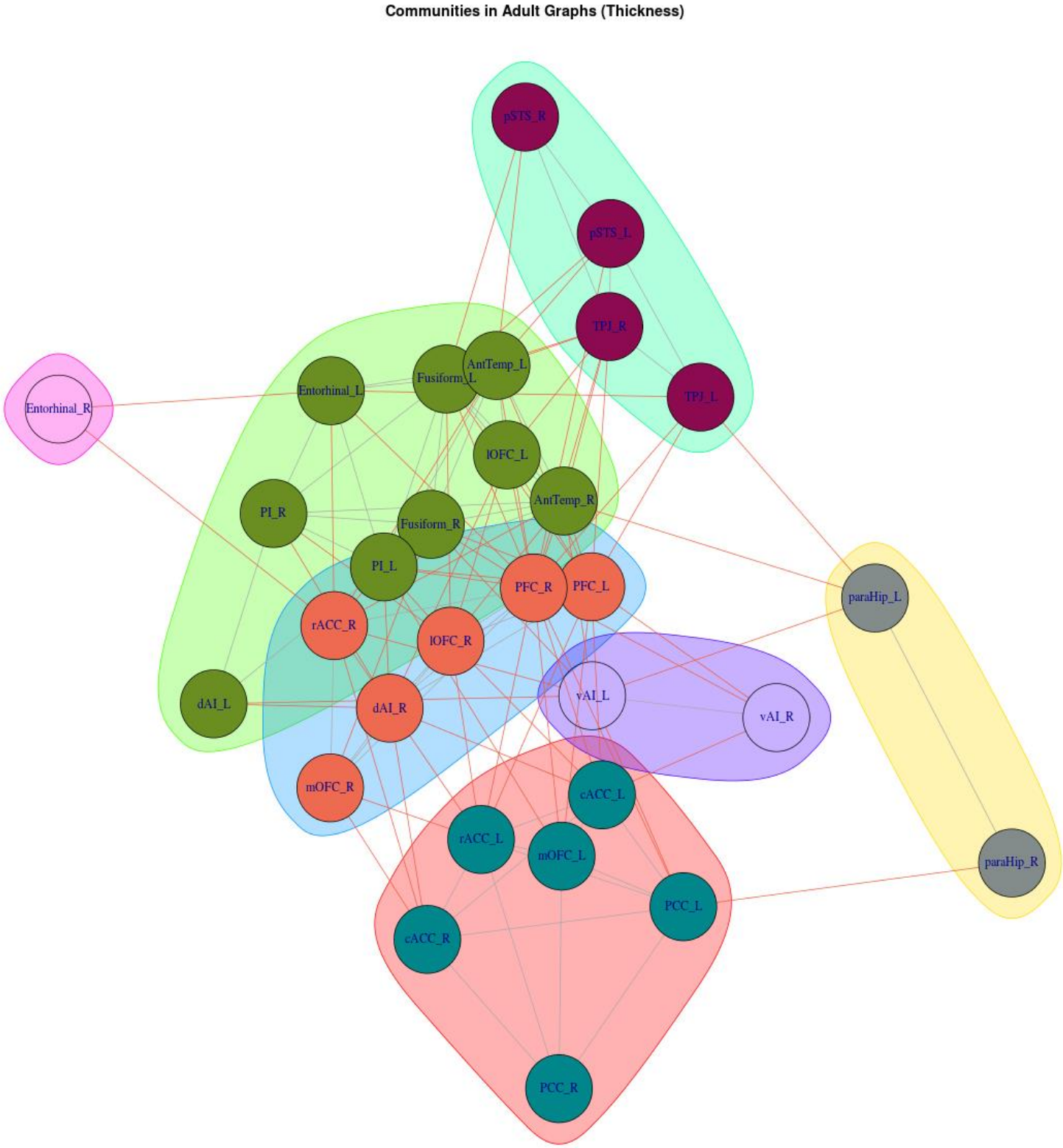

APPENDIX N

THEORY-BASED COMMUNITIES, ADULTS (CORTICAL THICKNESS)

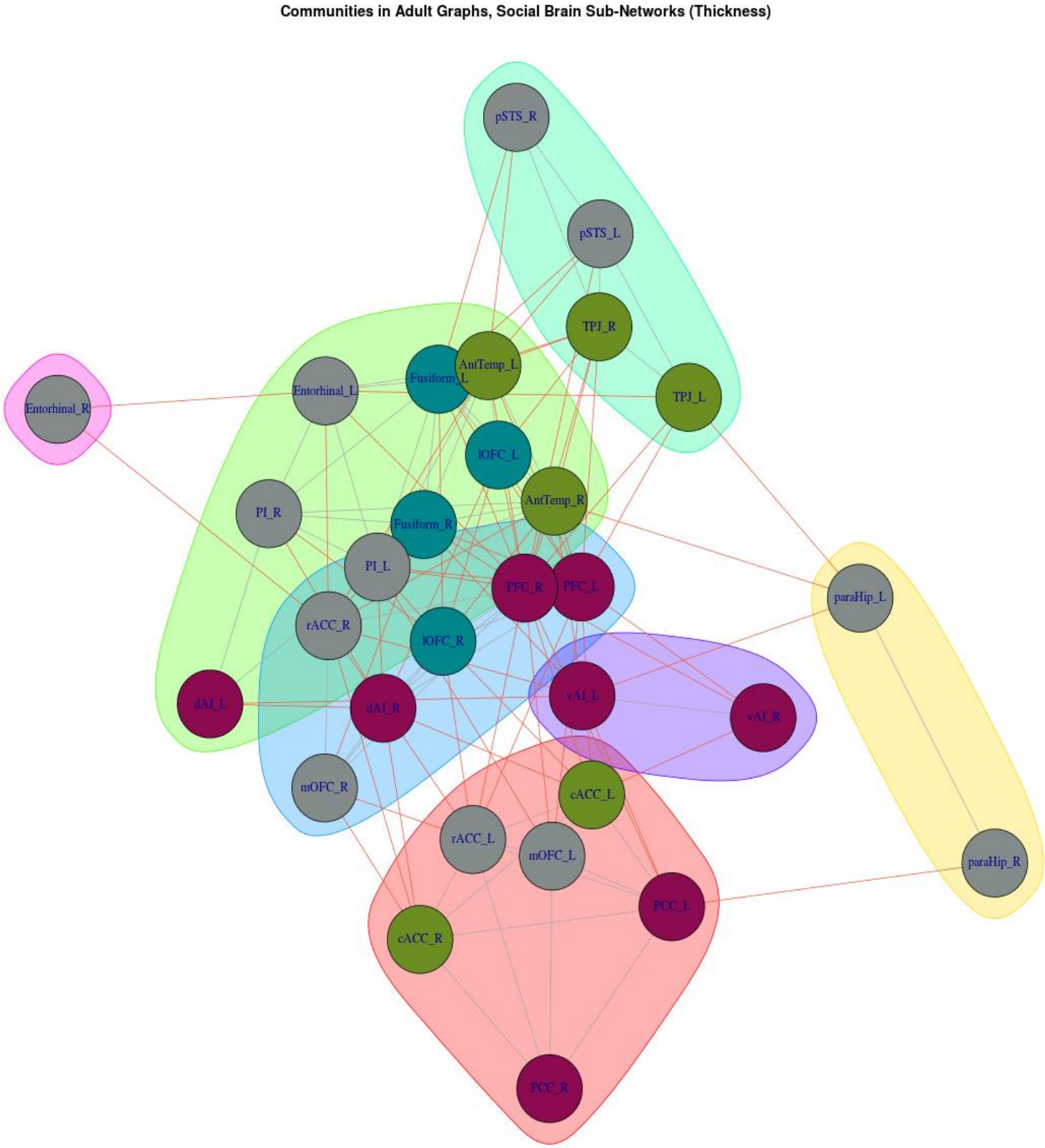

APPENDIX O

DATA-DRIVEN COMMUNITIES, YOUNG ADULTS (CORTICAL THICKNESS)

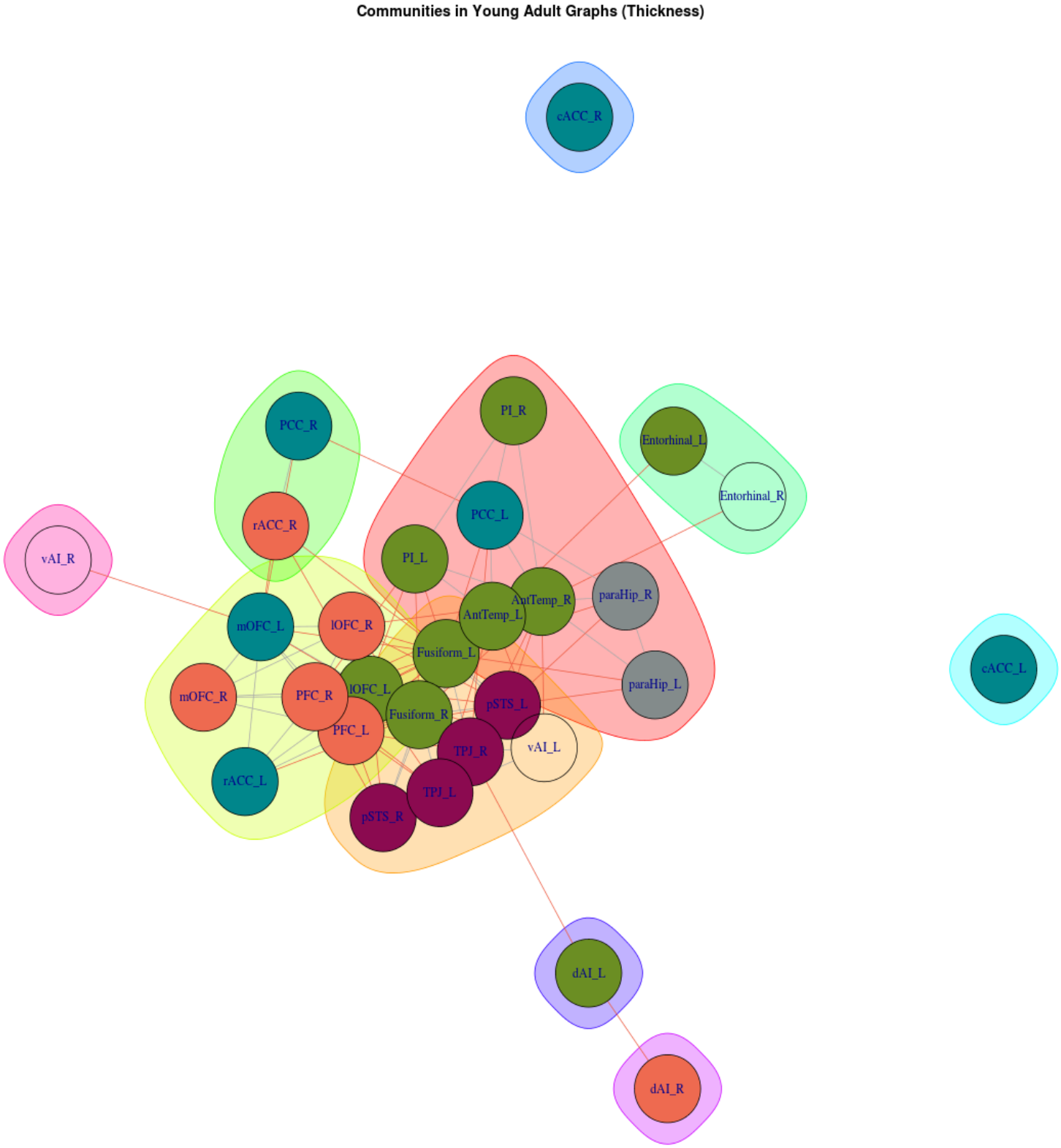

APPENDIX P

THEORY-BASED COMMUNITIES, YOUNG ADULTS (CORTICAL THICKNESS)

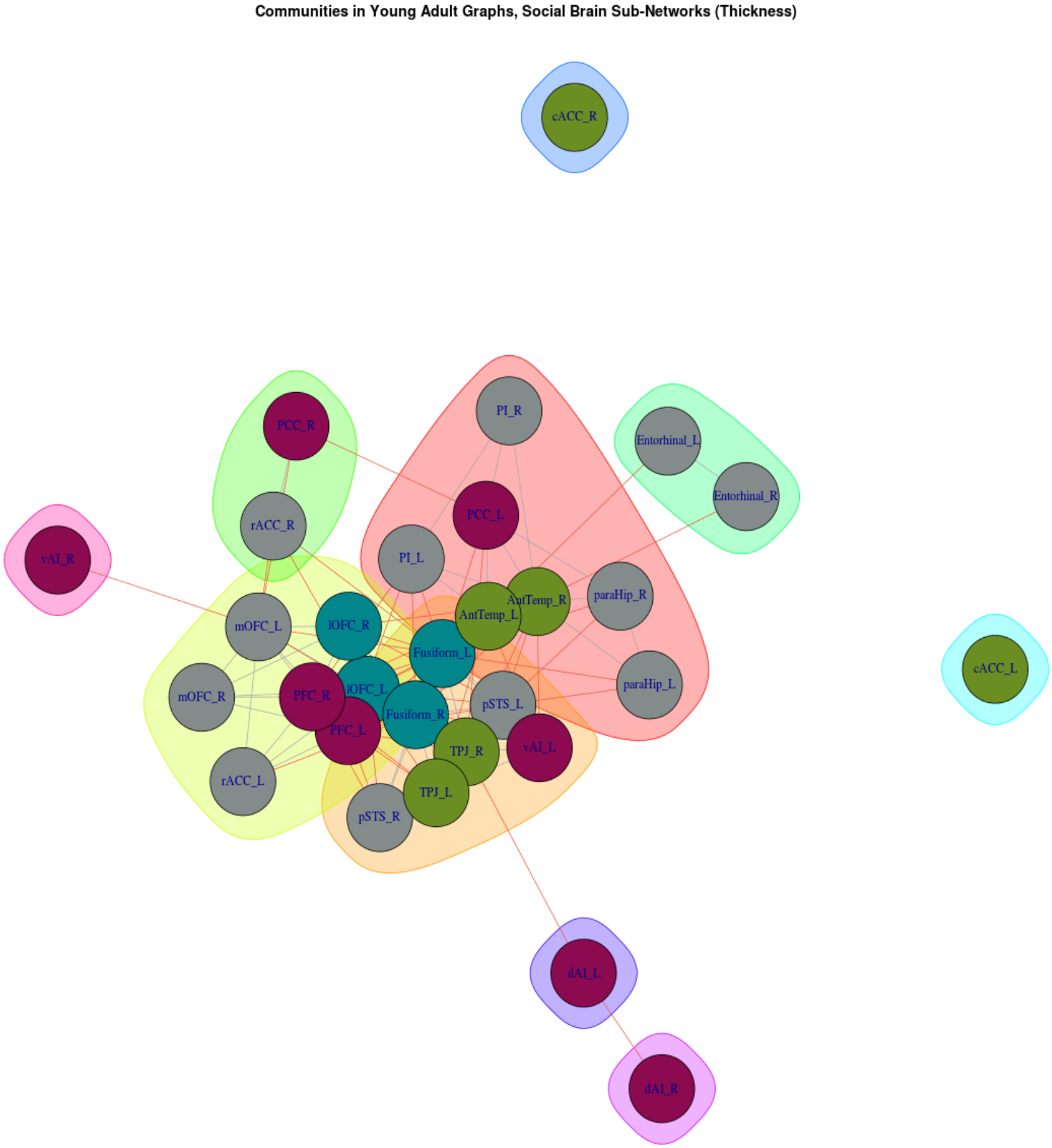

APPENDIX Q

DATA-DRIVEN COMMUNITIES, ADOLESCENTS (CORTICAL THICKNESS)

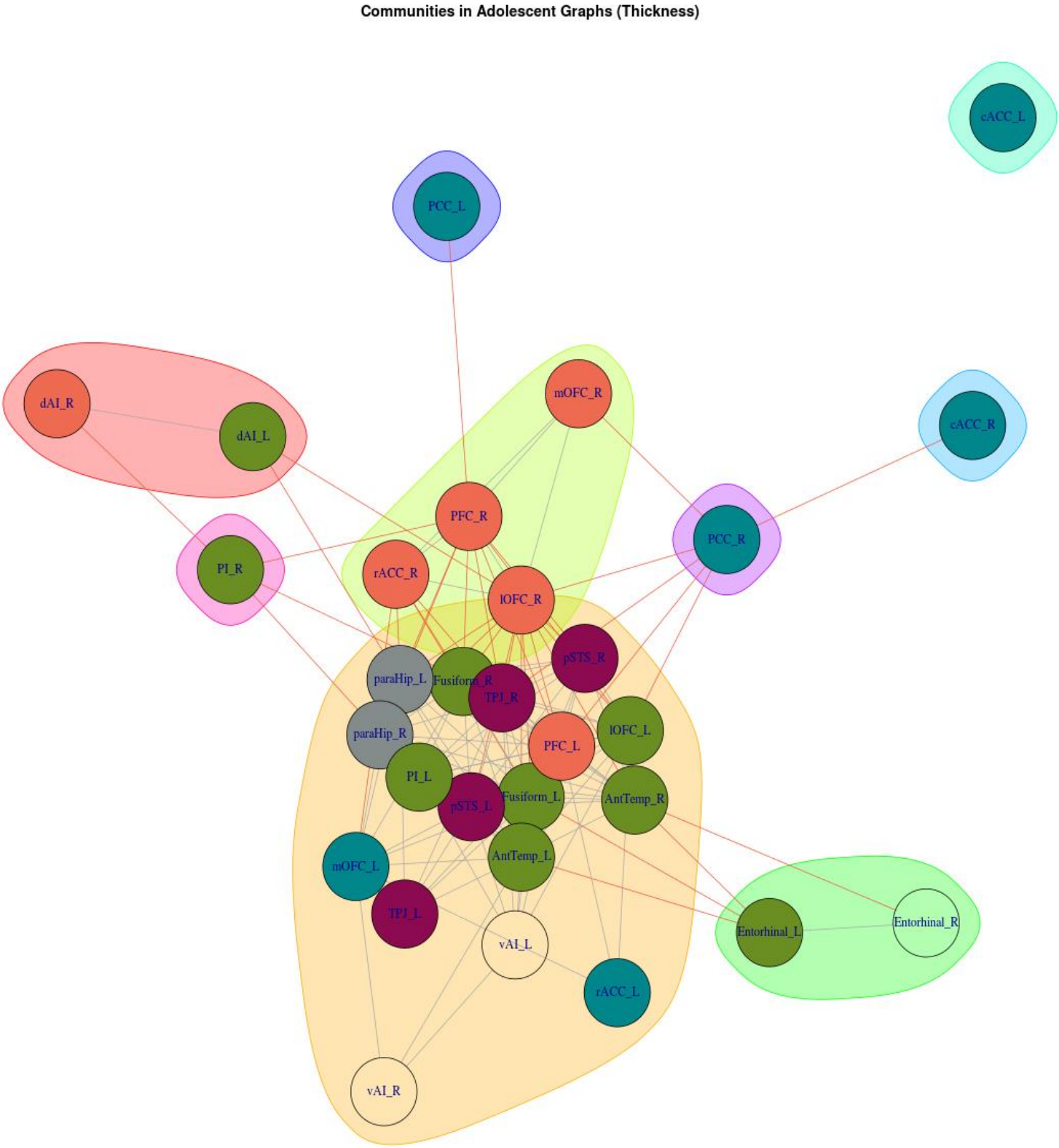

APPENDIX R

THEORY-BASED COMMUNITIES, ADOLESCENTS (CORTICAL THICKNESS)